CHARACTERISATION OF MAJOR METABOLITES OF WILD EVERLASTING, *HELICHRYSUM ARGYROSPHAERUM*

A THESIS SUBMITTED IN FULFILMENT

OF THE REQUIREMENTS FOR THE DEGREE OF

MASTER OF SCIENCE (CHEMISTRY)

OF

THE UNIVERSITY OF NAMIBIA

BY

TAONGA MOFFAT NAMATE

201047624

NOVEMBER 2017

MAIN SUPERVISOR: DR. STEFAN LOUW

CO-SUPERVISOR: DR. RENATE HANS

ABSTRACT

Plant species in the genus *Helichrysum*, are widely used in Southern African traditional medicine. Antibacterial and antifungal activities were reported for most of the *Helichrysum* species including *H. argyrosphaerum*. As a starting point to elucidate the structures of the compounds that may be responsible for these properties, phytochemical screening was performed to qualitatively identify the classes of compounds present. The results showed that the plant is rich in polyphenols and flavonoids, specifically flavones. This study employed a screening approach combining high pressure liquid chromatography – ultraviolet spectroscopy – high resolution tandem mass spectrometry (HPLC-UV-HRMS/MS) to elucidate the chemical structures of the major compounds of *H. argyrosphaerum*. First, suitable reversed phase liquid chromatography (RPLC) and hydrophilic interaction liquid chromatography (HILIC) separation methods were developed and the resulting methods were used for the HPLC-UV-HRMS/MS analysis of the methanol extracts of the flowers, stems and leaves of the plant. The UV spectra obtained for 5 of the 8 major constituents provided corroborating evidence that the compounds of interest are flavonoids. The high resolution MS/MS spectra provided accurate masses for the precursor and product ions from which the molecular formulae could be deduced. The molecular formulae was subsequently compared to those reported in literature and a number of possible known molecular structures that produced the same precursor and product ions were found. It was then possible to identify an aglycone, apigenin [5,7-Dihydroxy-2-(4-hydroxyphenyl)-4H-1-benzopyran-4-one], a cell permeable polyphenol bioactive (anti-inflammatory, antioxidant) component and four different kinds of apigenin-O-glycosides, as well as three chlorogenic acid analogues.

Table of Contents

ABSTRACT ii

LIST OF ABBREVIAIONS AND SYMBOLS vi

LIST OF FIGURES ix

LIST OF TABLES xvii

ACKNOWLEDGEMENTS xviii

DECLARATION xix

CHAPTER 1 1

1. INTRODUCTION 1

1.1. Orientation of the study 1

1.2. Statement of the problem 1

1.3. Objectives of the research 1

1.4. Significance of the study 2

1.5. Limitations of the study 2

CHAPTER 2 3

2. LITERATURE REVIEW 3

2.1 *Helichrysum argyrosphaerum* 3

2.2 Flavonoids 6

2.3. Chlorogenic acids 13

2.4. Polyphenols/Phenolics 13

2.5. Terpenes 15

2.6. HPLC-UV-HRMS and NMR of flavonoids 15

CHAPTER 3 27

3. MATERIALS AND METHODS 27

3.1. Chemicals and Reagents 27

3.2. Instrumentation 27

3.3. Sample Collection and Processing 27

3.4. Preparation of Extracts 28

3.5. Phytochemical Screens 29

3.5.1. Anthraquinones 29

3.5.2. Anthranoids 29

3.5.3. Cardenolides/cardiac glycosides 30

3.5.4. Saponins 30

3.5.5. Terpenoids 30

3.5.6. Iridoids 31

3.5.7. Polyphenols 31

3.5.8. Alkaloids 32

3.6. HPLC method development 33

3.7. LC-MS Method development 34

3.8. Semi-preparative RPLC Method development 35

3.9 Sample analysis and data acquisition 35

CHAPTER 4 36

4. RESULTS AND DISCUSSIONS 36

4.1. Phytochemical screening 36

4.2. HPLC method development 38

4.2.1. Development of a RPLC method 39

4.2.2. Development of the HILIC method 40

4.3. LC-MS method development 40

4.3.1. Development of the RPLC-MS method 44

4.3.2. Development of the HILIC-MS method 44

4.3.3. Semi-preparative RPLC 47

4.4. Identification of the major constituents in the MeOH extract of the flowers of *H. argyrosphaerum*. 56

4.4.1. Flavonoids 60

4.4.1.1 Apigenin and apigenin glycosides 60

4.4.2. Chlorogenic acids 74

CHAPTER FIVE 83

5. CONCLUSIONS 83

RECOMMENDATIONS 85

REFERENCES 86

APPENDIX 1: Apigenin glycosides commonly found in nature 94

APPENDIX 2: Research permission letter 95

APPENDIX 3: Ethical clearance certificate 96

LIST OF ABBREVIAIONS AND SYMBOLS

$[M+H]^+$	-	precursor ion or pseudo-molecular ion
λ	-	wavelength
AAc	-	ammonium acetate
ACN	-	acetonitrile
AF	-	ammonium formate
APCI	-	atmospheric pressure chemical ionisation
ca.	-	*circa* (approximately)
CGA	-	chlorogenic acid
CQA	-	caffeoylquinic acid
CoQA	-	coumaroylquinic acid
Da.	-	Dalton
DAD	-	diode array detector
DCM	-	dichloromethane
DNP	-	dictionary of natural products
EDA	-	effected directed analysis
ESI	-	electron spray ionisation
F1	-	initial flow rate

F2	-	final flow rate
FA	-	formic acid
FQA	-	feruloylquinic acid
G1	-	initial gradient time
G2	-	final gradient time
GC	-	gas chromatography
HILIC	-	hydrophilic interaction liquid chromatography
HPLC	-	high performance liquid chromatography
HRMS	-	high resolution mass spectrometry
LC-MS	-	HPLC coupled with MS
m/z	-	mass to charge ratio
MeOH	-	methanol
MIC	-	minimum inhibition concentration
MS	-	mass spectrometry
MS/MS	-	tandem mass spectrometry
MS^n	-	tandem mass spectrometry involving multiple fragmentation steps
NIST	-	National Institute of Standards and Technology (U.S)
NMR	-	nuclear magnetic resonance

NPLC	-	normal phase liquid chromatography
PDA	-	photo diode array
RPLC	-	reverse phase liquid chromatography
TIC	-	total ion chromatogram
TOF	-	time of flight
TWC	-	total wavelength chromatogram
UPLC	-	ultra performance liquid chromatography
UV	-	ultraviolet
UV-vis	-	ultraviolet to visible range

LIST OF FIGURES

Figure 2.1 *Helichrysum argyrosphaerum* (Photo: Taonga Namate, Instrumental analysis Laboratory, University of Namibia).

Figure 2.2 Distribution of Namibia's *Helichrysum* species (*H. tomentosulum*, *H. argyrosphaerum*, *H. roseo-niveum*, *H. zeyheri* and *H. herniarioides*).

Figure 2.3 Different groups of flavonoids and their backbone structures.

Figure 2.4 Basic structure of Flavonoids.

Figure 2.5 Common sugar moieties found in flavonoids.

Figure 2.6 Disaccharides found in flavonoids.

Figure 2.7 The structure of an O-neohesperidose.

Figure 2.8 Flavonoids isolated from *Helichrysum* species.

Figure 2.9 Structures of 5-caffeoylquinic acid and 5-feruloylquinic acid.

Figure 2.10 Acetoxytremetone isolated from *H. italicum*.

Figure 2.11 Some phenolics and a diterpene found in *Helichrysum species*.

Figure 2.12 Pelargonidin (an example of anthocyanidins).

Figure 2.13 The B-ring cinnamoyl system.

Figure 2.14 Delphinidin-glycoside structure versus quercetin-glycoside structure.

Figure 2.15 Fragmentation of a flavonoid glycoside illustrated on apigenin-7-O-rutinoside.

Figure 4.1 LC-UV chromatogram obtained at 280 nm for the RPLC analysis of the MeOH extract of the leaves of *H. argyrosphaerum* using a gradient time

of 40 minutes and a mobile phase containing 0.1 % FA in 5 % MeOH (phase A)/0.1 % FA in MeOH (phase B).

Figure 4.2 LC-UV chromatogram obtained at 280 nm for the RPLC analysis of the MeOH extract of the leaves of *H. argyrosphaerum* using a gradient time of 60 minutes and a mobile phase containing 0.1 % FA in 5 % MeOH (phase A)/0.1 % FA in MeOH (phase B).

Figure 4.3 LC-UV chromatogram obtained at 280 nm for the RPLC analysis of the MeOH extract of the stems of *H. argyrosphaerum* using a gradient time of 40 minutes and a mobile phase containing 0.1 % FA in 5 % MeOH (phase A)/0.1 % FA in MeOH (phase B).

Figure 4.4 LC-UV chromatogram obtained at 280 nm for the RPLC analysis of the MeOH extract of the stems of *H. argyrosphaerum* using a gradient time of 40 minutes and a mobile phase containing 0.1 % FA in 5 % ACN (phase A)/0.1 % FA in ACN (phase B).

Figure 4.5 LC-UV chromatogram obtained at 280 nm for the RPLC analysis of the MeOH extract of the flowers of *H. argyrosphaerum* using a gradient time of 40 minutes and a mobile phase containing 0.1 % FA in 5 % MeOH (phase A)/0.1 % FA in MeOH (phase B).

Figure 4.6 LC-UV chromatogram obtained at 280 nm for the RPLC analysis of the MeOH extract of the flowers of *H. argyrosphaerum* using a gradient time of 40 minutes and a mobile phase containing 1 % FA in 5 % MeOH (phase A)/1 % FA in MeOH (phase B).

Figure 4.7 LC-UV chromatogram obtained at 280 nm for the HILIC analysis of the MeOH extract of the flowers of *H. argyrosphaerum* using a gradient

time of 30 minutes and a mobile phase containing 5 mM AAc in 5 % ACN (phase A)/5 mM AAc in ACN (phase B).

Figure 4.8 LC-UV chromatogram obtained at 280 nm for the RPLC analysis of the MeOH extract of the leaves of *H. argyrosphaerum* using a gradient time of 16 minutes and a mobile phase containing 0.1 % FA in 5 % MeOH (phase A)/0.1 % FA in MeOH (phase B).

Figure 4.9 LC-UV chromatogram obtained at 280 nm for the RPLC analysis of the MeOH extract of the leaves of *H. argyrosphaerum* using a gradient time of 30 minutes and a mobile phase containing 0.1 % FA in 5 % MeOH (phase A)/0.1 % FA in MeOH (phase B).

Figure 4.10 LC-UV chromatogram obtained at 280 nm for the HILIC analysis of the MeOH extract of the leaves of *H. argyrosphaerum* using a gradient: 100→50 % B (8 min). Using a mobile phase consisting of 5 mM of AF in water with 5% ACN (phase A)/ 5 mM of AF in water with 95 % ACN (phase B). A Phenomenex Luna HILIC column was used.

Figure 4.11 LC-UV chromatogram obtained at 280 nm for the HILIC analysis of the MeOH extract of the leaves of *H. argyrosphaerum* using a gradient: 100→50 % B (20 min). Using a mobile phase consisting of 5 mM of AF in water with 5% ACN (phase A)/ 5 mM of AF in water with 95 % ACN (phase B). A Phenomenex Luna HILIC column was used.

Figure 4.12 LC-UV chromatogram obtained at 280 nm for the HILIC analysis of the MeOH extract of the leaves of *H. argyrosphaerum* using a gradient: 100→60 % B (20 min). Using a mobile phase consisting of 5 mM of

AF in water with 5% ACN (phase A)/ 5 mM of AF in water with 95 % ACN (phase B). A Phenomenex Luna HILIC column was used.

Figure 4.13 LC-UV chromatogram obtained at 280 nm for the HILIC analysis of the MeOH extract of the leaves of *H. argyrosphaerum* using a gradient: 100→65 % B (20 min). Using a mobile phase consisting of 5 mM of AF in water with 5 % ACN (phase A)/ 5 mM of AF in water with 95 % ACN (phase B). A Phenomenex Luna HILIC column was used.

Figure 4.14 LC-UV chromatogram obtained at 280 nm for the HILIC analysis of the MeOH extract of the leaves of *H. argyrosphaerum* using a gradient: 100→80 % B (20 min). Using a mobile phase consisting of 5 mM of AF in water with 5% ACN (phase A)/ 5 mM of AF in water with 95 % ACN (phase B). A Phenomenex Luna HILIC column was used.

Figure 4.15 LC-UV chromatogram obtained at 280 nm for the HILIC analysis of the MeOH extract of the leaves of *H. argyrosphaerum* using a gradient: 100→80 % B (20 min). Using a mobile phase consisting of 5 mM of AF in water with 5% ACN (phase A)/ 5 mM of AF in water with 95 % ACN (phase B). An Xbridge BEH Amide HILIC column was used.

Figure 4.16 LC-UV chromatogram obtained at 280 nm for the HILIC analysis of the MeOH extract of the leaves of *H. argyrosphaerum* using a gradient: 100→60 % B (20 min). Using a mobile phase consisting of 5 mM of AF in water with 5% ACN (phase A)/ 5 mM of AF in water with 95 % ACN (phase B).An Xbridge BEH Amide HILIC column was used.

Figure 4.17 LC-UV chromatogram obtained at 280 nm for the HILIC analysis of the MeOH extract of the leaves of *H. argyrosphaerum* using a gradient:

100→70 % B (20 min). Using a mobile phase consisting of 5 mM of AF in water with 5% ACN (phase A)/ 5 mM of AF in water with 95 % ACN (phase B). An Xbridge BEH Amide HILIC column was used.

Figure 4.18 LC-UV chromatogram obtained at 280 nm for the HILIC analysis of the MeOH extract of the leaves of *H. argyrosphaerum* using a gradient: 100→80 % B (20 min), 20 % A isocratic (8 min). Using a mobile phase consisting of 5 mM of AF in water with 5% ACN (phase A)/ 5 mM of AF in water with 95 % ACN (phase B). A 2.5 µm Xbridge BEH Amide column was used.

Figure 4.19 LC-UV chromatogram of the semi-preparative RPLC analysis of the MeOH extracts of the flowers of *H. argyrosphaerum* observed at 280 nm using a gradient: 100 % A to 100 % B in 70 minutes using a mobile phase consisting of 0.1 % FA in 5 % MeOH (phase A)/ 0.1 % FA in MeOH (phase B) for the isolation of compounds **1**-**7**.

Figure 4.20 LC-UV chromatogram of the semi-preparative RPLC analysis of the MeOH extracts of the flowers of *H. argyrosphaerum* observed at 280 nm using a gradient: 100 % A to 100 % B in 45 minutes using a mobile phase consisting of 0.1 % FA in 5 % MeOH (phase A)/ 0.1 % FA in MeOH (phase B) for the isolation of compounds **1**-**7**.

Figure 4.21 TWCs of the RPLC-UV-MS analysis of the isolated compounds **1**, **2**, **5** and **6** detected in the *H. argyrosphaerum* MeOH extract of the flowers.

Figure 4.22 TWC of the RPLC-UV-MS analysis of the *H. argyrosphaerum* MeOH extracts of the stems, leaves and flowers recorded in positive ionisation mode using the optimised RPLC-MS method.

Figure 4.23 TIC of the RPLC-UV-MS analysis of the *H. argyrosphaerum* MeOH extracts of the stems, leaves and flowers recorded in positive ionisation mode the optimised RPLC-MS method.

Figure 4.24 TWC of the HILIC-UV-MS analysis of the *H. argyrosphaerum* MeOH extracts of the stems, leaves and flowers recorded in positive ionisation mode using the optimised HILIC-MS method.

Figure 4.25 TIC of the HILIC-UV-MS analysis of the *H. argyrosphaerum* MeOH extracts of the stems, leaves and flowers recorded in positive ionisation mode of the optimised HILIC-MS method.

Figure 4.26 UV-vis spectra of compounds **3**-**7**, the major flavonoids detected in the MeOH extract of the flowers of *H. argyrosphaerum.*

Figure 4.27 UV-vis spectrum (A), MS spectrum (B) and MS/MS spectrum (C) of compound **7**, tentatively identified as apigenin in the MeOH extract of the flowers of *H. argyrosphaerum*.

Figure 4.28 Proposed MS/MS fragmentation reactions of apigenin.

Figure 4.29 UV-vis spectrum (A), MS spectrum (B) and MS/MS spectrum (C) of compound **5** tentatively identified as apigenin-7-O-β-D-glucoside-[6”-O-(4-Carboxy-3-hydroxy-3-methylbutanoyl)] in the MeOH extract of the flowers of *H. argyrosphaerum*.

Figure 4.30 Compound **5** is tentatively identified as apigenin-7-O-β-D-glucoside-[6”-O-(4-carboxy-3-methylbutanoyl)]. The cleavage of its O-glycosidic bond to produce its most abundant product ion (Y_0) observed at *m/z* 271.

Figure 4.31 UV-vis spectrum (A), MS spectrum (B) and MS/MS spectrum (C) of compound **6**, tentatively identified as an apigenin-7-O-diglycoside in the MeOH extract of the flowers of *H. argyrosphaerum*.

Figure 4.32 UV-vis spectrum (A), MS spectrum (B) and MS/MS spectrum (C) of compound **3**, tentatively identified as apigenin-7-O-galacturonopyranoside or apigenin-7-O-glucuronopyranoside in the MeOH extract of the flowers of *H. argyrosphaerum*.

Figure 4.33 Apigenin-7-O-glycosides with sugar acids as the sugar moieties that are possible structures of compound **3**.

Figure 4.34 UV-vis spectrum (A), MS spectrum (B) and MS/MS spectrum (C) of compound **4**, tentatively identified as apigenin-4'-O-glucopyranoside in the MeOH extract of the flowers of *H. argyrosphaerum*.

Figure 4.35 The possible chemical structures of compound **4**, apigenin-4'-O-α/β-D-glycoside.

Figure 4.36 TWCs of the RPLC-UV-MS analysis of the polyphenol standards against the MeOH extract of the flowers of *H. argyrosphaerum* reported in positive ionisation mode using a mobile phase containing 0.1 % FA in 5 % MeOH over a gradient of 30 minutes.

Figure 4.37 UV-vis spectra (A) and the MS^E spectra (B) of the chlorogenic acid standard and compound **1**, identified as chlorogenic acid in the MeOH extract of the flowers of *H. argyrosphaerum*.

Figure 4.38 The MS spectrum of compound **1**, identified as chlorogenic acid in the MeOH extract of the flowers of *H. argyrosphaerum*.

Figure 4.39 The chemical structure of compound **1**, chlorogenic acid.

Figure 4.40 UV-vis spectra of compounds **1**, **2** and **8**.

Figure 4.41 The MS spectrum (A) and MS^E spectrum (B) of compound **2**, tentatively identified as 1'→3-Lactone-4,5-di-O-caffeoylquinic acid in the MeOH extract of the flowers of *H. argyrosphaerum*.

Figure 4.42 The MS spectrum (A) and MS^E spectrum (B) of compound **8**, tentatively identified as a derivative of feruloylquinic acid in the MeOH extract of the flowers of *H. argyrosphaerum*.

Figure 4.43 1'→3-Lactone-4,5-di-O-caffeoylquinic acid.

Figure 4.44 Feruloylquinic acid.

LIST OF TABLES

Table 3.1 Extracts produced from different plant parts of *H. argyrosphaerum*.

Table 4.1 Phytochemical screens of the finely ground plant material of the different plant parts of *H. argyrosphaerum*.

Table 4.2 Major compounds tentatively identified in the methanol extract of the flowers of *H. argyrosphaerum*.

ACKNOWLEDGEMENTS

Firstly, I would like to extend my gratitude to The Almighty through him all things are made possible including this, my research project. Secondly, I would like to thank the following people and institutes; The National Commission of Research Science and Technology (NCRST) of Namibia, The National Research Fund (NRF) of South Africa and The University of Namibia Research and Publication Committee (URPC/2013/012) for their financial support, my knowledgeable and hardworking supervisors Dr. Louw (main supervisor) and Dr. Hans (co-supervisor)) for their guidance and encouragement through which we achieved good results in the end, The University of Namibia for their permission to carry out this project and to use their facilities (Laboratories and HPLC), Stellenbosch University for the permission to use their instruments (UPLC and LC-MS). I would also like to thank my collaborating team of Prof. André de Villiers, Dr. Marietjie Aletta Stander and Dr. Kathithileni M. Kalili for their guidance and respective contributions. I am so grateful for my mother (Mrs. Mary Gurure) for her motivation, my girlfriend (Miss Peo Baitsile) for her unwavering support and my grandmother (Mrs. Emily Gusha) for her prayers and believing in me. For financial support and providing for me, I thank my father (Mr. Nikowa Namate) and my step-mother (Mrs. Davidzo Namate). Last but not least, I thank all my family members and friends for their motivation and encouragement throughout the period of my research.

DECLARATION

I, Taonga Moffat Namate, hereby declare that this study is a true reflection of my own research, and that this work, or part thereof has not been submitted for a degree in any other institution of higher education.

No part of this thesis may be reproduced, stored in any retrieval system, or transmitted in any form, or by any means (e.g., electronic, mechanical, photocopying, recording or otherwise) without the prior permission of the author, or The University of Namibia on behalf of the author.

I, Taonga Moffat Namate, grant The University of Namibia the right to reproduce this thesis in whole or in part, in any manner or format, which The University may deem fit, for any person or institution requiring it for study and research; provided that The University of Namibia shall waive this right if the whole thesis has been or is being published in a manner satisfactory to the University.

Signature…… Date……..

CHAPTER 1

1. INTRODUCTION

1.1. Orientation of the study

Species of the genus *Helichrysum* species are widely used in Southern African traditional medicine (1). Although *H. argyrosphaerum* and *H. cephaloideum* are known to cause the poisoning of livestock (1,2), generally *Helichrysum* species are not known to cause poisoning in humans (3). In fact, most of the *Helichrysum* species including *H. argyrosphaerum* display antibacterial and antifungal activities (1,4). A number of different classes of chemical compounds have been isolated from many *Helichrysum* species (1,5–7). However, no studies have been performed to investigate the chemical composition of *H. argyrosphaerum* (1). The main aim of this study was to identify the major metabolites of *H. argyrosphaerum* that may be bioactive.

1.2. Statement of the problem

Although it was determined that *H. argyrosphaerum* display antibacterial and antifungal activity, the compound(s) that may be responsible for the bioactivity have not yet been identified (1,4). In addition, the chemical composition of *H. argyrosphaerum* has never been studied before.

1.3. Objectives of the research

The primary objective was to elucidate the chemical structures of the major compounds using a combination of high pressure liquid chromatography – ultraviolet spectroscopy – high resolution tandem mass spectrometry (HPLC-UV-HRMS/MS). The secondary objectives were to develop a suitable HPLC method that can be used for the HPLC-UV-HRMS/MS analysis as well as a semi-preparative high performance

liquid chromatography method (semi-prep HPLC) unique to this plant species, that will facilitate the isolation of all major constituents of the relevant plant extracts if further characterisation by NMR would be needed.

1.4. Significance of the study

This study will be the first of its kind to provide information on the chemical composition of *H. argyrosphaerum*. The bioactive compounds responsible for antibacterial and antifungal activities may be useful as possible new leads that may be used to develop better antibiotics and antifungals (or chemotherapeutic agents) in future.

1.5. Limitations of the study

The plants are seasonal and they do not flower throughout the year giving a restricted time frame for the collection of the samples, therefore it was necessary to collect large amounts of samples and carefully preserve the collected samples. This plant has not yet been extensively studied, and the chemistry has never been studied before, therefore providing a challenge in finding information on it.

CHAPTER 2

2. LITERATURE REVIEW

2.1 *Helichrysum argyrosphaerum*

Figure 2.1: *Helichrysum argyrosphaerum* (Photo: Taonga Namate, Instrumental Analysis Laboratory, University of Namibia).

H. argyrosphaerum (Figure 2.1) belongs to the daisy (*Asteraceae*) family under the genus, *Helichrysum*, which comprises of 1,699 species (8). The plant is commonly known as 'Wild/rosebud everlasting', 'Silver head' or 'Sewejaartjie' (1,9,10). Plants under this genus are widely distributed in Angola, Botswana, Namibia (Figure 2.2), Malawi, Mozambique, Zambia, Zimbabwe, Lesotho and South Africa (10). The plants from this genus prefer hot, dry and sandy habitats, but can often grow in stony and sometimes moist places. *Helichrysum* species are commonly found on disturbed grounds (roadsides, cultivated land and along railway lines) and they may become abundant on overgrazed areas (9,11).

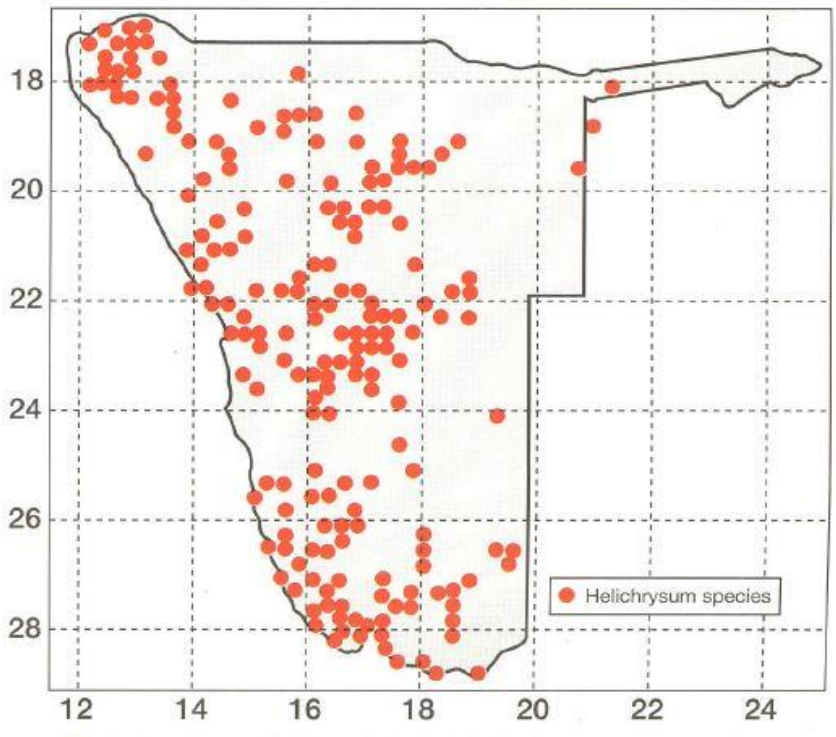

Figure 2.2: Distribution of Namibia's *Helichrysum* species (*H. tomentosulum*, *H. argyrosphaerum*, *H. roseo-niveum*, *H. zeyheri* and *H. herniarioides*) (9).

H. stoechas, *H. armenium*, *H. caespititium* and *H. plicatum* are medicinal plants from the genus, *Helichrysum*, whose methanol extracts were found to have cytogenetic effects on human lymphocyte cultures, their inhibitory effects on the mitotic index and replication index indicated that they can have genotoxic and mutagenic effects as well (5,12). *Helichrysum italicum* is one of the most investigated medicinal plants from this genus that is used as a traditional remedy for the treatment of intestinal complaints and are used as herbal tea for treating digestive, stomachic and intestinal diseases (13). The smoke of *H. caespititium* is inhaled by the Southern Sotho people for relief of head and chest colds and they also use it as a dressing for open wounds during circumcision rites (5). *H. caespititium* is used in the treatment of gonorrhoea by the Bakwena and Bakgatla people (4). The smoke of *H. aureonitens* is inhaled in order to induce trances

or invoke the goodwill of the ancestors (1). *H. cochleariforme* is drunk for the treatment of infections of the respiratory tract and the leaves of *H. appendiculatum* are used as wound dressings (1). Traditional uses of *H. argyrosphaerum* have not yet been found but its antibacterial and antifungal activities were determined *in vitro* (1,4).

H. argyrosphaerum was found to inhibit the growth of gram-positive bacteria (*Bacillus pumilus, Bacillus subtilis, Micrococcus kristinae, and Staphylococcus aureus*) and gram-negative bacteria (*Pseudomonas aeruginosa*) at minimum inhibition concentrations (MICs) of 1.00 mg/mL shaken and homogenised polar extracts (4). This plant also inhibited the growth of fungi (*Aspergillus flavus*, *Aspergillus niger*, *Cladosporium sphaerospermum* and *Phytophthora capsici*) at MICs of 1.00 mg/mL in shaken extracts (4), homogenised extracts did not inhibit growth. Although *H. argyrosphaerum* has been found to have antibacterial and antifungal activities, it has also been found to induce poisoning in ruminants causing amaurosis (blindness without visible change in the eye), paresis and paralysis (2,11,14). Blindness, paresis, and paralysis in sheep and cattle grazing on pastures where the *H. argyrosphaerum* DC. (*Asteraceae*) is abundant has been reported in Namibia (11).

Some species of the genus, *Helichrysum*, were studied further leading to the isolation and characterisation of their active compounds. An acylated phloroglucinol of *H. caespititium* was isolated, characterised and tested for antimicrobial activity (5). An acetophenone derivative isolated from *H. italicum* was tested for bioactivity in relation to the plant (6). In the review done by Lourens and colleagues (1), classes of isolated chemical compounds such as flavonoids, phloroglucinols, pyrones and terpenoids from most *Helichrysum* species were reported except those of *H. argyrosphaerum*.

2.2 Flavonoids

Flavonoids are an extensive family of phytochemicals and they are the most common and widely distributed group of plant phenolic compounds with a wide range of biological functions that include antioxidant, antibacterial, anticancer, antiviral, anti-inflammatory and hepatoprotective activities (15,16). They are plant secondary metabolites, which have been subjected to considerable scientific research for decades because of their occurrence, therapeutic importance and because they are vital for normal growth, development and defence mechanisms in plants (17). Interest in their analysis has increased due to their recognized physiological activities in humans and numerous studies have related the ingestion of polyphenols to lower the likelihood of developing cardiovascular diseases and cancers (15). The contribution of phenolics including quercetin and its derivatives (that provide cardio-protective benefits observed with the consumption of red wine) to the 'French Paradox' proved influential in stimulating further research in flavonoids and their contribution to the human diet (18,19). Flavonoids are considered to be one of the biggest classes of antibacterial compounds (1,20) and also one of the largest anti-staphylococcal classes of metabolites (20). Apigenin and luteolin are examples of flavonoids that have been reported to have activities against *Staphylococcus aureus* and its methicillin resistant strains with minimum inhibition concentrations recorded at 3.90-62.50 µg/mL (20). Flavonols and flavones are flavonoids (Figure 2.3) that are important in food components since they have been found to exhibit antioxidant activities (21). Apart from their beneficial properties in foods as nutraceuticals, polyphenols are also chemotaxonomic markers due to their specificity and ubiquity, and they have been proven to be chemical markers for food authentication (15).

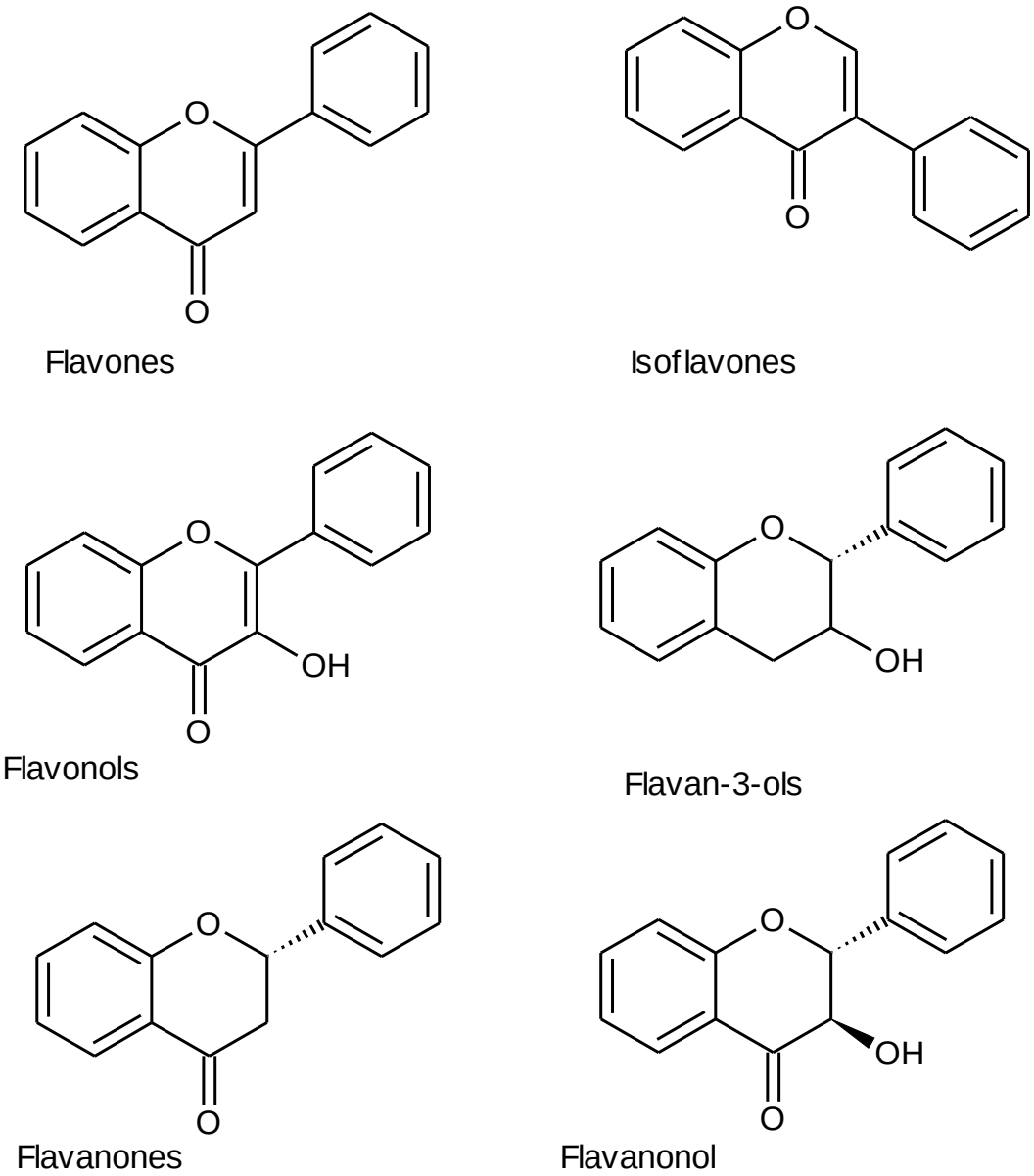

Figure 2.3: Different groups of flavonoids and their backbone structures (16).

Chemically flavonoids are characterised by a fifteen-carbon skeleton consisting of two benzene rings A and B linked via a heterocyclic pyrane ring C (Figure 2.4). The various classes of flavonoids differ in the level of oxidation and pattern of substitution of the C ring, while individual compounds within a class differ in the pattern of substitution of the A and B rings (Figure 2.4). Available reports tend to show that secondary metabolites of phenolic nature including flavonoids are responsible for the variety of

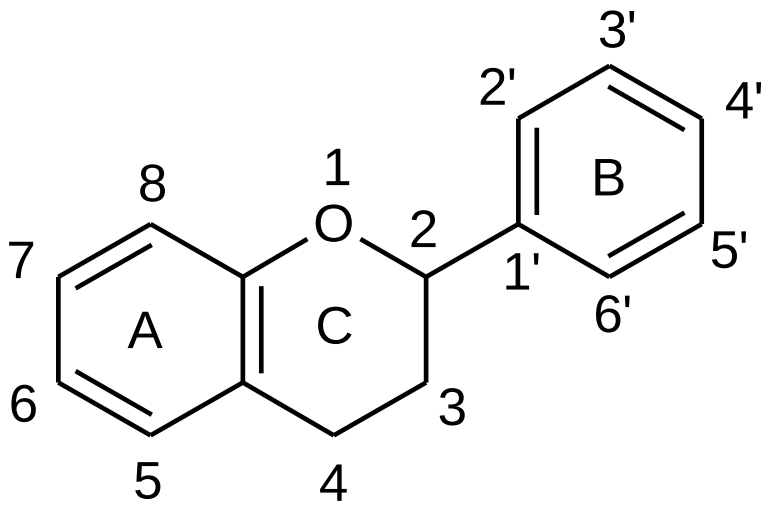

Figure 2.4: Basic structure of Flavonoids (16).

pharmacological activities as previously highlighted. In plants, flavonoids may occur in various forms corresponding to additional hydroxylation, methylation and glycosylation (15). Flavonoids occur in nature as aglycones, glycosides, and methylated derivatives (16). A glycoside can be any of a wide variety of naturally occurring substances in which a carbohydrate portion, consisting of one or more sugars or uronic acid (i.e., a sugar acid), is combined with a compound, in this case an aglycon, containing a hydroxyl group. The compound containing a hydroxyl group, usually a non-sugar entity (aglycon), such as a derivative of phenol or an alcohol, may also be another carbohydrate, as in cellulose, glycogen, or starch, which consist of many glucose monomers (22). Flavonoids commonly occur as flavonoid *O*-glycosides, in which one or more hydroxyl groups of the aglycone are bound to a sugar entity with formation of an acid labile glycosidic O–C bond (15,18). Flavones and flavonols are commonly found in plants in the form O-glycosides (23). Flavonoid-C-glycosides can also be found and they contain acid-resistant C-C bonds linking the sugar directly to the flavonoid nucleus (15,21). Glycosides are normally formed with the glycosidic

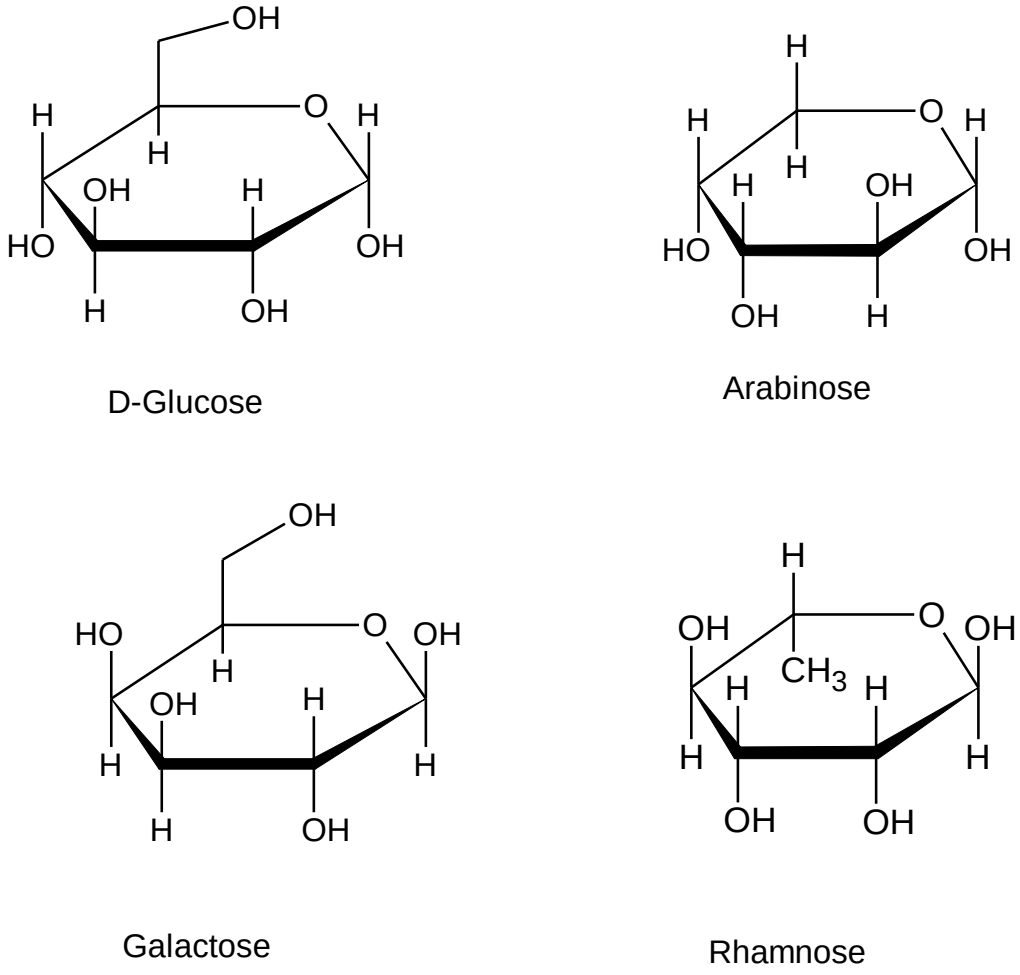

Figure 2.5: Common sugar moieties found in flavonoids.

linkage located in positions 3 or 7 (Figure 2.4) and the sugar moiety can be L-rhamnose, D-glucose, glucorhamnose, galactose, or arabinose (Figure 2.5) (16). Any of the hydroxyl groups can be glycosylated, but certain positions are more preferred/usual: for example, the 7-hydroxyl group in flavones and flavanones, the 3- and 7-hydroxyls in flavonols and flavan-3-ols are common glycosylation sites (15,18,21). The number of sugar rings that can be substituted on the aglycone varies from one to four (21). Glucose is the most commonly encountered sugar while galactose, rhamnose, xylose and arabinose are less common followed by mannose, fructose, glucuronic and galacturonic acids which are rare (15,18). Disaccharides

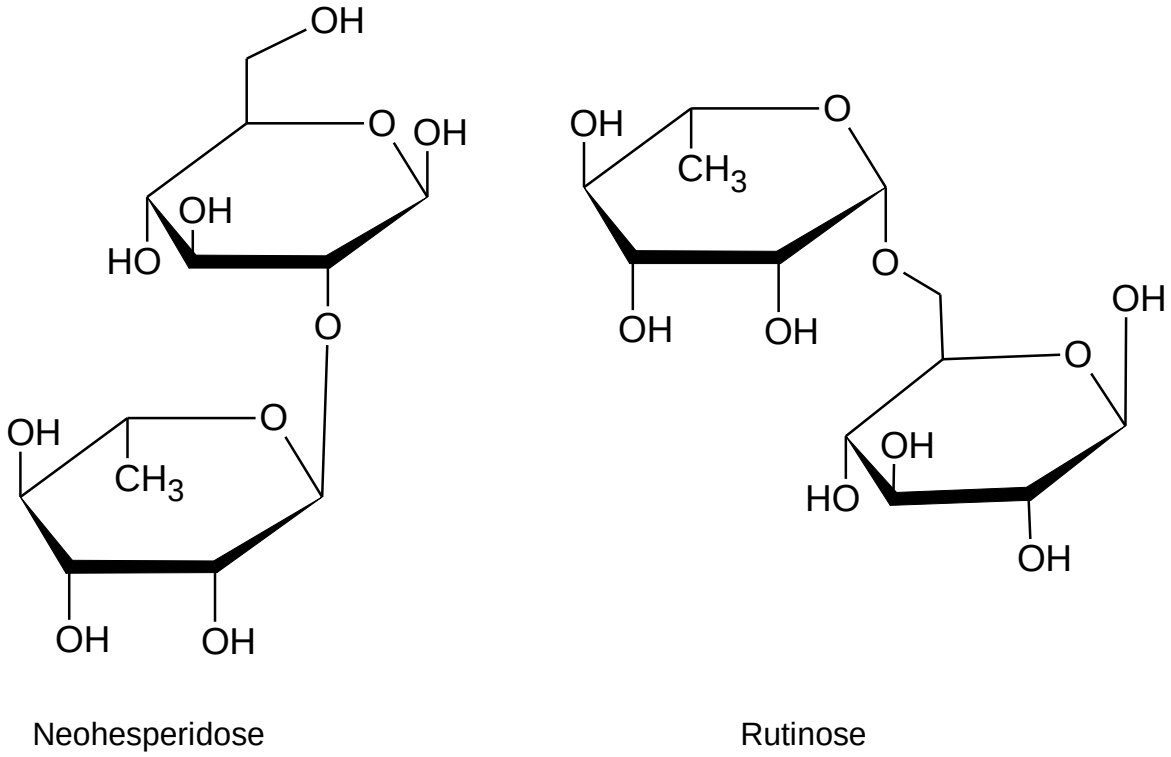

Figure 2.6: Disaccharides found in flavonoids.

(Figure 2.6) are also found in association with flavonoids, the most common ones being rutinose and neohesperidose (Figure 2.7), and occasionally, tri- or even tetra-saccharides are encountered (15,18). Acylated glycosides, in which one or more of the sugar hydroxyls are esterified with an acid also occur.

The flavonoids gnaphaliin and pinocembrin (Figure 2.8) were isolated from the methanol extract of *H. italicum* and were reported to have antimicrobial activities (6,24). Several flavonoids, isoastragalin, isosalipurposide, helichrysin A and B were isolated as the major constituents from the capitulums of *H. plicatum* (25). Also, apigenin, apigenin-7-glucoside, luteolin, naringenin and quercetin have been isolated from the capitulums of *H. compactum* and were shown to possess antioxidant activity (25). In addition, other different types of flavonoids and their derivatives have been found in *Helichrysum* species including, *H. tenuifolium*, *H. melanacme* and *H.*

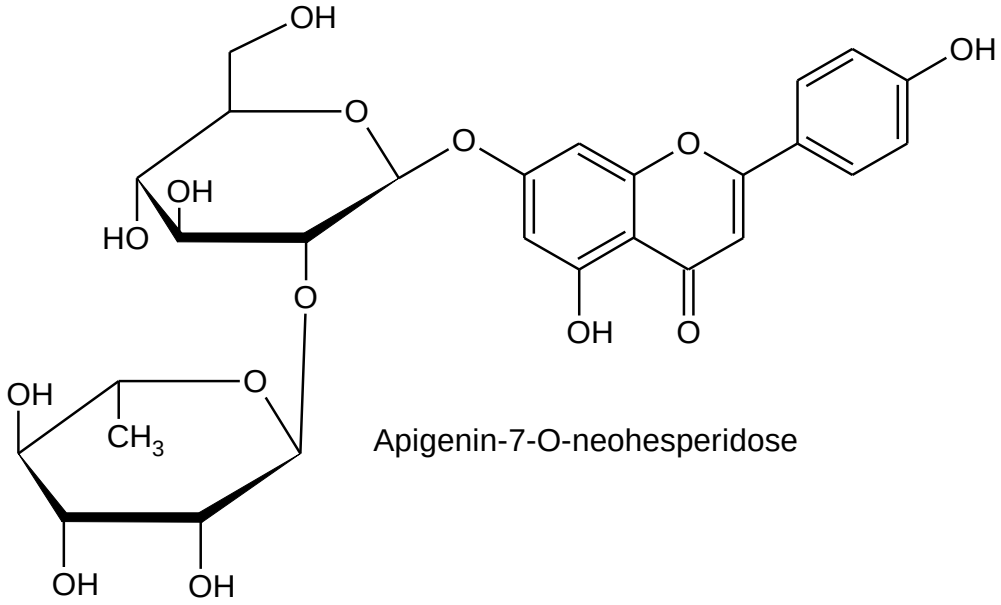

Figure 2.7: The structure of an O-neohesperidose.

cymosum (1). A phloroglucinol, 2-methyl-4-[2',4',6'-trihydroxy-3'-(2-methylpropanoyl)phenyl]but-2-enyl acetate, and an acetophenone derivative named gnaphaliol 9-O-propanoate were isolated from extracts of *H. caespititium* and *H. italicum* respectively, using HPLC (5,6). The phloroglucinol of *H. caespititium* was reported to have antibacterial and antifungal activities (5). However, antioxidant and anti-inflammatory activities of *H. italicum* have been attributed to the presence of flavonoids such as 4,2′,4′,6′-tetrahydroxychalcone-2′-glucoside, kaempferol-3-glucoside, naringenin-glycoside, gnaphaliin, pinocembrin and tiliroside which have been found active in assays of antioxidant and anti-inflammatory activities (6). *Helichrysum caespititium* was tested for antimicrobial activity which led to the isolation of an acylated phloroglucinol, 2-methyl-4-[2',4',6'-trihydroxy-3'-(2-methylpropanoyl) phenyl]but-2-enyl acetate, with significant biological activity against ten different gram-positive species of bacteria and six fungi species which were significantly inhibited at very low MIC values (5). Different *Helichrysum* species

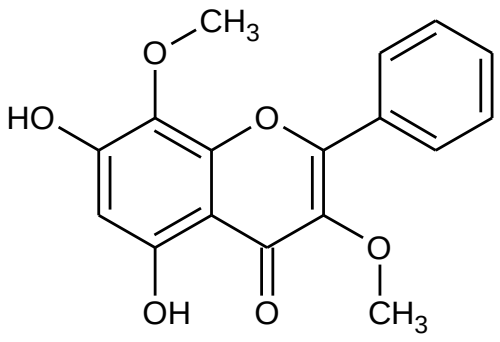

Gnaphaliin

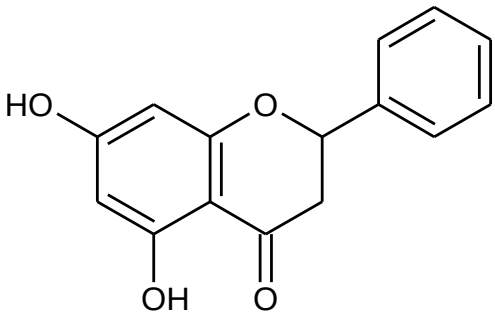

Pinocembrin

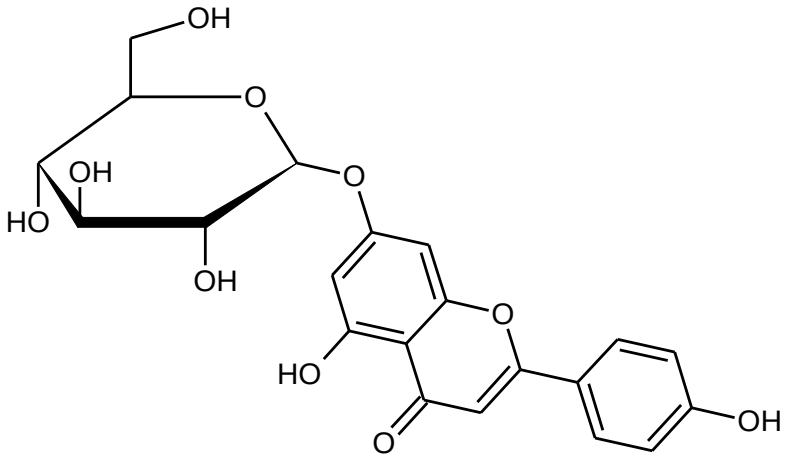

Apigenin-7-glucoside

Figure 2.8: Flavonoids isolated from *Helichrysum* species.

produce different secondary metabolites (acetophenones, flavonoids and phloroglucinols) as a biochemical defence mechanism (chemical barrier) against bacteria and fungi (5), thereby contributing to their antibacterial and antifungal properties.

2.3. Chlorogenic acids

Chlorogenic acids (CGAs) are natural antioxidants that form part of the most abundant polyphenols in the human diet (26,27). They are usually produced by plants as a part of the defence mechanism response against environmental stresses triggered by microbial pathogens, mechanical wounding and direct exposure to UV or visible light (26,28). CGAs are a large family of esters formed between quinic acid and one to four residues of certain trans-cinnamic acids (27,29,30). The cinnamic acids that are commonly encountered are caffeic, *p*-coumaric and ferulic acid which are precursors of *p*-coumaroylquinic (*p*CoQA), caffeoylquinic (CQA) and feruloylquinic acids (FQA) respectively (26). Typical CGA UV spectra display a λ_{max} of *ca.* 325 nm and they can be detected using LC-MS in both positive and negative ionisation modes (29). CGAs are found in various dietary sources including coffee, apples, citrus fruits, grapes, wines to name a few and many plant species from the family *Asteraceae* including lettuce, artichoke (*Cynara scolymus*), *Artemesia absinthium* and *A. vulgaris* (28). Two examples of these compounds are 5-caffeoylquinic acid (Figure 2.9) that was isolated from *Baccharis oxyodonta* and 5-feruloylquinic acid (Figure 2.9) that was detected and identified in *Moringa ovalifolia* (26,27). Chlorogenic acid was reported to be very abundant in the methanol extracts of various *Helichrysum* species including *H. compactum* (25).

2.4. Polyphenols/Phenolics

Acetophenones are non-flavonoid phenolics that are involved in biological activities of plants such as *H. italicum* (6). Six acetophenones were identified and isolated from *H. italicum* including a new gnaphaliol-9-O-propanoate and a known acetoxytremetone (6,31). Acetoxytremetone (Figure 2.10) was observed to be involved in the antioxidant effect of *H. italicum* and was reported to exert spasmolytic activity

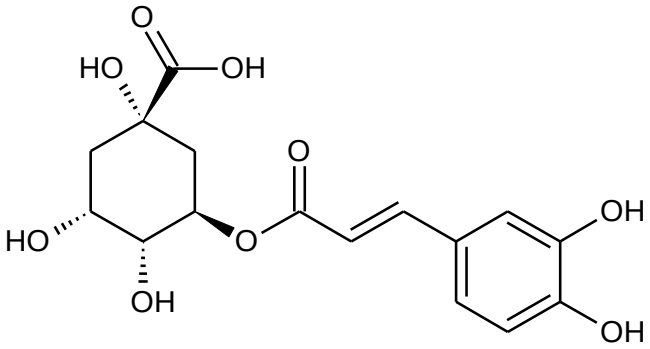

Caffeoylquinic acid

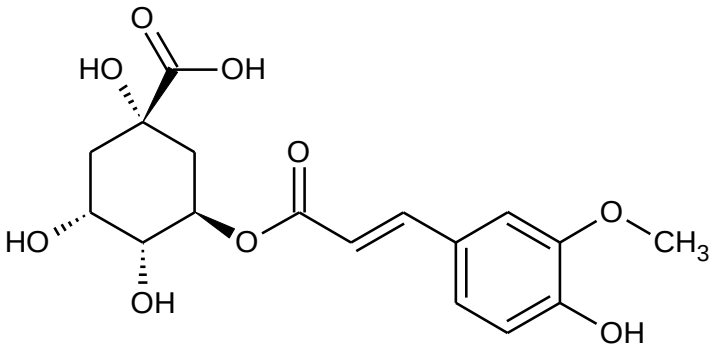

Feruloylquinic acid

Figure 2.9: Structures of 5-caffeoylquinic acid and 5-feruloylquinic acid (27,32).

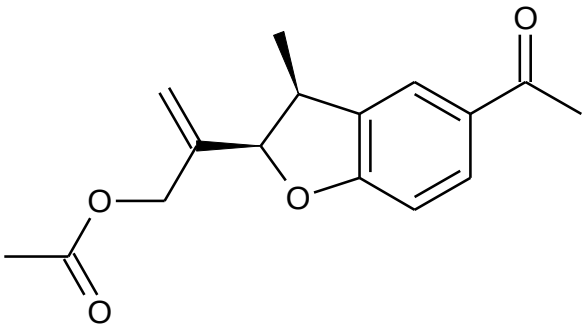

Acetoxytremetone

Figure 2.10: Acetoxytremetone isolated from *H. italicum* (6).

as well (6). However, no record was found reporting acetophenones of *H. argyrosphaerum* (1).

Other groups of phenolics (Figure 2.11) isolated from *Helichrysum* species include antimicrobial phloroglucinols, helihumulone and acylphloroglucinol, and a chalcone (2'-hydroxy-4',6'-dibenzyloxychalcone) from the flowers of *H. gymnocomum* (1,33,34). Coumaric acid was found in *H. obconicum* among other polyphenols including apigenin (35).

2.5. Terpenes

Terpenes are hydrocarbons that are built up from isoprene units (C_5H_8), named terpenoids when they are oxygenated derivatives, which widely occur in plants and animals (36). These compounds are abundant in essential oils of plants as diterpenes (e.g. vitamin A), monoterpenes or sesquiterpenes while triterpenes and tetraterpenes are also found in animals (36). Diterpenes have been reported to be very abundant in Australian *Helichrysum* species including *H. ambiguum* but not the case for South African species (7). A sesquiterpene aldehyde derivative of cadalene (Figure 2.11) is an example of one of many diterpenes that were isolated and identified from Australian *Helichrysum* species (7).

2.6. HPLC-UV-HRMS and NMR of flavonoids

The techniques that were employed in this study to elucidate chemical structures were HPLC-UV separation and detection, semi-preparative HPLC isolation of the compounds of interest from complex mixtures, followed by LC-MS analysis to elucidate their structures. NMR is the technique that will allow complete characterisation of the chemical structures of compounds of interest.

2.6.1 HPLC-UV

HPLC was first used for the determination of food flavonoids in 1976 by Fisher and Wheaton and the HPLC analysis of flavonoids was reviewed by Daigle and Conkerton in 1983 followed by an update to this review in 1988 (23). Although other methods of separation for the separation of flavonoids have been used, HPLC was by far the most widely used method by the end of the 90's (23). In general, acetonitrile and/or methanol are the mobile phases that have been used with reversed phase HPLC (RPLC) columns in combination with water containing an acid (23). These two commonly used organic modifiers (methanol and acetonitrile) in RPLC analysis of flavonoids have little direct effect on the ionisation of molecules, although nebulization efficiency will be affected by the percentage of the organic modifier in the mobile phase (18). Contemporary HPLC separation of flavonoids is exclusively performed using RPLC, with the exceptions of normal phase liquid chromatography (NPLC) used for oligomeric proanthocyanins and hydrophilic interaction chromatography (HILIC) (18).

The two driving forces behind improvements in HPLC, particularly in the HPLC analysis of flavonoids, are the need for shorter analysis times and higher resolution (18). Decreased analysis times are greatly appreciated especially in routine laboratories where a lot of samples need to be analysed on a daily bases, this is also very useful in cases where analytical data is needed within a short period of time and can result in cheaper analytical methods. It was discovered that ultra-high pressure liquid chromatography (UPLC) offers two advantages compared to conventional HPLC that are increased speed, achieved by shorter columns and high flow rates and increased efficiency, achieved by maintaining column lengths (18). The application of UPLC technology, in flavonoid HPLC analysis, is mainly to achieve faster separation

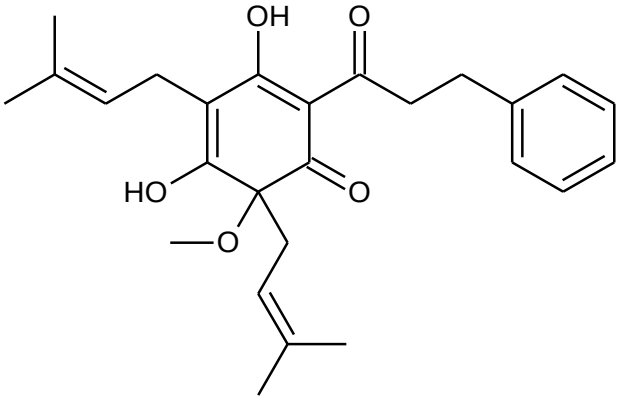

Helihumulone

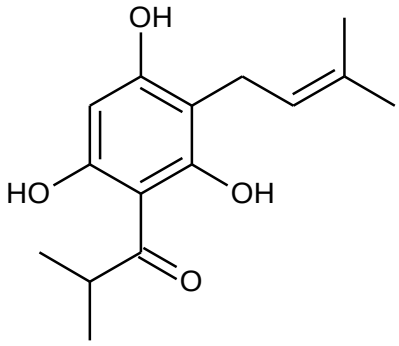

Acylphloroglucinol

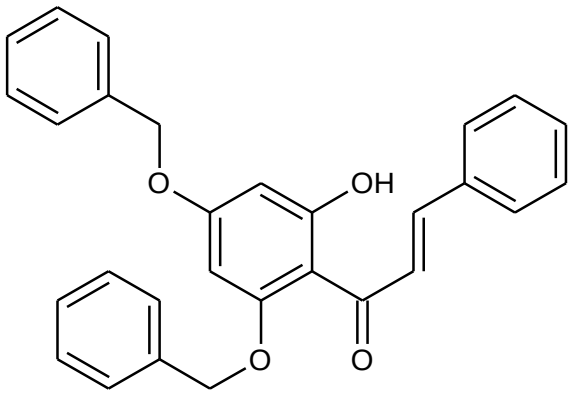

2'-hydroxy-4',6'-dibenzyloxychalcone

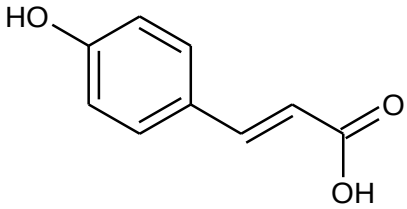

Coumaric acid

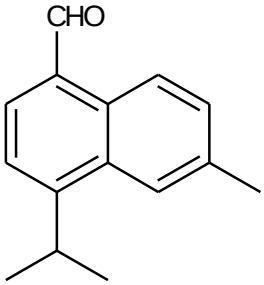

Aldehyde cadalene derivative

Figure 2.11: Some phenolics and a diterpene found in *Helichrysum* species.

and higher output (18). This is achieved in shorter analysis times for UPLC columns because the column is short and the optimal mobile phase linear velocity is high (18). HPLC is quite limited compared to traditional fractionation approaches (e.g. flash chromatography), due to its low sample capacity. However, it is possible to overcome this limitation to some degree by using semi-preparative HPLC (larger HPLC columns on the same instrumentation), which is carried out for preparative purposes and capable of purifying a significant quantity of a component of a mixture (37).

The major driving forces behind the interest in HILIC for flavonoid analysis is that it this separation mode offers an alternative separation mechanism to RPLC, which typically results in class–type separations of flavonoids according to the degree of glycosylation and/or acylation (18). RPLC chromatograms with detection at UV-370 nm have been reported to display released flavonoid aglycones, namely quercetin, kaempferol and apigenin in spinach aqueous extract after acid hydrolysis (21). RPLC was demonstrated to be very suitable for the separation of flavonoids based on the nature of the aglycone, oxidation state, substitution patterns, stereochemistry, the nature and degree of glycosylation as well as the nature and degree of acylation (18).

NPLC is not suitable for flavonoid analysis because of the limited solubility of these compounds in typical NPLC mobile phases with the few exceptions of apolar flavonoids such as polymethoxylated flavones and acetylated flavonoids (18). Besides ‘the extensively used’ RPLC, in recent years HILIC has been established as a complementary method. HILIC has been reported to be powerful for separating highly polar compounds that are usually not retained in RPLC, such as certain pharmaceuticals, organophosphorus pesticides and drugs of abuse (38), but RPLC is most often the mode of choice because of its compatible with MS and it achieves good performance for fast separations (18).

Method development for HPLC, extensively in industries such as the chemical, pharmaceutical, food industry clinical as well as environmental analysis, has become an essential task in the analytical laboratory of today (39). Method development is traditionally carried out on a single column with a given length and as a means to improve the quality of the separation the stationary phase, the mobile phase composition, and/or the temperature are varied (39). Whereas in this study column conditions were varied keeping the stationary phase constant. Since method development is such an important and time demanding task, a number of hardware and software tools have been developed to facilitate the development of a method such as a computer simulation software that predicts the outcome of either isocratic or gradient experiments as a function of changes in experimental conditions saving time and providing better resolution and shorter run times (39). In this study, the experimental conditions (HPLC and LC-MS) that were varied included mobile phase conditions and column conditions.

Studies on flavonoids by UV spectroscopy have revealed that most flavones and flavonols exhibit two major absorption bands: Band I (300–400 nm) represents the B ring absorption, while band II (240–285 nm) corresponds to the A ring absorption (17,18). Band I is more useful because it is specific and provides more selective information, since all flavonoids absorb in the region of 240-285 nm (17,18). Flavanones and flavones absorb intensely in the 270–280 nm region (band II), whereas in the 320–330 nm region (band I) flavones and flavonols show significant absorption (40). Flavanols, flavanones, dihydroflavonols and isoflavones exhibit only band II absorption (269–279 nm) because they lack conjugation between A and B rings (18). Flavonols and flavones show band I absorption between 300 and 380 nm, as an indication of their presence, whereas anthocyanidins (Figure 2.12) are easily

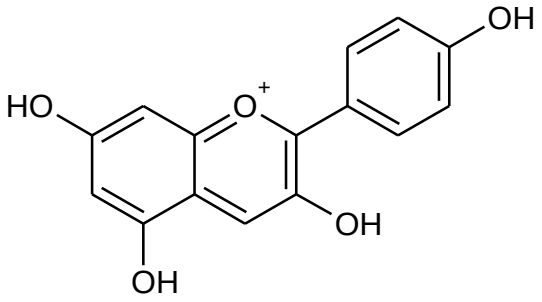

Pelargonidin

Figure 2.12: Pelargonidin (an example of anthocyanidins).

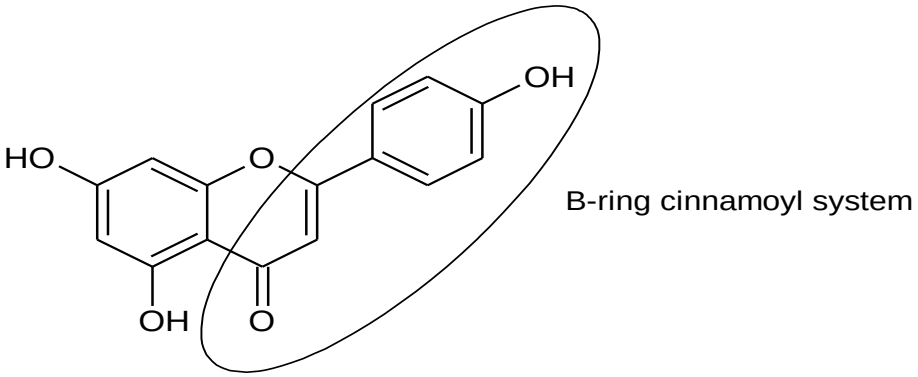

Figure 2.13: The B-ring cinnamoyl system.

distinguished by their band I absorption between 460 and 550 nm in the visible range (18). This significant difference may be attributed to the presence of a charge in the ring system (Figure 2.12) resulting in a high wavelength (low energy visible range) being observed. UV spectra (in the mobile phase: methanol-acidic water) of flavones and flavonols exhibit two major absorption peaks in the region 240–400 nm, commonly referred to as band I (300–380 nm) and band II (240–280 nm) (17,18). Band I was considered to be associated with the absorption by the B ring cinnamoyl system (Figure 2.13), and band II with the absorption by the A ring benzoyl system (15).

In the study by Abad-García *et al.*, (15), it was discovered that three different apigenin glycosides (Figures 2.7, 2.8 and 2.15) showed absorption bands at 267.3 nm which is the characteristic band I. UV spectra of flavonoids also helps with the characterisation of the substitution pattern of A and B rings. Additional hydroxyl groups in B or A rings cause bathochromic shifts of bands I or II since the lone pairs of the oxygen are delocalized into the conjugated ring system, therefore changing the amount of energy absorbed by the ring. Methylation of hydroxyl groups decreases this effect, especially if they are in a resonant position 4' (Figure 2.4). In addition to this effect, methylation has an important effect on the elution order due to the increase of apolarity of the methoxylated flavonoid (15). In the UV spectroscopy of flavone glycosides, it has been observed that *O*- and *C* glycosylation of ring A has little or no effect on their UV spectra, but glycosylation of ring B causes shifts of band I to lower wavelengths. Again this effect is more pronounced for a resonant position 4' than for a non-resonant position 3' (Figure 2.4) (15). However, it is impossible to detect and differentiate the type of glycosylation (*O*-, *C*- or *O*,*C*-) with the aid of UV-vis spectra only (15). Glycosylation and the nature of the sugar moiety do not have a significant effect on the absorbance spectra of most flavonoids. However, glycosylation at C-3 which causes ahypsochromic shift of 15–20 nm in absorption band I for flavonols and flavones is an exception (18). Irrespective of the phenolic subclass and type of glycosidic bond (C–C vs C–O), an increase in the degree of glycosylation (hence molecular weight) leads to a decrease in the optimal linear velocity (41). This suggests that flavonoids with a high degree of glycosylation will elute later than those with low degree of glycosylation.

Although some useful structural information e.g. the chemical class of flavonoids can be obtained based on UV-vis spectral properties, it is still important to use MS and

NMR for full characterisation since they provide more structural information (18). UV spectra can be used to distinguish between different classes of flavonoids as previously reported, this may sound trivial bur this information in many has proven to be pivotal e.g. several glycosylated flavonoids exhibit identical MS behaviours because they have identical molecular formulae and fragmentation patterns but belong to different flavonoid families (18). As an example, accurate mass MS cannot distinguish between two molecules with the same formula, delphinidin (an anthocyanin) and quercetin (flavonol) glycosides (Figure 2.14), unless high-collision energy CID experiments are performed since they have identical product ions (18). However, UV spectra of anthocyanins and flavonols are clearly distinct as described earlier and therefore allow facile assignment of the chemical class without additional experiments.

2.6.2 LC-HRMS

Single-stage MS in combination with UV detection is usually used in routine analytical applications to facilitate the confirmation of the identity of flavonoids in samples with the help of standards and reference data (17). However, tandem mass spectrometry (MS/MS or MS^n) is the preferred technique for the analysis of unknowns because of its capability to provide additional selectivity required for unambiguous identification (17). A wide range of detectors have been used in combination with HPLC separation to detect and/or identify flavonoids but by far the most common are diode array detectors (DAD) and MS (18). The structural analysis of flavonoids based on their UV spectra has recently been surpassed by more powerful tools (MS and NMR), however, useful information can still be obtained based on UV spectral properties, the most important being the chemical class of flavonoids (18). The diode array detector can be connected before other detectors such as MS (compatible with high mobile phase flow rates and provides extremely reliable quantification provided that co-elution of

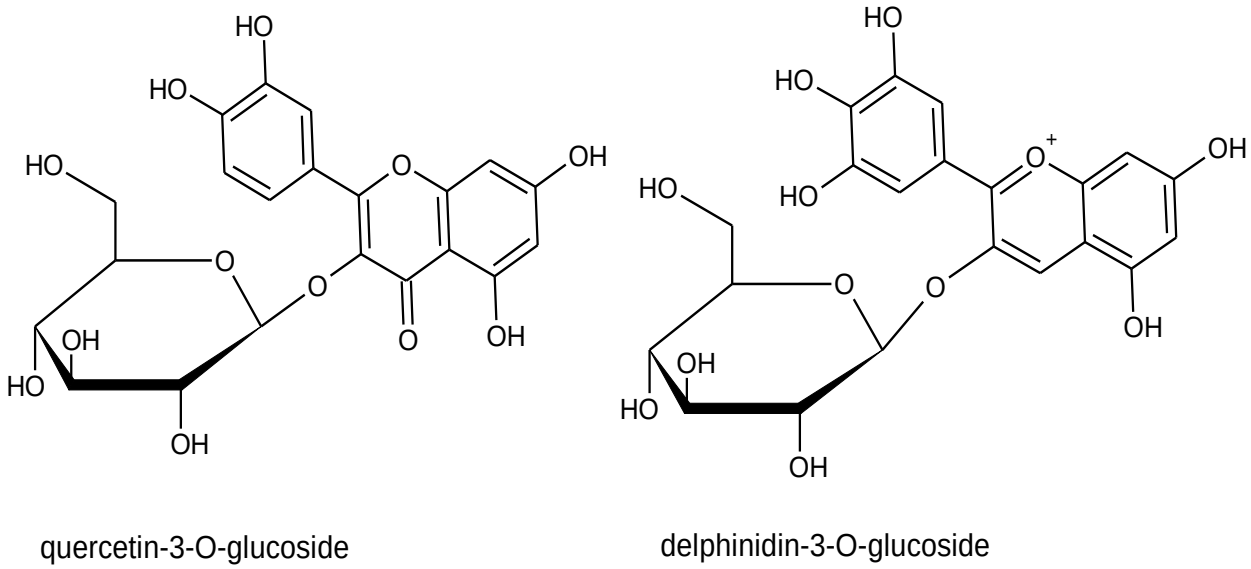

Figure 2.14: Delphinidin-glycoside structure versus quercetin-glycoside structure.

compounds with similar absorbance properties can be avoided), resulting in LC-MS analysis, because UV detection is non-destructive (18). LC-MS techniques provide rapid, selective and sensitive analysis, which allow structure determination of multiple trace compounds in complex matrices to be done at the same time where compound isolation is not necessary and there is minimal consumption of material in the analysis (42). The Combination of information from the LC-MS and NMR analyses has been extensively used for unknown structure elucidation (42).

Technological advances in MS instrumentation over the last fifteen years have overshadowed those in HPLC, from the perspective of LC-MS (18). LC-MS has become one of the most important and extensively used techniques for the identification of target flavonoids and the structural characterisation of unknown compounds (17,18). Non-target screening for the identification and structure elucidation of unknown compounds can be performed by coupling HPLC with modern

high resolution mass spectrometry (HRMS) (38). Research of flavonoids in different fields relies heavily on accurate analytical data, and LC-MS has played an influential role by allowing fast tentative identification and accurate quantification of low levels of flavonoids in a variety of matrices (18). Electrospray ionisation (ESI) is used almost exclusively in the LC-MS analysis of flavonoids, though the application of atmospheric pressure chemical ionisation (APCI) has also been reported (17). LC-MS has become an obligatory tool in flavonoid characterisation as a complementary technique to NMR because it can be used to identify individual compounds in complex mixtures without the need for isolation (18).

Time of flight (TOF) mass spectrometers work on the principle that lighter ions travel faster than heavier ions following an initial acceleration by an electric field. All ions acquire the same kinetic energy during this initial acceleration period, and are separated in the field-free flight tube according to their different velocities. The physical property that is measured is flight time, which is directly related to the mass-to-charge ratio of the ion. Due to this mode of operation, TOF instruments offer very high mass ranges (without compromising sensitivity, as is the case in scanning mass spectrometers), very high acquisition rates and for the latest generation of instruments, relatively high resolving power and good sensitivity (although the latter decreases with high acquisition rates). (43).

In LC-MS positive electrospray ionisation mode in the presence of mobile phase, standards of quercetin, kaempferol, myricetin, apigenin and luteolin form abundant peaks of the protonated molecules/pseudo-molecular ion ($[M+H]^+$) at *m/z* 303; 287; 319; 271 and 287, respectively (21). The presence of adducts in the MS spectra is very useful in the identification of the $[M+H]^+$ ion because only the pseudo-molecular ions are able to form adducts (clusters and/or molecular complexes with mobile phase

species in the electrospray ionisation source) and hence determining the molecular weight of the unknown compounds (15). In this sense, the sodium adduct $[M+Na]^+$ at 22 amu above the proposed pseudo-molecular ion is of great relevance. In LC-MS, the positive ionisation mode (protonation of the pseudo-molecular ion) are more popular because they provide more extensive fragmentation in ionisation whereas, in negative ionisation mode (deprotonation of the pseudo-molecular ion) higher collision energies are required for fragmentation and may lack some diagnostic ions in the product ion spectra due to limited fragmentation (17,18). In first-order MS spectra of flavonoids, with low cone voltages ~30 V, pseudo-molecular ions ($[M+H]^+$ and $[M-H]^-$) are most common, with little fragmentation displayed (18). The flavonoid aglycone fragment ions were displayed according to the nomenclature proposed by Ma *et al.*, (1997), as illustrated in Figure 2.15 (15). It was proposed that "For free aglycones, the ${}^{i,j}A^+$ and ${}^{i,j}B^+$ labels refer to the fragments containing intact A and B-rings, respectively, in which the superscripts *i* and *j* indicate the C-ring bonds that have been broken" (Figure 2.15). "For conjugated aglycones, an additional subscript 0 to the right of the letter is used to avoid confusion with the A_i^+ and B_i^+ ($i \geq 1$) labels that have been used to designate carbohydrate fragments containing a terminal (non-reducing) sugar unit" (15). The nomenclature, proposed by Domon and Costello (1988) for glycoconjugates, was adopted by Abad-García (15) to denote the fragment ions as shown in Figure 2.15. Ions that contain the aglycone were labelled ${}^{k,l}X_j$, Y_j and Z_j, where *j* represents the number of the interglycosidic linkage broken (counting from the aglycone) and the superscripts *k* and *l* indicate the cleavages within the carbohydrate rings (15). The glycosidic bond linking the sugar unit to the aglycone was given the number '0' (15).

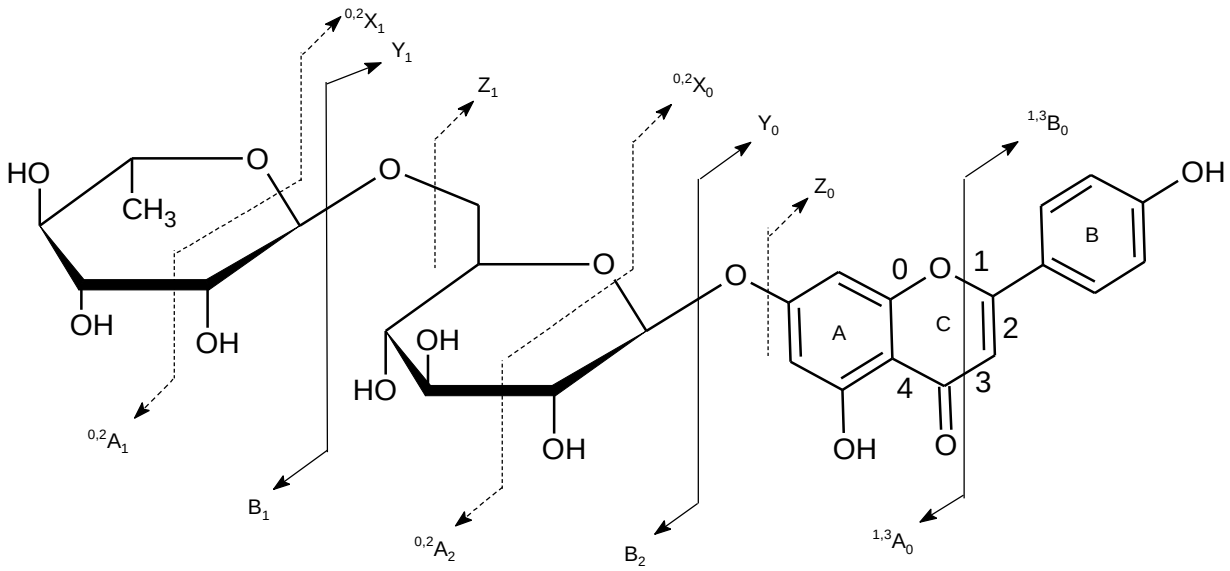

Figure 2.15: Fragmentation of a flavonoid glycoside illustrated on apigenin-7-O-rutinoside (15).

2.6.3 NMR

In structural elucidation of flavonoids, NMR is indispensable because it allows the complete assignment of flavonoid structures, including the aglycone identity, stereochemistry, nature and position of sugars and acylated sugars etc.(18). It is however hampered by cost and throughput limitations and is not suited to all applications, especially because it requires sufficient concentrations of relatively pure analytes (18). While NMR only provides average compositional information on complex mixtures, MS can be used to determine the structures of individual molecules present in mixtures (18). HPLC and structural information from MS^n spectra provided the combination of chromatographic resolution that enables routine separation and tentative identification of complex mixtures of flavonoids spanning several orders of magnitude in concentration, something that was not possible 25 years ago (18).

CHAPTER 3

3. MATERIALS AND METHODS

3.1. Chemicals and Reagents

All chemicals and reagents used were analytical grade. The acetonitrile and methanol used for mobile phase and sample preparation for HPLC and LC-MS analysis were HPLC grade. Milli-Q water was used for mobile phase preparation. Two 100 mM stock solutions of the buffers (ammonium acetate and ammonium formate) were prepared.

3.2. Instrumentation

HPLC analyses were performed on a Perkin Elmer Flexar HPLC consisting of a quaternary pump, degasser, auto sampler, photodiode array detector and column oven. Chromera software (version 3.4.1.5904) was used for instrument control and data acquisition. LC-MS, LC-MS^E and LC-MS/MS analyses were performed on a Waters Acquity UPLC system consisting of a binary pump, degasser, auto-sampler, column oven and a photodiode array (PDA) detector (500 nL flow cell, 10 mm path length), interfaced through an electron spray ionisation (ESI) source to a Waters Synapt G2 quadrupole - time-of-flight (Q-TOF) high resolution mass spectrometer. LC-MS instrument control and data acquisition were performed using MassLynx (version 4.1) software (Waters).

3.3. Sample Collection and Processing

Plant material was collected from Döbra Farm Plot 46 (22°19'51.1"S 17°05'59.7"E) (Research/collection permit number: 1869/2014) (National Herbarium of Namibia identification report number: 2014/360). Plant samples were collected during the flowering season. It has been reported that extracts of some medicinal plants were

generally richest in antibacterial agents after the flowering (sexual) stage of their growth is complete, and plants taken from stressful environments were particularly active (4). Eight plants were uprooted in order to have approximately 10.0 grams of each plant part. The plant material was separated into the respective plant parts; flowers, stems and leaves. Only the aerial parts of the plant were studied. For consistency, only mature flowers and fresh green leaves were considered. The separated parts of the plant were air dried and ground into a fine powder.

3.4. Preparation of Extracts

The constituents of the different plant parts were extracted using sequential extractions with solvents of increasing polarity during each step; firstly hexane, then dichloromethane and finally methanol (44). Hexane (200 mL) was added to 10 g of ground plant material (leaves, flowers and stems) in a separate Erlenmeyer flask. The flasks were sealed with aluminium foil and were placed on the orbital shaker for 24 hours. The extraction was performed at 200 rpm and room temperature (~ 25 °C). Each extract was filtered using a Buchner funnel in order to retain the dry plant residue for the next extraction. The filtrate was transferred to a weighed 250 mL round bottom flask. Dichloromethane (200 mL) was added to the dry plant residue (leaves, flowers and stems) from the previous extraction in a separate Erlenmeyer flask. The extraction was performed in the same way as the previous extraction and the dry plant residue was subsequently used for the preparation of the methanol extract, again following the same procedure. The filtrates in separate 250 mL round bottom flasks were concentrated using a rotary evaporator at ~150 rpm under reduced pressure and a temperature of 20-25 °C for the DCM extract, 40 °C for the hexane and methanol extracts to volumes less than 10 mL in order to transfer them to pre-weighed 10 mL vials. The remaining solvent was evaporated in a nitrogen atmosphere (to avoid loss

of volatile compounds) in order to obtain dry extracts for storage. The extracts (Table 3.1) were stored at -20 °C.

3.5.Phytochemical Screens

The powdered material of *H. argyrosphaerum* were screened for phytochemicals according to the procedures described by Farnsworth (45). All phytochemical screens were performed

Table 3.1: Extracts produced from different plant parts of *H. argyrosphaerum*

Plant part	Mass of Material (g)	Mass of dried extract (g)		
		Hexane	DCM	Methanol
Leaves	10.1012	0.6275	0.3226	1.4059
Stems	10.0098	0.1373	0.1103	0.7579
Flowers	10.0376	0.4042	0.1177	1.3795

with negative controls in order to compare colour changes. A weak colouration was assigned a + while a strong colouration got +++.

3.5.1. Anthraquinones

To test for anthraquinones, an ether-chloroform maceration (1.0 g of plant material in 5.00 mL of $CHCl_3$ and 5.00 mL of ether) was filtered and 1.00 mL of the solution was treated with 1.00 mL 10 % NaOH solution. A red colouration confirmed the presence of anthraquinones in the leaves only.

3.5.2. Anthranoids

A portion of finely ground plant material (0.2 g) was boiled for two minutes with 0.50 mL of 1 N KOH and 0.50 mL of 5 % H_2O_2. After cooling, the mixture was filtered.

The filtrate was treated with 6 drops of acetic acid (the universal indicator paper was yellow-to-red) and the resulting solution was mixed with 5.00 mL of toluene. The toluene (upper) layer was separated with a pipette and transferred to a test tube and 2.00 mL of 0.5 N KOH was added. Lack of a red colour in the aqueous layer confirmed the absence of anthranoids.

3.5.3. Cardenolides/cardiac glycosides

Finely ground plant material (2.0 g) was mixed with 20.00 mL of distilled water in a test tube and was kept at room temperature for 2 hours. The mixture was filtered using a Buchner funnel and the filtrate was divided into two parts, test tubes A and B. Four drops of Kedde reagent (4.00 mL of 3,5-dinitrobenzioc acid and 0.60 mL of 1 N KOH in methanol) were added to portion A. The lack of a blue-violet colour confirmed the absence of cardenolides in all plant parts. Part B was used as a control.

3.5.4. Saponins

Finely ground plant material (1.0 g) was mixed with 15.00 mL of water in a test tube. The mixture was heated in a water bath for 5 minutes. The mixture was filtered and left to cool to room temperature. The filtrate was added in a 16 x 160 mm test tube and it was shaken for 10 seconds forming a honey comb froth. The height of the honeycomb froth which persists was measured. Froth higher than 1.0 cm confirmed the presence of saponins in the flowers and leaves.

3.5.5. Terpenoids

Three millilitres of chloroform was added to 0.5 g of finely ground plant material. The mixture was shaken and filtered. Ten drops of acetic anhydride followed by 2 drops of conc. sulphuric acid were added to the filtrate. Lack of a red-to-brown colouration at the interface confirmed the absence of terpenes in all plant parts.

3.5.6. Iridoids

One hundred milligrams of finely ground plant material was suspended in 3.00 mL of water. The extract was filtered off and concentrated to a volume of 0.50 mL. The mother liquor was treated with 1.00 mL of a reagent composed of; 10 mL acetic acid, 1.00 mL of 2 % copper sulphate solution and 0.50 mL of conc. HCl. The colouration in the tonalities of blue after gentle heat confirmed the presence of iridoids in the leaves only.

3.5.7. Polyphenols

Two solvents, water (15.00 mL) or ethanol (10.00 mL) may be used in this section. In the case of ethanol green parts of the plant should not be used, therefore, water was used in this case. Plant material (1.0 g) in solvent was heated in a water bath for 15 minutes and the mixture was filtered. Three drops of ferric cyanide solution [1.00 mL of 1% $FeCl_3$ and 1.00 mL of $K_3Fe[CN]_6$, freshly prepared] were added to the filtrate (2.00 mL). The blue-green colour confirmed the presence of polyphenols in all plant parts.

3.5.7.1. Flavonoids

Finely ground plant material (1.0 g) was extracted with 10.00 mL of water with 5.00 mL of methanol and filtered. A few magnesium turnings were added to a 3.00 mL portion of the filtrate. Concentrated HCl was then added, drop wise (cyanidin reaction) to the 3.00 mL portion. The orange colour confirmed the presence of flavones in all plant parts (orange colour = flavones; red colour = flavonols; pink = flavanones).

3.5.7.2. Anthocyanins

Anthocyanins are plant pigments and vary in colour from orange-red to blue-red. One gram of the finely ground plant material was mixed with 15.00 mL of cold 1 % HCl

and boiled. The colour change at and during boiling confirmed the presence of anthocyanins.

3.5.7.3. Leucoanthocyanins

Finely ground plant material (1.0 g) was mixed with 20.00 mL of water. A portion of 0.50 mL of this mixture was mixed with 2.00 mL of 2 N HCl and heated in a water bath to 100 °C. A slow development of red-to-violet colour confirmed the presence of leucoanthocyanins in the leaves only.

3.5.7.4.Tannins

Finely ground plant material (2.0 g) was put in a test tube with 15.00 mL of water. The mixture was heated in a water bath for 5 minutes. After cooling the mixture was filtered and 2 % NaCl solution (5.00 mL) was added to the filtrate. Any suspensions were further filtered out and 5.00 mL of 1 % gelatine was added. No formation of a precipitate indicated the absence of tannins in the precipitate test, while the polyphenol test served as proof for the presence of tannins as well as a green to black colouration observed with 1 % $FeCl_3$ solution test confirmed the presence of tannins in all plant parts.

3.5.8. Alkaloids

Two grams of powdered material was boiled with 25.00 mL of 1 % HCl for 15 minutes in a water bath and then the suspension was filtered into a test tube. The filtrate was divided into test tube A and test tube B. Two drops of the Dragendorff's reagent was added to test tube A and 2 drops of Mayer's reagent added to test tube B. Lack of a red precipitate for the Dragendorff's test confirmed a negative result in all plant parts while a creamy white precipitate for Mayer's test indicated a positive result in flowers only.

3.6. HPLC method development

RPLC and HILIC separation methods were developed for the analysis of the methanol extracts of the different plant parts of *H. argyrosphaerum*. All subsequent HPLC experiments were performed with the suitable concentration of 2.00 mg/mL of the extract using a flow rate of 1.00 mL/min and an injection volume of 20.00 µL. The samples were filtered into HPLC vials using 0.45 µm nylon syringe filters. The column and samples were maintained at room temperature (*ca.* 25 °C). RPLC experiments were performed on a Kinetex C_{18} column of length 250.0 mm and a diameter of 4.6 mm packed with 5.0 µm particles. The mobile phase A consisted of either 5 % methanol (MeOH) or acetonitrile (ACN) with 0.1 or 1.0 % formic acid (FA) while B consisted of MeOH or ACN with 0.1 or 1.0 % FA. Two gradients were evaluated, the 40 minute gradient was set up as follows: 0 % → 100 % B linear gradient (0-40 min), 100 % B isocratic (40-49 min) and 100 % → 0 % B (49-50 min) and the 60 minute gradient was as follows: 0 % → 100 % B linear gradient (0-60 min), 100 % B isocratic (60-69 min) and 100 % → 0 % B (69-70 min). HILIC experiments were performed on a Phenomenex Luna HILIC column of length 250.0 mm and a diameter of 4.6 mm packed with 3.0 µm particles. The mobile phase A consisted of 5 % ACN with 5 mM ammonium acetate (AAc) at pH 7 and mobile phase B consisted of 95 % ACN with 5 mM AAc at pH 7. For HILIC experiments, compound retention was tested and the gradient was set up as follows: 100 % B isocratic (0-10 min), 100 % → 50 % B (10-40 min) and 50 % → 100 % B (40-41 min). All HILIC-MS experiments were performed using an injection volume of 5.00 µL. Samples were dissolved in MeOH for RPLC experiments and ACN for HILIC experiments. Detection of flavonoids was with UV-vis spectroscopy at wavelengths of 254, 280, 320 and 370 nm. Column pressure was observed and kept below 400 bar. Chromera software (version

3.4.1.5904) was used for instrument control and data acquisition for the conventional HPLC instrument (Perkin Elmer Flexar).

3.7. LC-MS Method development

In order to have fresh samples, a portion of dried methanol extract of each plant part was dissolved in MeOH at a concentration of 10.0 mg/mL and was filtered into HPLC vials using 0.45 µm nylon syringe filters. Subsequently the samples were diluted to 2.0 mg/mL using MeOH. A RPLC method was translated from the optimised HPLC method (4.6 mm I.D. column) for the UPLC (2.1 mm I.D. column) instrument that was used for the LC-MS experiments. RPLC-MS experiments were performed on a Phenomenex Kinetex C_{18} column with dimensions of 150.0 mm length × 2.1 mm I.D. packed with 2.6 µm particles. A flow rate of 0.30 mL/min with column and sample temperature at room temperature (*ca.* 25 °C) and 20 °C respectively. Gradient times of 30 and 40 minutes were evaluated to retain the shape of chromatograms obtained in RPLC experiments. The mobile phases used for RPLC were A (5 % MeOH; 0.1 % FA) and B (MeOH; 0.1 % FA). For HILIC experiments, the developed method was translated for the UPLC instrument and was further optimized. Optimisation of the HILIC method was performed on two different columns; a Phenomenex Luna HILIC column with dimensions of 150.0 mm length × 2.0 mm I.D. packed with 3.0 µm particles and an Xbridge BEH Amide column XP with dimensions of 150.0 mm length × 4.6 mm I.D. packed with 2.5 µm particles. Column and sample temperatures were kept at 40 °C and 20 °C respectively. The mobile phase A consisted of 5 % ACN with 5 mM ammonium formate (AF) and mobile phase B consisted of 95 % ACN with 5mM AF. The HILIC method was optimised using different injection volumes, flow rates, equilibration times, gradients, gradient times and mobile phase compositions in order to find the most suitable method for the HILIC-MS experiments. Waters

Empower software (Waters, Milford, MA, USA) was used for the UPLC instrument control and data acquisition (HILIC). Detection of flavonoids was with UV-vis spectroscopy at wavelengths of 254, 280, 320 and 370 nm.

3.8. Semi-preparative RPLC Method development

The main objective of the semi-preparative RPLC method development was to isolate the compounds detected in RPLC experiments. This was achieved by translating methods used on a Phenomenex Kinetex C_{18} column with a length of 150 mm and a 2.1 mm I.D. packed with 2.6 µm particles to a larger Supelco Ascentis C_{18} column with a length of 250.0 mm and a 10.0 mm I.D. packed with 5.0 µm particles. The mobile phase conditions were restricted to those of the optimised analytical RPLC method: phase A (0.1 % FA in 5 % MeOH) and B (0.1 % FA in MeOH). The translated method was further optimised in order to achieve short runs and save mobile phase.

3.9 Sample analysis and data acquisition

The samples were analysed in both ESI positive and negative modes. However, since the ESI negative analyses did not reveal any additional information compared to the ESI positive results, only the ESI positive results are reported here. LC-Q-TOF-MS data, where ions formed in the ion source are measured and no fragmentation occurs in the collision cell, were acquired in positive ionisation mode with a scan range of 100–1500 amu, lock mass of 557 amu and a cone voltage of 30 V. LC-MS^E (an acquisition mode performed concurrently with full scan acquisition in a single analysis, where fragmentation is performed using a collision energy ramp of 50-100 V) data were acquired across a mass range of 40–1500 amu. Targeted MS/MS data, where a particular precursor ion is fragmented in the collision cell and the fragments are measured, were acquired across ranges of 100-600 amu, 100-750 amu and 100-900 amu depending on the analytes using a static collision energy of 30 V.

CHAPTER 4

4. RESULTS AND DISCUSSIONS

Phytochemical screening was performed in order to determine which classes of compounds were present in *H. argyrosphaerum* as a guiding step to subsequent characterisation of the major metabolites. This was followed by High Pressure Liquid Chromatography – Ultraviolet Spectroscopy – High Resolution Tandem Mass Spectrometry (HPLC-UV-HRMS/MS) characterisation of eight major compounds and semi-preparative HPLC isolation of six of these compounds.

4.1. Phytochemical screening

Phytochemicals are plant based chemical compounds that exhibit disease preventive properties and are found in cereals, fruits, vegetables, legumes, herbs, spices, nuts, weeds and beverages (such as tea, wine and beer) (46). They are known to provide therapeutic effects on pathological conditions through modulating signalling pathways (46). Phytochemical screening (Table 4.1) was performed as a guiding step to identify classes of compounds that are abundant in the plant and to provide a target of focus for further experiments. The most abundant phytochemicals were found to be polyphenols, including flavonoids, which were present in all plant parts in relatively large amounts. Other sub-classes of polyphenols (anthocyanins) were present in large quantities in the leaves and stems, but not in the flowers. Terpenes, anthranoids and cardiac glycosides were not detected. Besides the abundant polyphenols, alkaloids and saponins were also present with the alkaloids present only in small quantities in the flowers. In the test for tannins, the precipitate test was observed to be negative because the solution was maybe too dilute for low concentration tannin precipitate to be visible or formed. This is supported by low concentrated positive results in the ferric chloride

Table 4.1: Phytochemical screens of the finely ground plant material of the different plant parts of *H. argyrosphaerum*

Compound classes		Results		
		Flowers	Leaves	Stems
Anthraquinones		-	+	-
Anthranoids		-	-	-
Cardenolides/ Cardiac glycosides		-	-	-
Saponins		+	++	-
Terpenes		-	-	-
Iridoids		-	+	-
Polyphenols		+++	+++	++
Flavonoids		++ (flavones)	++ (flavones)	+ (flavones)
Anthocyanins		-	++	++
Leucoanthocyanins		-	+	-
Tannins	**Precipitate**	-	-	-
	Ferric chloride	+	++	+
Alkaloids	**Dragendorff's test**	-	-	-
	Mayer's test	+	-	-

Key: - not detected; + present in small quantities; ++ present in medium quantities; +++ present in large quantities.

test. The Dragendorff's reagent was not freshly prepared and this led to an assumption that the organic acid (tartaric acid) may have degraded which, in turn might lead to the negative result observed.

Different *Helichrysum* species produce different secondary metabolites or phytochemicals (acetophenones, flavonoids, and phloroglucinols) as a biochemical defence mechanism against bacteria and fungi (5). The high abundance of polyphenols observed in *H. argyrosphaerum* is in correlation with other findings highlighted in section 2.2, 2.4 and 2.5 where *Helichrysum* species were found to possess high CGA and flavonoid (phenolics) content. The absence of terpenes is consistent with the findings by Jakupovic and colleagues (7), where the chemistry difference between

Australian and South African *Helichrysum* species was based on the accumulation and no accumulation of diterpenes respectively.

4.2. HPLC method development

The principal challenge in identifying the major compounds of the *H. argyrosphaerum* responsible for the plant's biological activities is the complexity of the sample. However, based on the results of the phytochemical screens polyphenols, flavonoids and anthocyanins, mostly polar compounds, are present in appreciable quantities in the different plant parts. Therefore, the most polar extract (MeOH extract) was investigated further.

HPLC is the most suitable technique for the analysis of polar compounds and has been the most widely employed technique in analysis of, for instance flavonoids in foods (23). "LC-MS is one of the most important techniques used for the identification of flavonoids and the structural characterisation of unknown compounds" (17). Contemporary HPLC separation of flavonoids is almost exclusively performed using RPLC with the exception of HILIC application which has increased recently (18). The most widely used methods among those for the determination of polyphenols, are based on RPLC coupled to DAD and/or MS or tandem MS (15). RPLC is often used because of its compatibility with MS and because good performance is obtained in this mode for faster separations (18) as observed in this study whereas HILIC produces a lot of overlapping peaks. Therefore, RPLC became the mode of choice because it has demonstrated its suitability for the separation of flavonoids based on the nature of the aglycone, the nature and degree of glycosylation and acylation and because the two most common organic modifiers used in the RPLC analysis of flavonoids (MeOH and ACN) have little to direct effect on the ionisation of molecules (18). Concentrations of

2.00 mg/mL, 2.86 mg/mL and 4.00 mg/mL extract solutions in methanol were analysed in order to find a suitable concentration that provides acceptable peak intensities.

4.2.1. Development of a RPLC method

The use of MeOH and ACN as organic modifiers was evaluated, as well as the effect of the concentration of FA in the mobile phase. The gradient time and mobile phase composition were optimised to achieve the optimal separation of all the constituents detected in the MeOH extracts of the different plant parts of *H. argyrosphaerum*.

RPLC analyses were first performed using a mobile phase that contain 0.1 % FA and MeOH using a 40 minute gradient (Figure 4.1) and a 60 minute gradient (Figure 4.2) in order to determine which one is the most suitable gradient time. Since the separation did not improve when using the longer gradient time, the shorter gradient time, 40 minutes, was chosen in order to provide shorter analysis times and save mobile phase. The results for analysis of the leaves were shown here, but the same conclusion was reached for the stems and flowers. Using the same gradient time, but comparing MeOH with ACN (Figures 4.3 and 4.4), ACN resulted in poor retention of the compounds in which case the majority of the compounds eluted in the first 15 minutes and in the void. Hence, MeOH was chosen as the organic modifier for all subsequent experiments. Subsequently a mobile phase with a higher acid content of 1 % FA was evaluated. The mobile phase with an acid content of 0.1 % FA produced sharper and more resolved peaks than the mobile phase with 1 % FA content in the case of the MeOH extract of the flowers (Figures 4.5 and 4.6) between retention times, 5-25 minutes indicated by the dashed box. This shows that in the case of flowers the mobile phase with a 0.1 % FA content showed better separation than the mobile phase with 1 % FA. Although the mobile phase with 1 % FA content produced extra peaks observed

from 20 minutes to 25 minutes in Figure 4.6, the main aim of this analysis was to achieve better separation of the majority of the detected peaks (Figure 4.5).

4.2.2. Development of the HILIC method

The HILIC method was evaluated to determine whether the mobile phase provided good retention for the separation of compounds (section 3.6). A mobile phase consisting of ACN as the organic modifier and AAc as the buffer provided the chromatogram in Figure 4.7. The peaks observed between retention time ranges of 4-10 and 18-22 minutes (Figure 4.7) were poorly resolved. Better separation, sharper and more resolved peaks, was observed using RPLC method (Figure 4.5 and 4.6) compared to the HILIC method (Figure 4.7).

4.3. LC-MS method development

The main objective of these experiments was to transfer methods developed using a conventional HPLC instrument to methods more suitable for LC-MS analyses (e.g. using 2.1 mm I.D. columns that require low mobile flow rates) on an Acquity UPLC instrument. These methods were then optimized for LC-MS analysis. Unfortunately, the quantities of the samples prepared for LC-MS (RPLC and HILIC) were underestimated in relation to the quantities needed. Therefore, as a result only the leaves extract was used for method development while the flowers extract was saved for analyses using only the optimised methods.

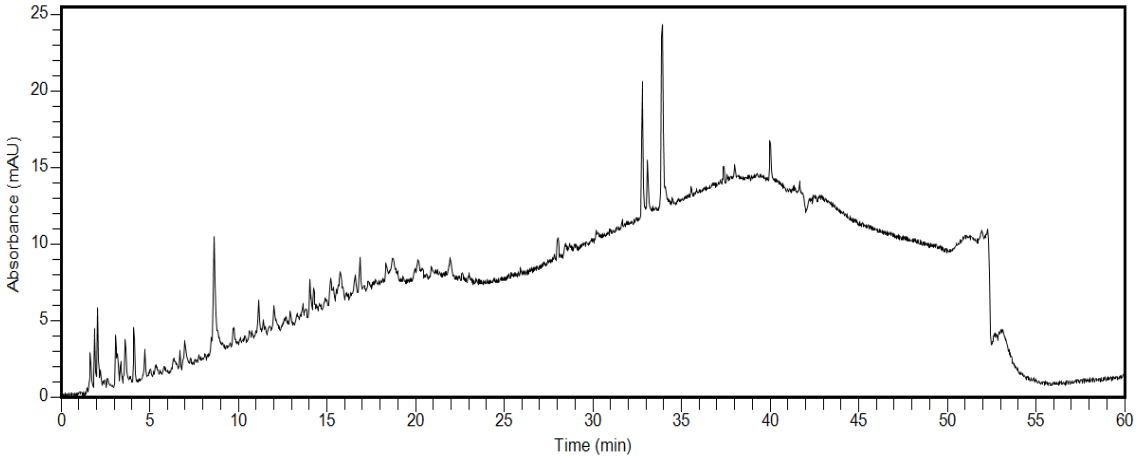

Figure 4.1: LC-UV chromatogram obtained at 280 nm for the RPLC analysis of the MeOH extract of the leaves of *H. argyrosphaerum* using a gradient time of 40 minutes and a mobile phase containing 0.1 % FA in 5 % MeOH (phase A)/0.1 % FA in MeOH (phase B).

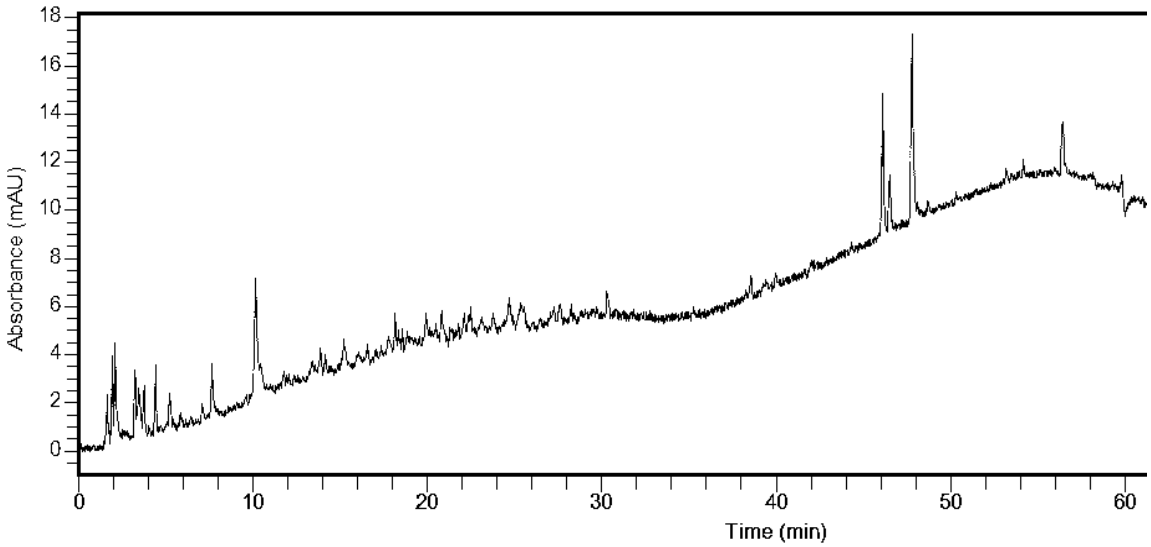

Figure 4.2: LC-UV chromatogram obtained at 280 nm for the RPLC analysis of the MeOH extract of the leaves of *H. argyrosphaerum* using a gradient time of 60 minutes and a mobile phase containing 0.1 % FA in 5 % MeOH (phase A)/0.1 % FA in MeOH (phase B).

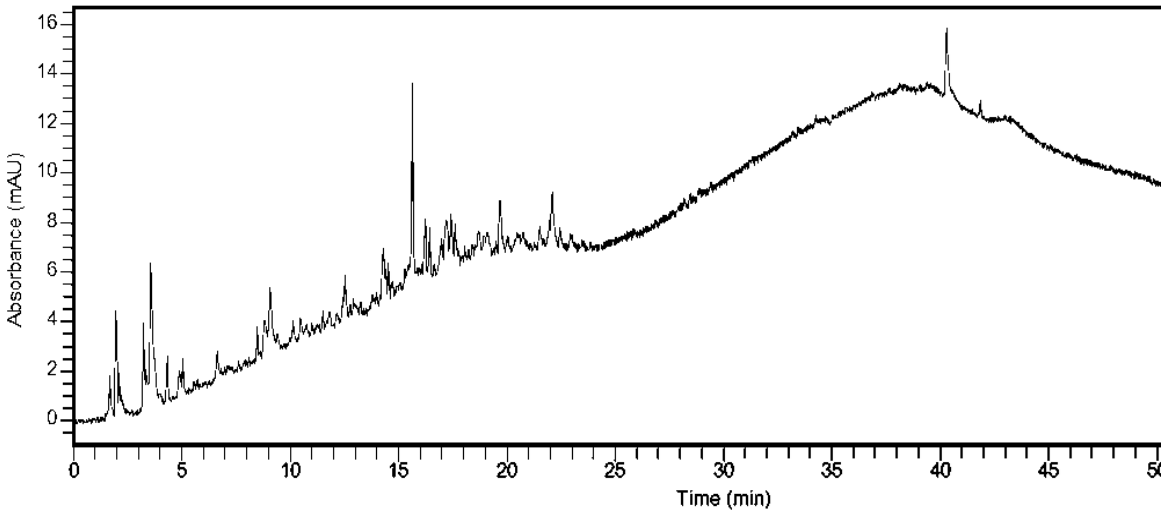

Figure 4.3: LC-UV chromatogram obtained at 280 nm for the RPLC analysis of the MeOH extract of the stems of *H. argyrosphaerum* using a gradient time of 40 minutes and a mobile phase containing 0.1 % FA in 5 % MeOH (phase A)/0.1 % FA in MeOH (phase B).

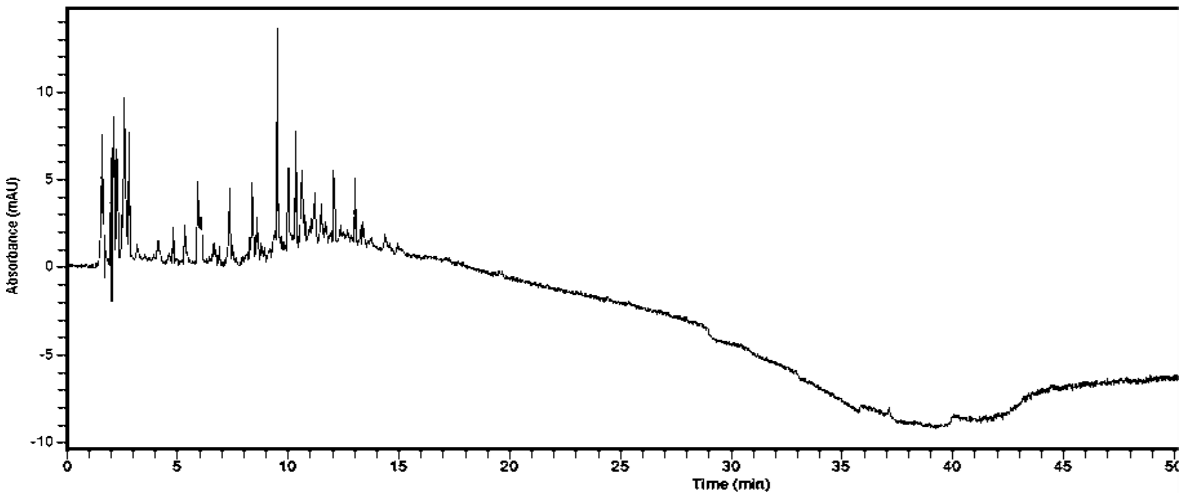

Figure 4.4: LC-UV chromatogram obtained at 280 nm for the RPLC analysis of the MeOH extract of the stems of *H. argyrosphaerum* using a gradient time of 40 minutes and a mobile phase containing 0.1 % FA in 5 % ACN (phase A)/0.1 % FA in ACN (phase B).

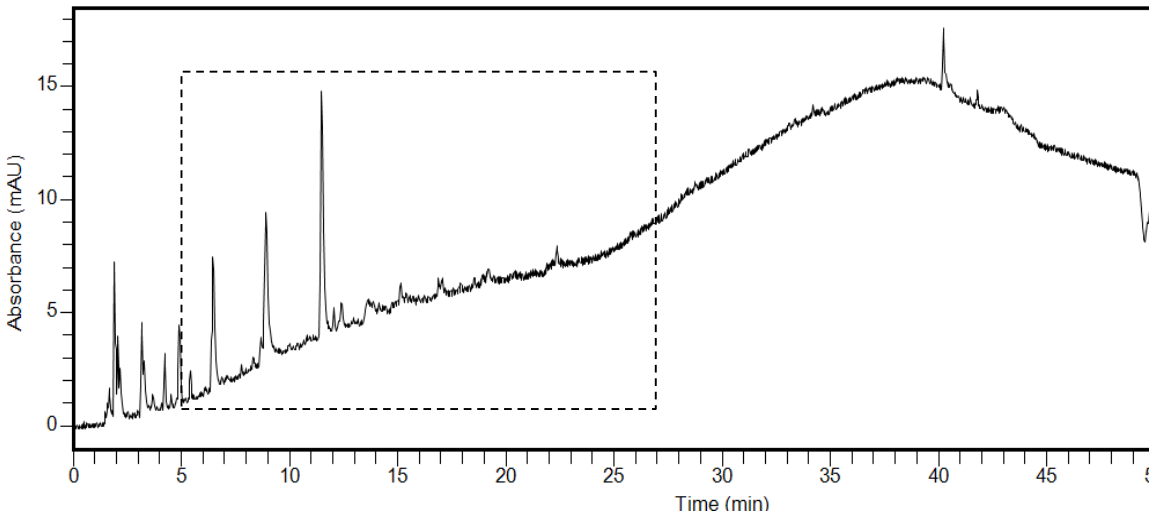

Figure 4.5: LC-UV chromatogram obtained at 280 nm for the RPLC analysis of the MeOH extract of the flowers of *H. argyrosphaerum* using a gradient time of 40 minutes and a mobile phase containing 0.1 % FA in 5 % MeOH (phase A)/0.1 % FA in MeOH (phase B).

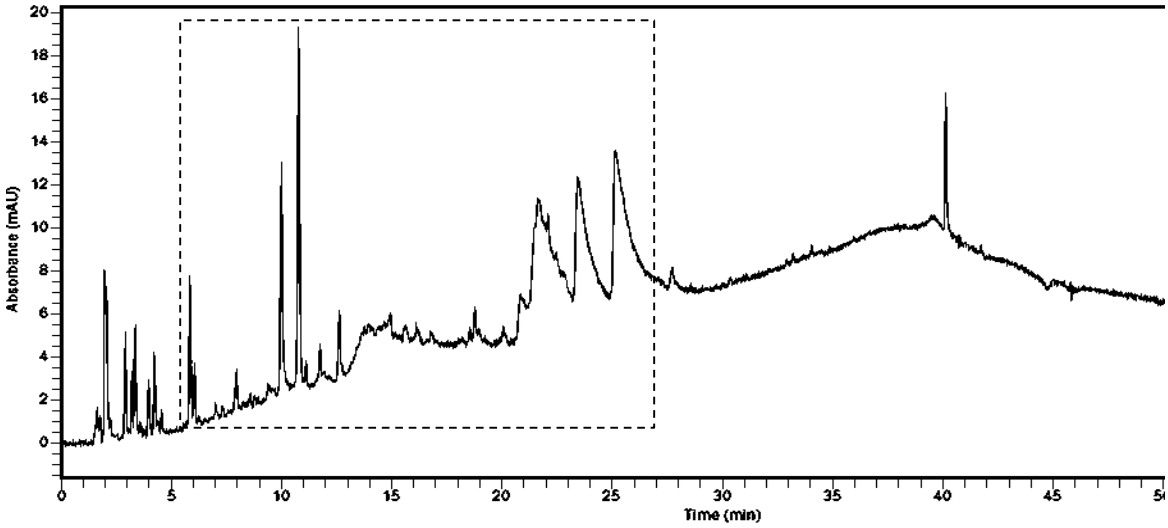

Figure 4.6: LC-UV chromatogram obtained at 280 nm for the RPLC analysis of the MeOH extract of the flowers of *H. argyrosphaerum* using a gradient time of 40 minutes and a mobile phase containing 1 % FA in 5 % MeOH (phase A)/1 % FA in MeOH (phase B).

4.3.1. Development of the RPLC-MS method

The optimised mobile phase conditions determined during HPLC method development, were subsequently used as a starting point for the RPLC-MS method development. Since the 2.1 mm I.D column that was available was only 15.0 cm in length (as opposed to the 25.0 cm, 4.6 mm I.D column that was used for HPLC method development), the only parameter to be optimised was the gradient time. Two different gradient times, 16 and 30 minutes, were evaluated and it produced the chromatograms shown in Figures 4.8 and 4.9. In both cases the mobile phase was changed from 100 % A (5 % MeOH: 0.1 % FA) to 100 % B (MeOH: 0.1 % FA). The 30 minute gradient (Figure 4.9) allowed sufficient partition time for constituents to separate, avoiding co-elution of peaks as seen between 8 and 9 minutes when using a 16 minute gradient time (Figure 4.8). All the subsequent RPLC-MS analysis were performed using a 30 minute gradient that was set up as follows: 0 % → 100 % B linear gradient (0-30 min), 100 % B isocratic (30-31 min), and returned to initial conditions (31-31.5 min).

4.3.2. Development of the HILIC-MS method

The optimised mobile phase conditions and gradient times that were tested during HPLC method development, were subsequently used as a starting point for the HILIC-MS method development. Extensive optimisation of the developed method was performed (including evaluation of different columns) in order to resolve the peaks observed during the compound retention test (Figure 4.7).

The initial method (Figure 4.10) involved the use of an 8 minute gradient using a flow rate of 0.30 mL/min. An injection volume of 2.00 µL was used. The initial gradient was set up as follows: 100 % B isocratic (0-4 min), 100→50 % B (4-12 min), and returned to initial conditions (12-12.2 min). The Phenomenex Luna HILIC column and the Xbridge BEH Amide column were the two columns that were evaluated.

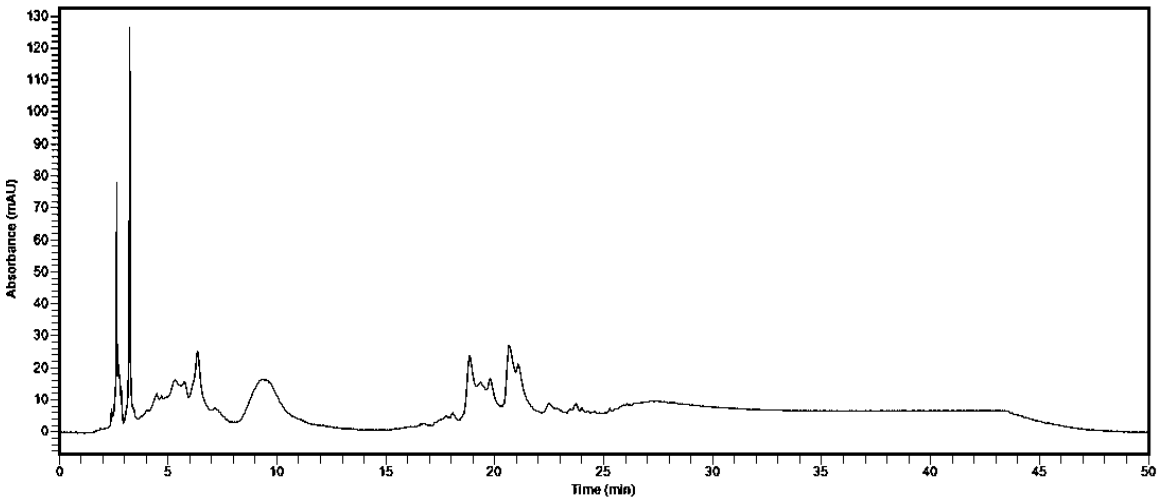

Figure 4.7: LC-UV chromatogram obtained at 280 nm for the HILIC analysis of the MeOH extract of the flowers of *H. argyrosphaerum* using a gradient time of 30 minutes and a mobile phase containing 5 mM AAc in 5 % ACN (phase A)/5 mM AAc in ACN (phase B).

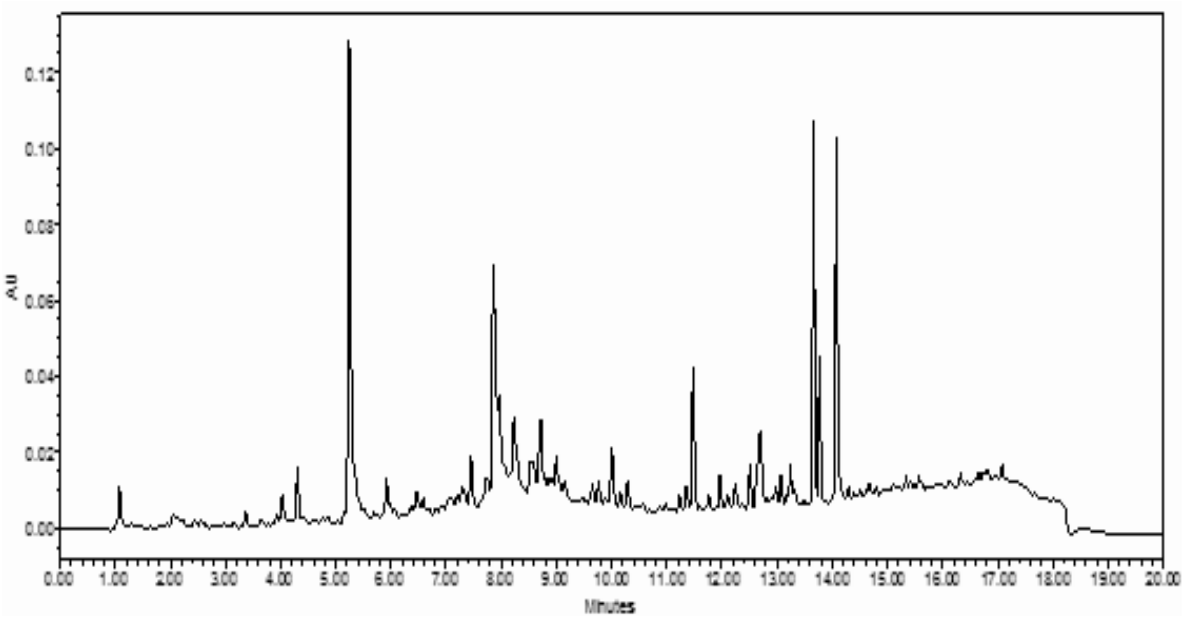

Figure 4.8: LC-UV chromatogram obtained at 280 nm for the RPLC analysis of the MeOH extract of the leaves of *H. argyrosphaerum* using a gradient time of 16 minutes and a mobile phase containing 0.1 % FA in 5 % MeOH (phase A)/0.1 % FA in MeOH (phase B).

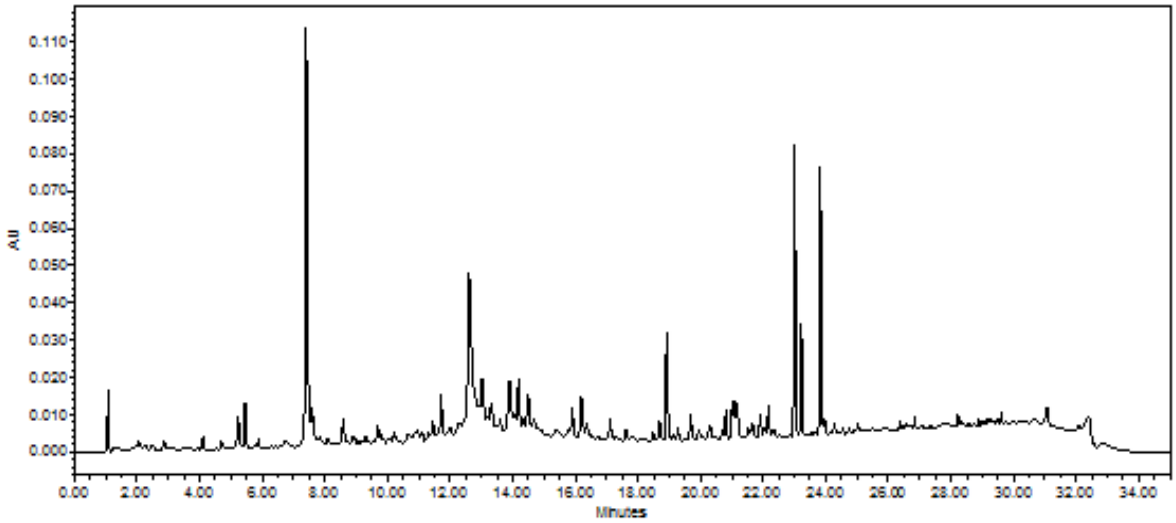

Figure 4.9: LC-UV chromatogram obtained at 280 nm for the RPLC analysis of the MeOH extract of the leaves of *H. argyrosphaerum* using a gradient time of 30 minutes and a mobile phase containing 0.1 % FA in 5 % MeOH (phase A)/0.1 % FA in MeOH (phase B).

Firstly, the Phenomenex Luna column was evaluated using the initial method mentioned above. A gradient set up as follows: 100 % B isocratic (0-6 min), 100→50 % B (6-26 min), and returned to initial conditions (26-26.2 min), was evaluated. The 20 minute gradient (Figure 4.11) provided a better separation for late eluting peaks compared to the 8 minute gradient (Figure 4.10) and was therefore used for all subsequent experiments. The mobile phase composition at the end of the gradient was then varied between 60 % B (Figure 4.12), 65 % B (Figure 4.13) and 80 % B (Figure 4.14) in order to improve resolution under the 20 minute gradient. A mobile phase composition of 80 % B (Figure 4.14) at the end of the gradient improved resolution of the late eluting peaks.

Secondly, an Xbridge BEH Amide column XP (150.0 mm × 4.6 mm I.D., 2.5 µm particles) was then evaluated (Figure 4.15). And this experiment was performed at a

mobile phase flow rate of 0.70 mL/min. All the amide column experiments were performed using an injection volume of 5.00 µL. The 20 minute gradient and the mobile phase composition of 80 % B at the end of the gradient (i.e. 100→80 % B in 20 minutes) were then evaluated on the amide column (Figure 4.15). This column provided more resolved peaks and better retention of compounds as observed in Figure 4.15 under these conditions compared to the Phenomenex column (Figure 4.14). This is because the amide column finally resolves a cluster of peaks observed from 2 to 4 minutes and co-eluting peaks from 8 to 11 minutes in all experiments performed with the Phenomenex column (Figures 4.10-14). Other mobile phase compositions were also evaluated using this amide column: 60 % B (Figure 4.16), 70 % B (Figure 4.17) and 80 % B with an isocratic section of 8 minutes (Figure 4.18) at the end of the gradient. The separation performed under the gradient set up as follows: 100 % B isocratic (0-6 min), 100→80 % B (6-26 min), 80 % B isocratic (26-34 min) and returning to initial conditions at 34.2 minutes produced the best observed separation (Figure 4.18). Therefore, all subsequent HILIC-MS experiments were performed using this method.

4.3.3. Semi-preparative RPLC

The mobile phase conditions from the developed RPLC-MS separation method served as starting point for semi-preparative HPLC separation in order to isolate the detected major compounds. This method provided the initial gradient (G1) that was set up as: 0→100 % B (0-30 min), 100 % B isocratic (30-31 min) and returned to initial conditions at 31.5 minutes. A flow rate (F1) of 0.3 mL/min was used, the column temperature was kept at 25 °C and the sample was kept at 20 °C. This method however had to be translated from a Phenomenex Kinetex column with dimensions of 150.0 mm (L_1) in length and a 2.1 mm I.D. packed with 2.6 µm particles to a larger Supelco

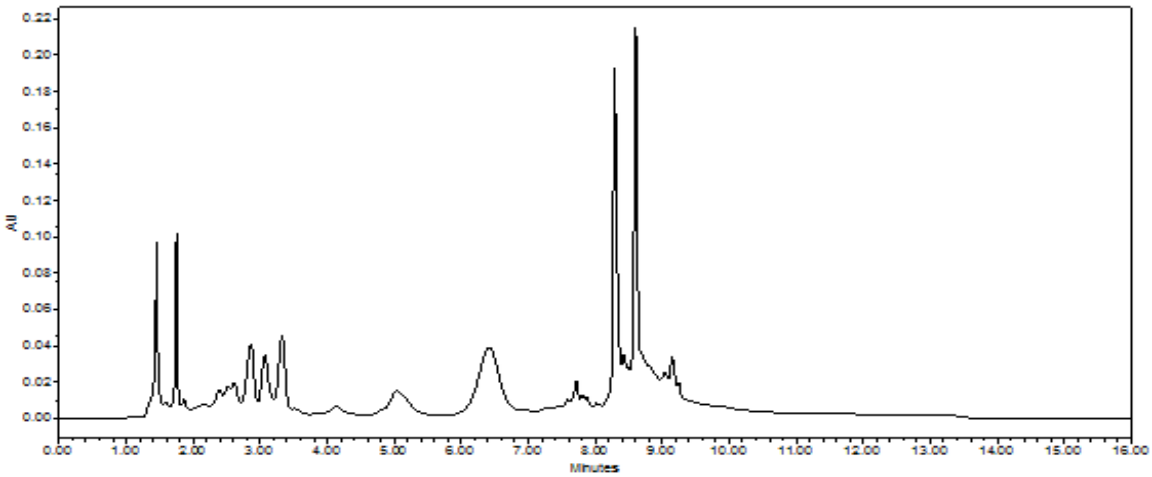

Figure 4.10: LC-UV chromatogram obtained at 280 nm for the HILIC analysis of the MeOH extract of the leaves of *H. argyrosphaerum* using a gradient: 100→50 % B (8 min). Using a mobile phase consisting of 5 mM of AF in water with 5% ACN (phase A)/ 5 mM of AF in water with 95 % ACN (phase B). A Phenomenex Luna HILIC column was used.

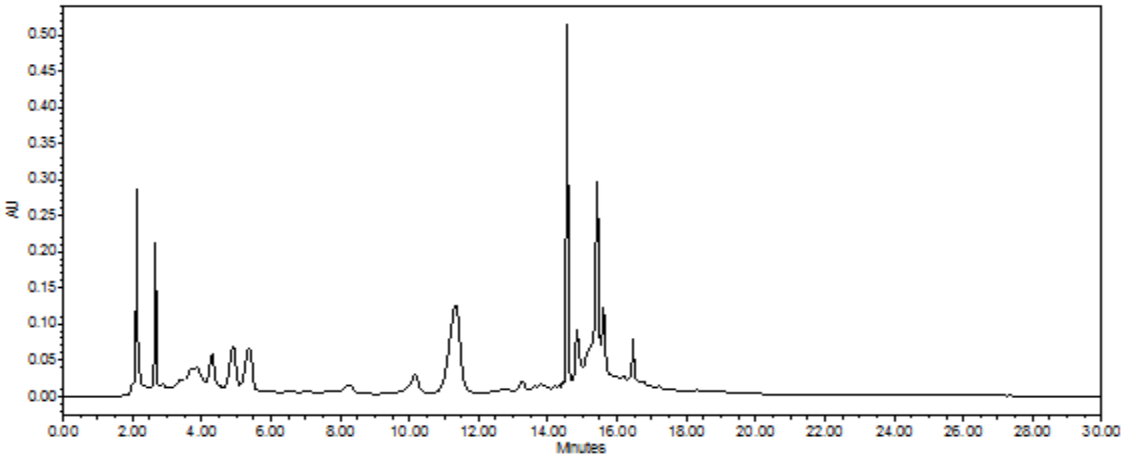

Figure 4.11: LC-UV chromatogram obtained at 280 nm for the HILIC analysis of the MeOH extract of the leaves of *H. argyrosphaerum* using a gradient: 100→50 % B (20 min). Using a mobile phase consisting of 5 mM of AF in water with 5% ACN (phase A)/ 5 mM of AF in water with 95 % ACN (phase B). A Phenomenex Luna HILIC column was used.

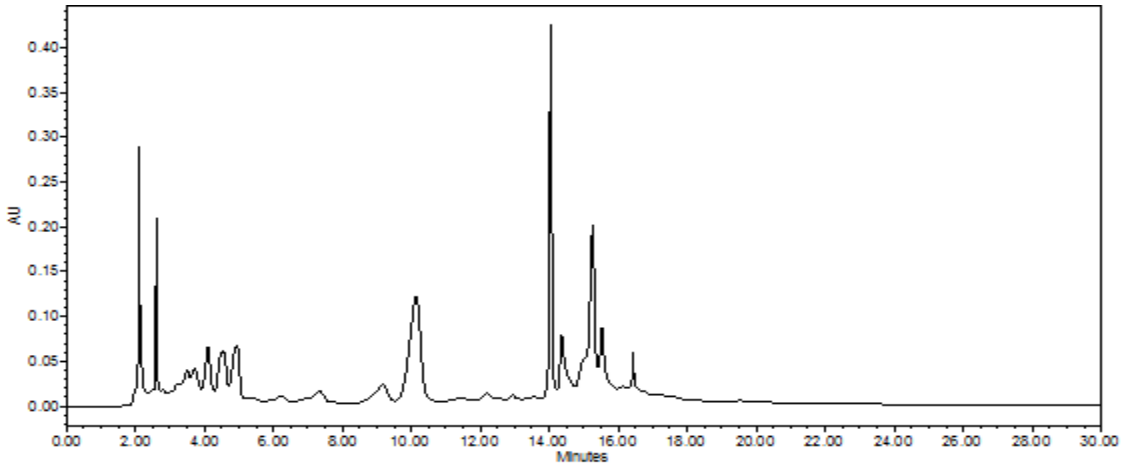

Figure 4.12: LC-UV chromatogram obtained at 280 nm for the HILIC analysis of the MeOH extract of the leaves of *H. argyrosphaerum* using a gradient: 100→60 % B (20 min). Using a mobile phase consisting of 5 mM of AF in water with 5% ACN (phase A)/ 5 mM of AF in water with 95 % ACN (phase B). A Phenomenex Luna HILIC column was used.

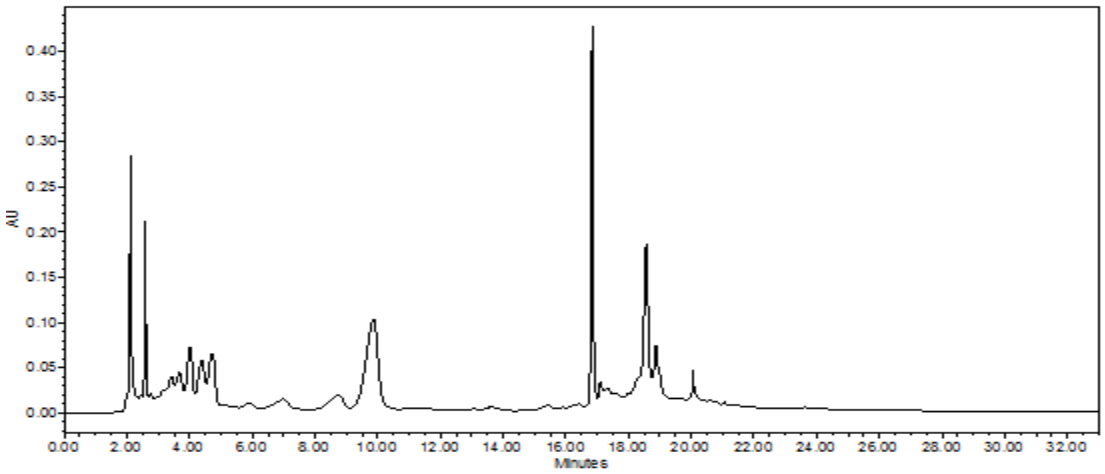

Figure 4.13: LC-UV chromatogram obtained at 280 nm for the HILIC analysis of the MeOH extract of the leaves of *H. argyrosphaerum* using a gradient: 100→65 % B (20 min). Using a mobile phase consisting of 5 mM of AF in water with 5 % ACN (phase A)/ 5 mM of AF in water with 95 % ACN (phase B). A Phenomenex Luna HILIC column was used.

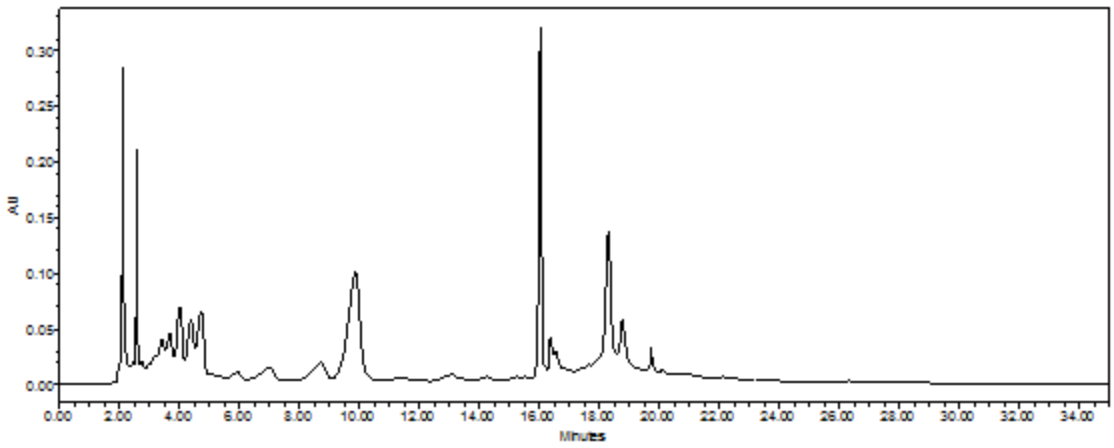

Figure 4.14: LC-UV chromatogram obtained at 280 nm for the HILIC analysis of the MeOH extract of the leaves of *H. argyrosphaerum* using a gradient: 100→80 % B (20 min). Using a mobile phase consisting of 5 mM of AF in water with 5% ACN (phase A)/ 5 mM of AF in water with 95 % ACN (phase B). A Phenomenex Luna HILIC column was used.

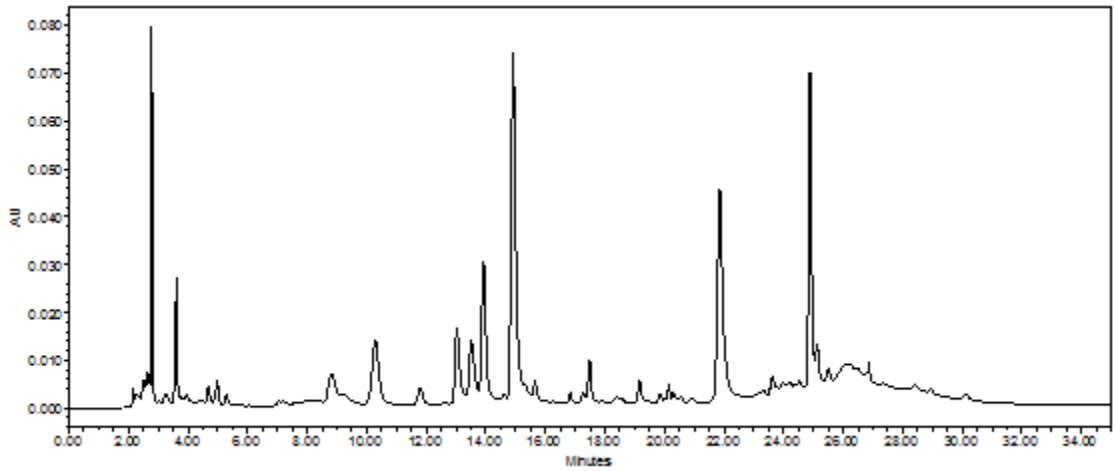

Figure 4.15: LC-UV chromatogram obtained at 280 nm for the HILIC analysis of the MeOH extract of the leaves of *H. argyrosphaerum* using a gradient: 100→80 % B (20 min). Using a mobile phase consisting of 5 mM of AF in water with 5% ACN (phase A)/ 5 mM of AF in water with 95 % ACN (phase B). An Xbridge BEH Amide HILIC column was used.

Ascentis column with dimensions of 250.0 mm in length (L_2) and a 10.0 mm I.D. packed with 5.0 µm particles. The flow rate was translated to 6.8 mL/min (F2) using the equation (1) and the gradient time was translated to 50 minutes (G2) using equation (2). The 50 minute gradient was set up as follows: 0→100 % B (0-50 min), 100 % B isocratic (50-51.6 min) and returned to initial conditions at 52.4 minutes. However, the calculated gradient time of 50 minutes was changed to 70 minutes to allow better separation by increasing time for complete partition (Figure 4.19) since the diameter of the Ascentis column is almost double to that of the Kinetex column. The flow rate was reduced to 4.00 mL/min due to observed high pressures from higher flow rates.

$$F2 = F1 \times \left(\frac{\pi r_2}{\pi r_1}\right)^2 \quad (1)$$

$$G2 = G1 \times \frac{L_2}{L_1} \quad (2)$$

F1 = initial flow rate, F2 = final flow rate, G1 = initial gradient, G2 = final gradient, r_1 = initial column radius, r_2 = final column radius, L_1 = initial column length, L_2 = final column length.

The injection volume of 50.00 µL was used. The 70 minute gradient time was shortened in order to save mobile phase and time of fraction collection. This method was further optimised to a short-run method with the gradient set up: 0→64 % B (0-45 min), 64→100 % B (45-46 min), 100 % B isocratic (46-50 min) and returned to initial conditions at 51 minutes (Figure 4.20). All subsequent semi-preparative HPLC separation experiments were performed using this method. The separation was repeated 16 times, each time collecting six fractions into six separate 250.00 mL round bottom flasks. These fractions, compounds **1**-**3**, **5**-**7** (Figures 4.19 and 4.20), were then concentrated and stored in HPLC vials for further analysis. Unfortunately, one fraction (compound **4**) could not be collected and two fractions were lost with the solvent during nitrogen (N_2) drying and not enough material was obtained after N_2 drying for

the rest of the fractions which in turn were not enough for NMR analysis. LC-MS analysis was done to determine the purity of four of the isolated compounds (Figure 4.21). Compound **1** and **2** were >70 % pure, compound **6** was >80 % pure and compound **5** was relatively pure (>90 %) (Figure 4.21) proving that the developed method is suitable for the isolation of flavonoids of *H. argyrosphaerum* in the future.

In a study by Albayrak and co-workers (25), phenolics and flavonoids of 16 difference *Helichrysum* species from Turkey were identified using HPLC-DAD analysis (RPLC). The identities of the compounds were confirmed using reference standards. An Eclipse XDB-C_{18} column (Agilent) with 5 µm particles and dimensions, of 250 mm × 4.6 mm i.d., similar to the Kinetex C_{18} column used in this study was used. In addition, MeOH extracts were analysed and MeOH was also used as the organic modifier in the mobile phase. In another study, a phloroglucinol derivative from *H. caespititium* was isolated in a pure form by HPLC in H_2O-Ethanol (1:1) on a reverse phase Phenomenex column with dimensions (250 mm × 4.60 mm i.d.) and 5 µm particle size (5).

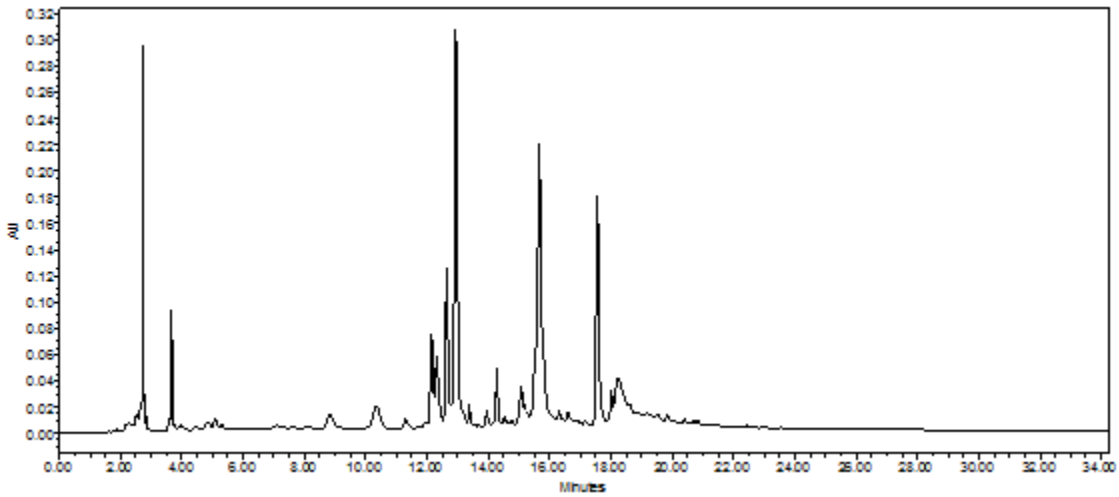

Figure 4.16: LC-UV chromatogram obtained at 280 nm for the HILIC analysis of the MeOH extract of the leaves of *H. argyrosphaerum* using a gradient: 100→60 % B (20 min). Using a mobile phase consisting of 5 mM of AF in water with 5% ACN (phase A)/ 5 mM of AF in water with 95 % ACN (phase B).An Xbridge BEH Amide HILIC column was used.

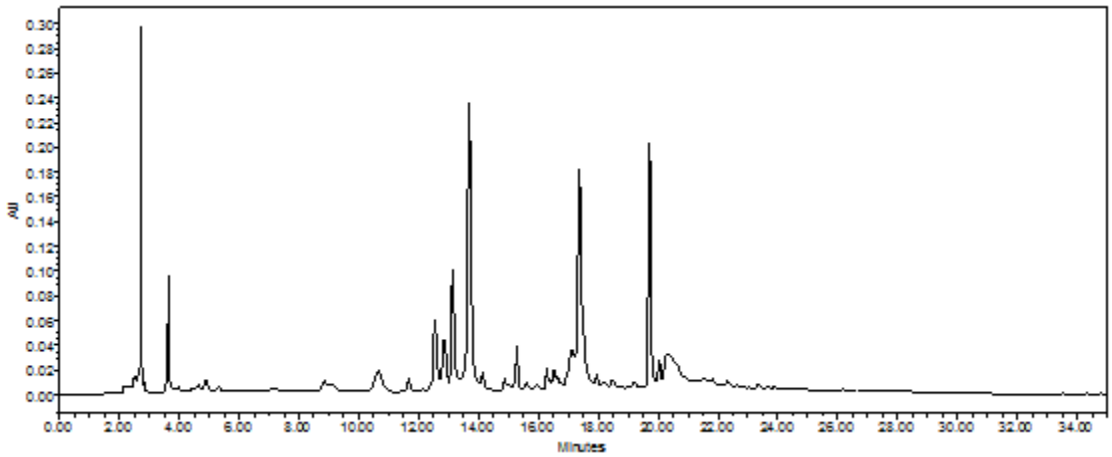

Figure 4.17: LC-UV chromatogram obtained at 280 nm for the HILIC analysis of the MeOH extract of the leaves of *H. argyrosphaerum* using a gradient: 100→70 % B (20 min). Using a mobile phase consisting of 5 mM of AF in water with 5% ACN (phase A)/ 5 mM of AF in water with 95 % ACN (phase B). An Xbridge BEH Amide HILIC column was used.

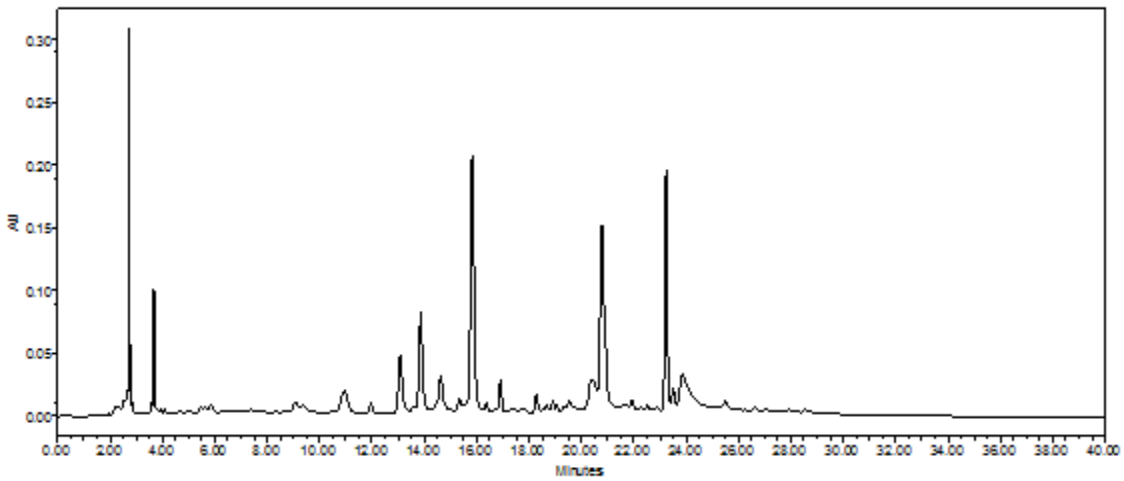

Figure 4.18: LC-UV chromatogram obtained at 280 nm for the HILIC analysis of the MeOH extract of the leaves of *H. argyrosphaerum* using a gradient: 100→80 % B (20 min), 80 % B isocratic (8 min). Using a mobile phase consisting of 5 mM of AF in water with 5% ACN (phase A)/ 5 mM of AF in water with 95 % ACN (phase B). A 2.5 µm Xbridge BEH Amide column was used.

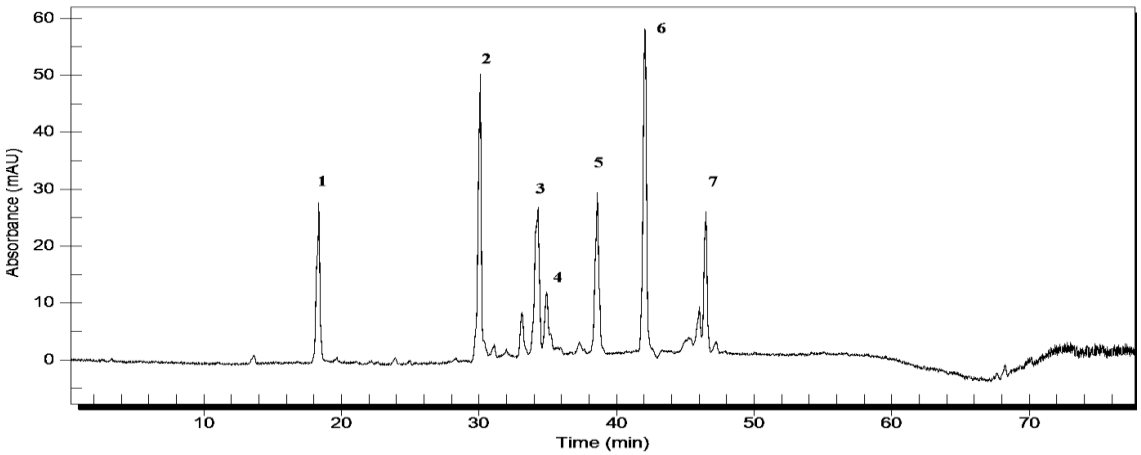

Figure 4.19: LC-UV chromatogram of the semi-preparative RPLC analysis of the MeOH extracts of the flowers of *H. argyrosphaerum* observed at 280 nm using a gradient: 100 % A to 100 % B in 70 minutes using a mobile phase consisting of 0.1 % FA in 5 % MeOH (phase A)/ 0.1 % FA in MeOH (phase B) for the isolation of compounds **1-7**.

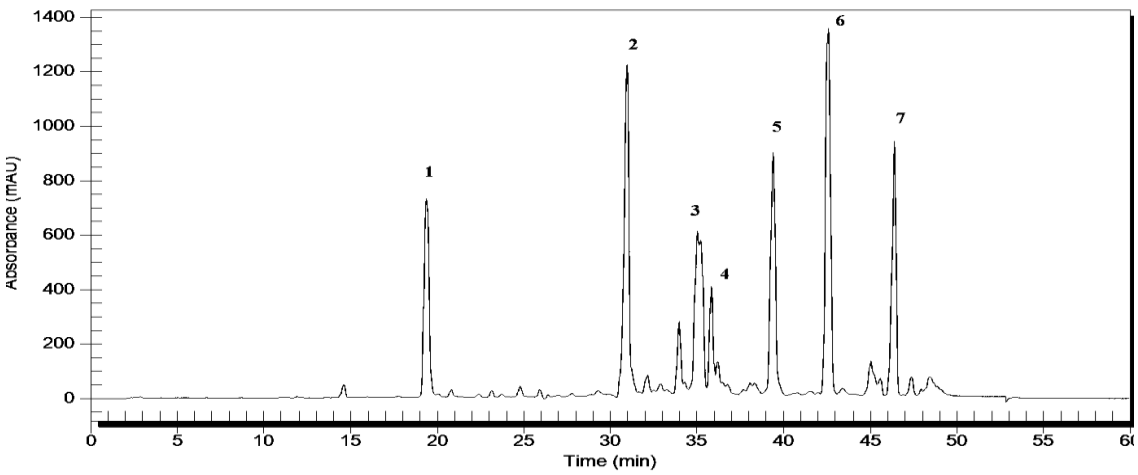

Figure 4.20: LC-UV chromatogram of the semi-preparative RPLC analysis of the MeOH extracts of the flowers of *H. argyrosphaerum* observed at 280 nm using a gradient: 100 % A to 100 % B in 45 minutes using a mobile phase consisting of 0.1 % FA in 5 % MeOH (phase A)/ 0.1 % FA in MeOH (phase B) for the isolation of compounds **1-7**.

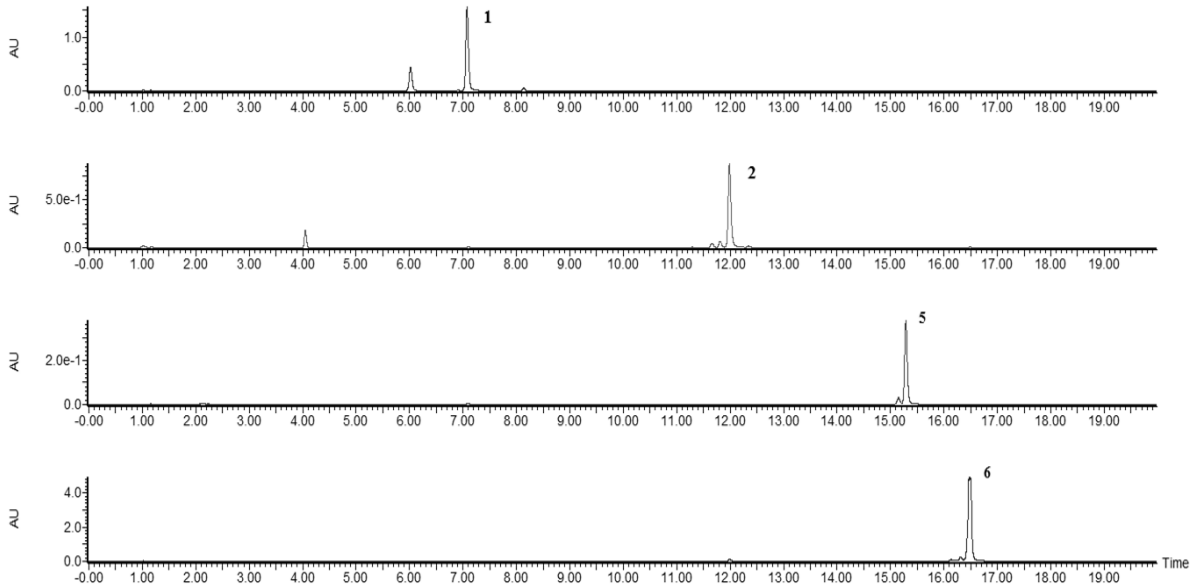

Figure 4.21: TWCs of the RPLC-UV-MS analysis of the isolated compounds **1**, **2**, **5** and **6** detected in the *H. argyrosphaerum* MeOH extract of the flowers.

4.4. Identification of the major constituents in the MeOH extract of the flowers of *H. argyrosphaerum*.

Solutions of the MeOH extracts (*ca.* 10 mg/mL in MeOH) of the flowers, stems and leaves of *H. argyrosphaerum* were analysed by HPLC-UV-HRMS/MS using the optimised RPLC-MS and HILIC-MS methods (Figure 4.22 and 4.24). Eight prominent peaks were observed in the total wavelength chromatogram (TWC) (acquired by the PDA detector) of the MeOH extract of the *H. argyrosphaerum* flowers (Figure 4.22) which corresponds to the total ion chromatogram (TIC) in Figure 4.23. Only two of these compounds, were present in appreciable abundance in the MeOH extracts of the stems and the leaves.

Since the RPLC-UV-MS analysis of the MeOH extract of the flowers contain a higher number of prominent and better resolved peaks (Figure 4.22), only the MeOH extract of the flowers was further investigated. The HILIC-UV-MS only contained a few prominent but overlapping peaks from 22 to 26 minutes (Figure 4.24 and 4.25). The eight major compounds listed in Table 4.2 were tentatively identified based on the UV and the MS data obtained from the RPLC-UV-MS/MS analysis. The MS/MS spectra of five of the major compounds (**3**, **4**, **5**, **6** and **7**) contain the same major product ion peak at *m/z* 271.0597 Da from which the same molecular formula, $C_{15}H_{11}O_5$, could be calculated which was found to be the formula of the compound that elutes at 17.56 minutes (**7**) which was subsequently identified as apigenin. The compounds that elute at 13.36 (compound **3**), 13.68 (compound **4**), 15.31 (compound **5**), 16.52 (compound **6**) and 17.56 (compound **7**) minutes are unique to the flower extract (Figure 4.22). The UV data of these compounds show that they are flavonoids.

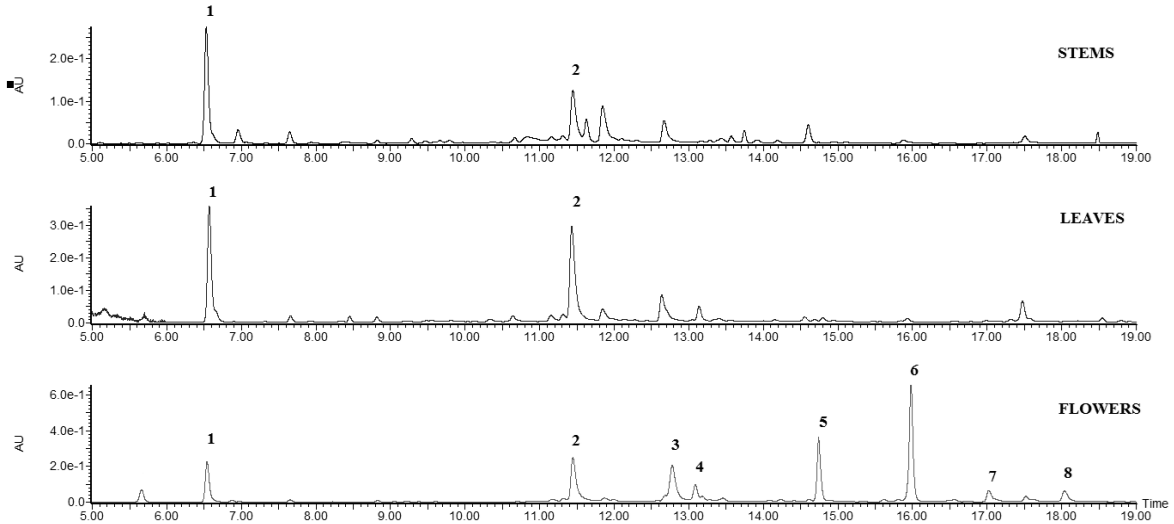

Figure 4.22: TWC of the RPLC-UV-MS analysis of the *H. argyrosphaerum* MeOH extracts of the stems, leaves and flowers recorded in positive ionisation mode using the optimised RPLC-MS method.

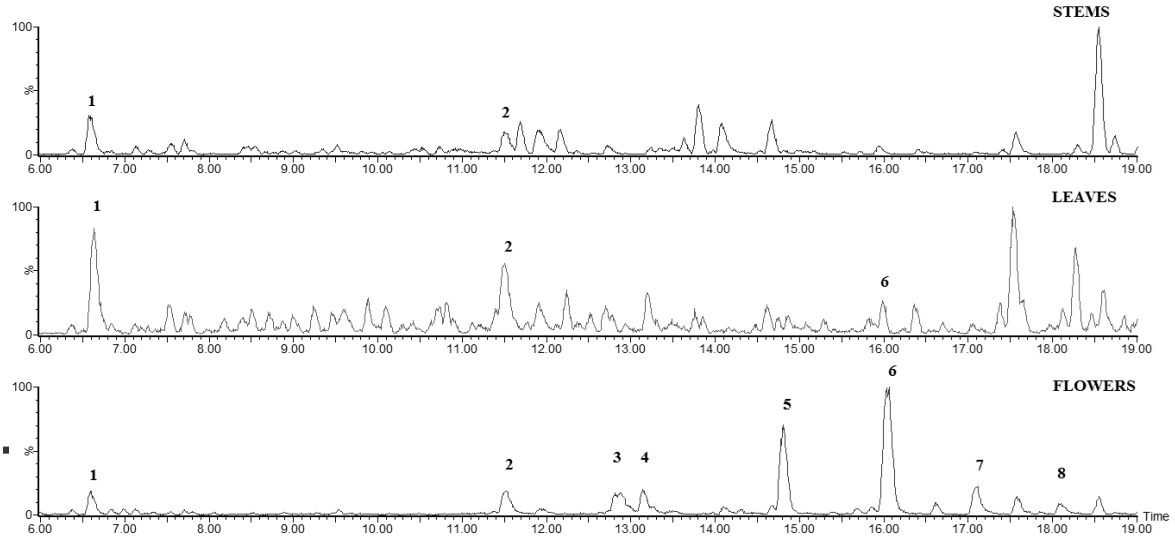

Figure 4.23: TIC of the RPLC-UV-MS analysis of the *H. argyrosphaerum* MeOH extracts of the stems, leaves and flowers recorded in positive ionisation mode using the optimised RPLC-MS method.

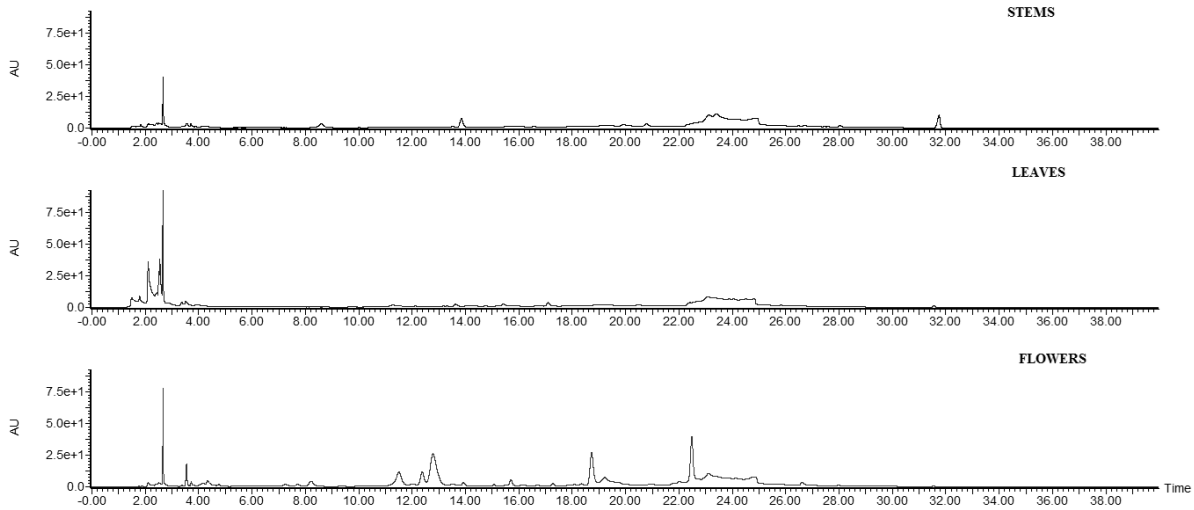

Figure 4.24: TWC of the HILIC-UV-MS analysis of the *H. argyrosphaerum* MeOH extracts of the stems, leaves and flowers recorded in positive ionisation mode using the optimised HILIC-MS method.

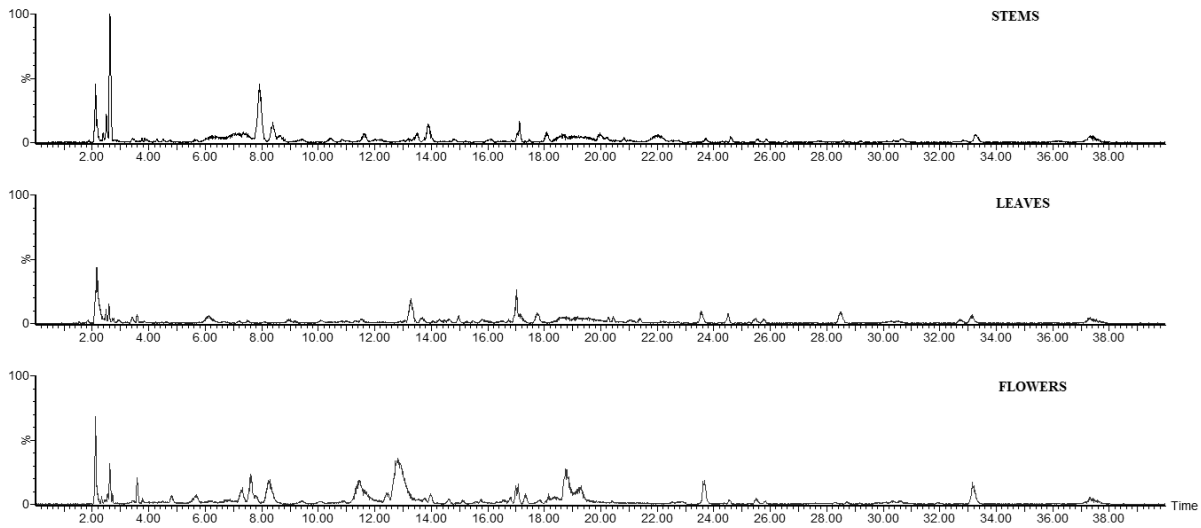

Figure 4.25: TIC of the HILIC-UV-MS analysis of the *H. argyrosphaerum* MeOH extracts of the stems, leaves and flowers recorded in positive ionisation mode of the optimised HILIC-MS method.

Table 4.2: Major compounds tentatively identified in the methanol extract of the flowers of *H. argyrosphaerum*

Peak number	Retention time	Constituent	Mass of $[M+H]^+$	$[M+H]^+$ ion formula	Mass of major product ion	Product ion formula	Flowers	Stems	Leaves
1	7.12	Chlorogenic acid[a]	355.1021	$C_{16}H_{19}O_9$	163.0402	$C_9H_7O_3$	√	√	√
2	12.01	1'→3-Lactone-4,5-di-O-caffeoylquinic acid	499.1238	$C_{25}H_{23}O_{11}$	163.0393	$C_9H_7O_3$	√	√	√
3	13.36	Apigenin-7-O-glucuronopyranoside or Apigenin-7-O-galacturonopyranoside	447.0911	$C_{21}H_{19}O_{11}$	271.0591	$C_{15}H_{11}O_5$	√	×	×
4	13.68	Apigenin-4'-O-glucopyranoside	433.1134	$C_{21}H_{21}O_{10}$	271.0595	$C_{15}H_{11}O_5$	√	×	×
5	15.31	Apigenin-7-O-glucoside-[6"-O-(4-carboxyl-3-methylbutanoyl)]	577.1545	$C_{27}H_{29}O_{14}$	271.0598	$C_{15}H_{11}O_5$	√	×	×
6	16.52	Unknown apigenin-7-O-substituted diglycoside	619.1663	$C_{29}H_{31}O_{15}$	271.0603	$C_{15}H_{11}O_5$	√	×	√
7	17.56	Apigenin	271.0597	$C_{15}H_{11}O_5$	153.0193	$[^{1,3}A]^+$	√	×	×
8	18.51	Feruloylquinic acid derivative	877.4039	unknown	177.0551	$C_{10}H_{11}O_4$	√	×	×

[a]Identity confirmed with authentic standard.

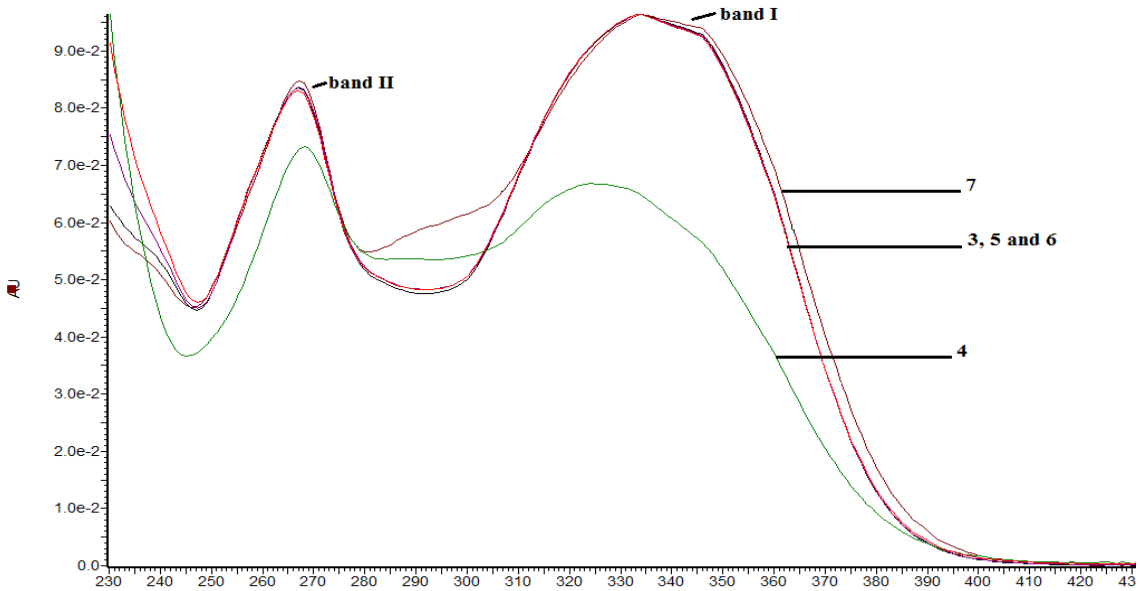

Figure 4.26: UV-vis spectra of compounds **3-7**, the major flavonoids detected in the MeOH extract of the flowers of *H. argyrosphaerum*.

4.4.1. Flavonoids

The UV spectra of compounds **3-7** (Figure 4.26) have major absorbance bands at *ca.* 265 and 335 nm. The UV spectra of flavones and flavonols exhibit two major absorption peaks in the region 240–400 nm (in the mobile phase: MeOH-acidic water), commonly referred to as band I (300–380 nm) and band II (240–280 nm) (15,16,18). Band I is considered to be the absorption due to the B-ring cinnamoyl system, and band II the absorption involving the A-ring benzoyl system (15). Based on this evidence, it was deduced that compounds **3-7** are flavonoids.

4.4.1.1 Apigenin and apigenin glycosides

The MS spectrum of compound **7** (Figure 4.27B) has a base peak at *m/z* 271. Another prominent peak is observed at *m/z* 293 which represents an ion with a mass of 22 Da more than the former ion. Hence, it is assumed that the ions at *m/z* 271 and 293 are the precursor ($[M+H]^+$) and sodium adduct ($[M+Na]^+$) ions, respectively. The accurate

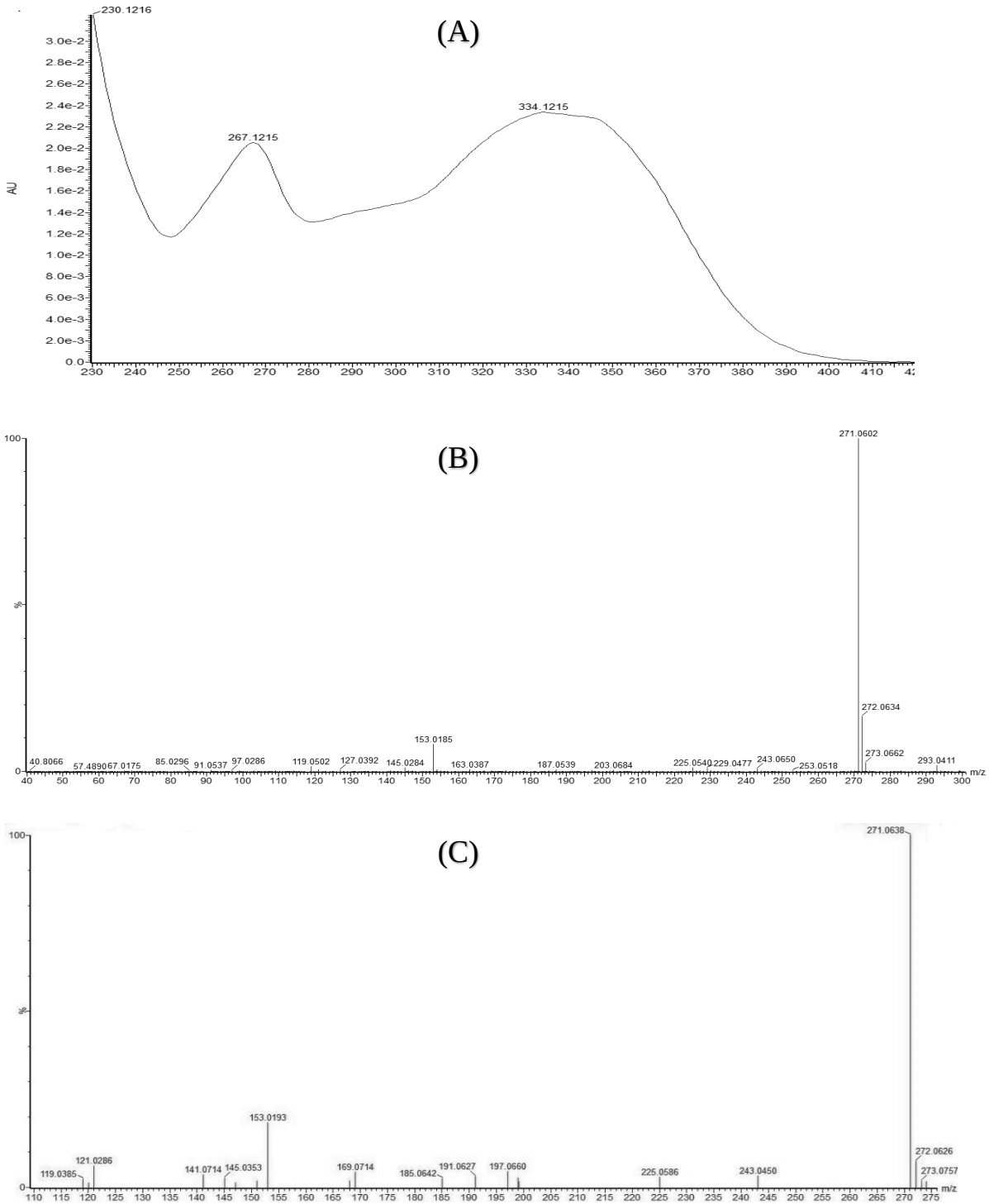

Figure 4.27: UV-vis spectrum (A), MS spectrum (B) and MS/MS spectrum (C) of compound **7**, tentatively identified as apigenin in the MeOH extract of the flowers of *H. argyrosphaerum*.

mass of the $[M+H]^+$ ion was measured (271.0602 Da), the elemental composition was calculated to be $C_{15}H_{11}O_5$ and hence the molecular formula of the neutral molecule is $C_{15}H_{10}O_5$. The MS spectra of only two flavones with this formula, apigenin and trihydroxyisoflavone, were found in the NIST mass spectra search database software version 2.0 (NIST MS Search 2.0). The $[M+H]^+$ ion also appear at *m/z* 271 in the MS/MS spectrum of compound 7 (Figure 4.27C). The fragmentation of the $[M+H]^+$ ion produces the most abundant peak at *m/z* 153 with the second most abundant peak observed at *m/z* 121 (Figure 4.27C). The ions that are expected to be formed during the fragmentation of apigenin (Figure 4.28) were compared to the peaks observed in the MS/MS spectrum of compound **7** (Figure 4.27C), and the following similarities were detected. The $[^{1,3}A]^+$ ion was observed at *m/z* 153, $[^{0,2}B]^+$ at *m/z* 121, $[^{1,3}B]^+$ at *m/z* 119, $[^{1,3}B\text{-}CO]^+$ at *m/z* 91, $[^{1,3}B\text{-}H_2O\text{-}CO]^+$ at *m/z* 73, $[^{0,4}B]^+$ at *m/z* 163, $[^{1,4}A_0]^+$ at *m/z* 125 and $[^{0,4}B\text{-}H_2O]^+$ at *m/z* 145. Therefore the proposed fragmentation mechanisms and the MS/MS spectrum indicated that compound **7** may be apigenin. However, there are two isobaric aglycones, genistein and pelargonidin that have similar but not identical mass spectra to that of apigenin (17).

According to the MS experiments performed by Abrankó and Szilvássyin (17), the four diagnostic ions to distinguish between apigenin, genistein and pelargonidin are observed at *m/z* 215, 153, 141 and 121 which are present in the MS/MS spectrum of compound **7** except the ion at *m/z* 215 which was not detected. The ions observed at *m/z* 119, 153 and 271 are the characteristic ions found in the MS/MS spectrum of apigenin, with the ion observed at *m/z* 153 being the most abundant fragment of the precursor ion observed at *m/z* 271 (21). Apart from the base peak, the most prominent peak in the MS/MS spectrum of compound **7** is the peak observed at *m/z* 153. This is the case for apigenin and genistein but not the case for pelargonidin (17). In the

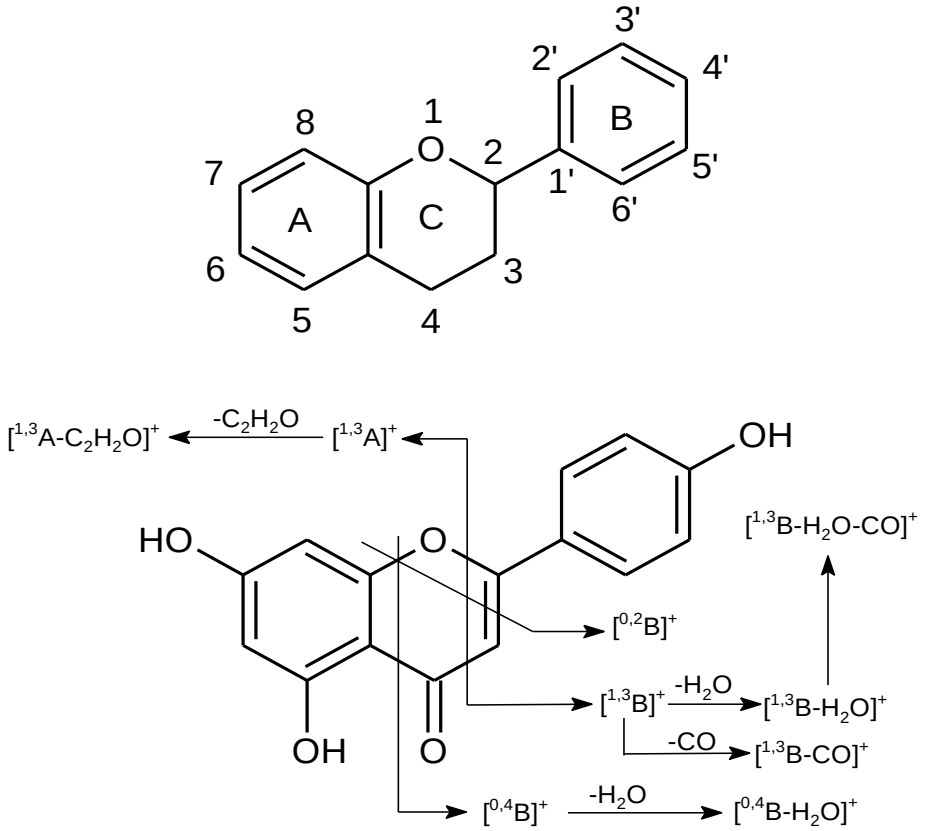

Figure 4.28: Proposed MS/MS fragmentation reactions of apigenin.

MS/MS spectrum of apigenin, the $[^{0,2}B]^+$ ion at *m/z* 121 was present at a higher relative abundance than the ion at *m/z* 141 (17) which compares well with what is observed in the MS/MS spectrum of compound **7** in Figure 4.27C. In addition, the MS/MS spectrum has $[^{1,3}B]^+$ and $[^{0,4}B\text{-}H_2O]^+$ ions at *m/z* 119 and 145 respectively, which were reported to be unique to the spectrum of apigenin (17). Based on this information, compound **7** was tentatively identified as apigenin (Figure 4.28).

Apigenin is a cell permeable polyphenol and bioactive (anti-inflammatory, antioxidant) component commonly found in red wine, buck wheat, red pepper, tomato skin, grape fruit, onions, oranges, tea, chamomile, and many vegetables such as parsley, mainly isolated from the buds and flowers of *Hypericum perforatum* (47,48).

It has a typical flavone structure with hydroxyl groups attached to positions 4', 5 and 7 (Figure 4.28). The ring system is also conjugated through the carbonyl at position 4 and the double bond present at position 2. Sugar moieties can attach to any of the hydroxyl groups of this aglycone to form O-glycosides with added bioactivities and are found in nature. This polyphenol aglycone has *in vitro* anticancer activity against malignant cancers such as colon, skin, lung, prostate (cancer stem cells and prostate cancer PC3 cells), ovarian (ovarian carcinoma HO-8910PM cells) and breast cancer (16,47,48). Apigenin has been reported to exhibit anti-bacterial activities against *Staphylococcus aureus* and methicillin-resistant *S. aureus* strains with tested MIC values of 3.9 – 15.6 µg/mL (20,49).

Since the MS/MS spectra of compounds **3** – **6** also contain the diagnostic ions that appear in the MS/MS spectrum of compound **7**, it was deduced that they are all flavones that contain apigenin as the aglycone (i.e. apigenin glycosides). However, compounds **3** - **6** are specifically apigenin-glycosides because diagnostic ions observed for apigenin (m/z 119, m/z 121, m/z 145, m/z 153 and m/z 271) are also observed in the MS/MS spectra of these compounds. In addition, their UV spectra are similar suggesting that their aglycone is the same. These compounds are also specifically O-glycosides because of the presence of the Y_0 ion observed at m/z 271 in their respective MS spectra that is evidence of the presence of the O-glycosidic bond found in flavonoid-O-glycosides that is cleaved under low collision energy conditions during fragmentation, leading to the loss of neutral sugar residues leaving the aglycone ion (Y_0) (Figure 4.30), in the case of monoglycosides, but the acid resistant C-C bonds found in flavonoid-C-glycosides will follow a different fragmentation pattern (15,18,21). It was reported that *O*- and *C*- glycosylation in A-ring has little or no effect on UV–vis spectra, but glycosylation in B-ring causes shifts of band I to lower

wavelengths, this effect being higher for a resonant position 4' than for a non-resonant position 3'(15). However, the detection of glycosylation or the differentiation between the type of glycosylation (*O*-, *C*- or *O, C*-) is impossible with the aid of UV spectra alone (15). In the UV spectrum of compound **4** (Figure 4.26) such a shift is observed compared to the other compounds. UV spectra can be used, however, to determine if there is a substitution at position 4' on the aglycone. This causes a shift of band I to a lower wavelength. Hence, this compound was tentatively identified as an apigenin-4'-O-glycoside. On the other hand substitution at position **7** of the aglycone causes no shift, hence compounds **3**, **5** and **6** were tentatively identified as apigenin-7-O-glycosides.

The MS spectrum of compound **5** (Figure 4.29B) shows a base peak at *m/z* 577 which is the $[M+H]^+$ ion. The peak found 22 units higher, at *m/z* 599, appears to be the corresponding sodium adduct, hence confirming that the $[M+H]^+$ ion is indeed observed at *m/z* 577, and hence the molecular weight of the compound is 576 Da. A molecular formula of $C_{27}H_{29}O_{14}$ was calculated for the $[M+H]^+$ ion from its accurate mass (577.1546 Da). Subsequently the molecular formula of the neutral molecule, $C_{27}H_{28}O_{14}$, was entered in the DNP (50) yielding a number of matches including maysin, cassiaoccidentalin B and 5, 7-dihydroxy-4'-methoxy-8-C-hexosyl-6-C-pentosylflavone. A number of flavonoid-C-glycosides and flavonoid-O-glycosides were found. However, because of the labile nature of the O-glycosidic bond found in flavonoid-O-glycosides ensures cleavage that leads to loss of neutral sugar residues leaving the aglycone ion (Y_0), and the acid resistant C-C bonds found in flavonoid-C-glycosides will follow a different fragmentation pattern. Based on this information, it was concluded that compound **5** is an O-glycoside. Since this is true for compound **5**,

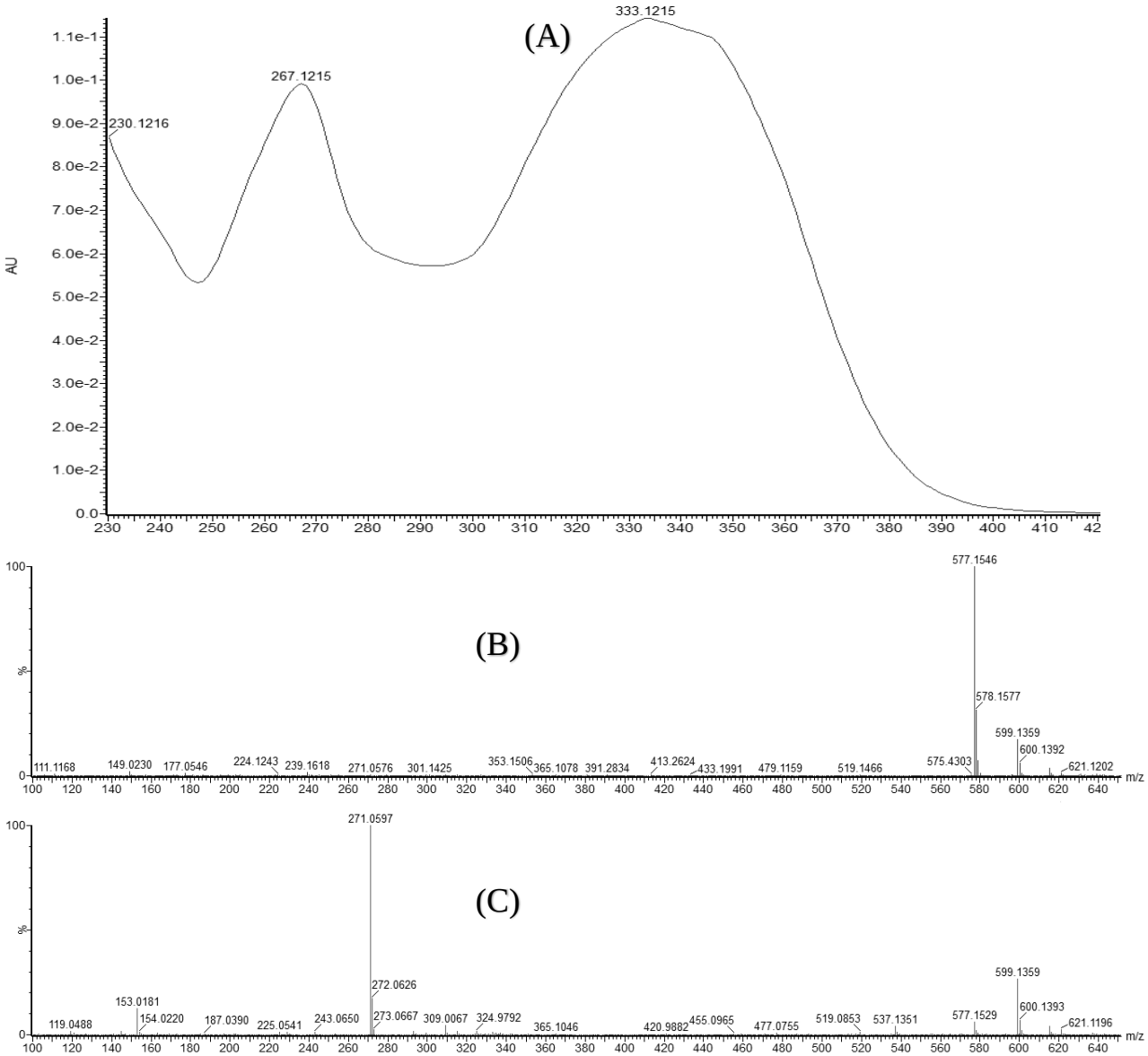

Figure 4.29: UV-vis spectrum (A), MS spectrum (B) and MS/MS spectrum (C) of compound **5** tentatively identified as apigenin-7-O-β-D-glucoside-[6”-O-(4-Carboxy-3-hydroxy-3-methylbutanoyl)] in the MeOH extract of the flowers of *H. argyrosphaerum*.

the list of possible compounds was then reduced to apigenin-7-O-β-D-glucoside-[6”-O-(4-Carboxy-3-hydroxy-3-methylbutanoyl)].

The MS/MS spectrum of compound **5** (Figure 4.29C) shows the fragments of the $[M+H]^+$ ion and a significant reduction in the size of the peak at *m/z* 577 serving as further proof that this peak represents the $[M+H]^+$ ion. Further confirmation of the sodium adduct is that it does not fragment hence no significant reduction in the relative abundance of the peak at *m/z* 599 will be observed (Figure 4.29C). The most abundant ion (Y_0) will be observed at *m/z* 271 as the product ion resulting from the cleavage of the O-C glycosidic bond. The MS/MS spectrum of compound **5** similar to that of compound **7** displays ions at *m/z* 119, 153 and 271 that are characteristic to the MS/MS spectrum of apigenin confirming that the aglycone is also apigenin. Since the aglycone of compound **5** is apigenin, the compound, apigenin-7-O-β-D-glucoside-[6”-O-(4-Carboxy-3-methylbutanoyl)] (Figure 4.30), was the only possible match in the DNP search that contain apigenin as its aglycone. The additional ions B_1 at *m/z* 145 and B_2 at *m/z* 309 observed in the MS/MS spectrum of compound **5** support that this compound is apigenin-7-O-β-D-glucoside-[6”-O-(4-carboxy-3-methylbutanoyl)]. However, without NMR analysis it is not possible to confirm if the molecule is the β anomer and if it is the D enantiomer. Compound **5** can be the substituted apigenin-7-O-β-D-glucopyranoside, an anti-HIV active principle that was isolated from *Kummerowia striata*. It was also isolated from *Centaurea urvillei* and displayed antiproteasomal (anticancer) activity (51,52). This compound has glucose as its sugar moiety and has extra functional groups that appear to alter its bioactivity from that of an unsubstituted apigenin-7-O-β-D-glucopyranoside.

The MS spectrum of compound **6** (Figure 4.31B) displays a base peak at *m/z* 619 which is the precursor ion $[M+H]^+$ and the presence of the sodium adduct at *m/z* 641 confirms it. The isotope peak at *m/z* 620 is observed next to the base peak. The calculated

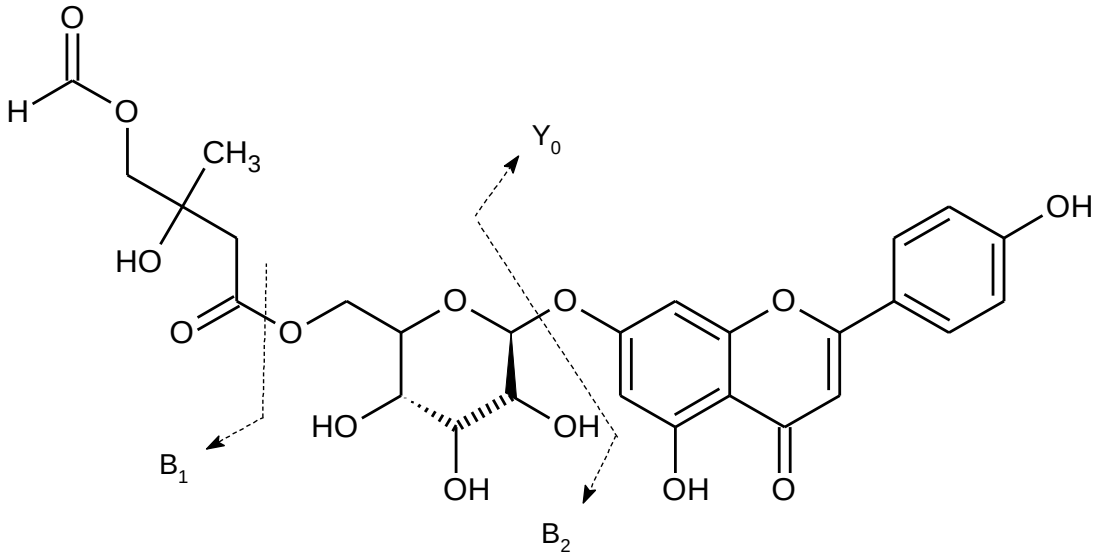

Figure 4.30: Compound **5** is tentatively identified as apigenin-7-O-β-D-glucoside-[6”-O-(4-carboxy-3-methylbutanoyl)]. The cleavage of its O-glycosidic bond to produce its most abundant product ion (Y_0) observed at *m/z* 271.

elemental composition of the $[M+H]^+$ ion was $C_{29}H_{31}O_{15}$. The MS/MS spectra (Figure 4.31C) shows the fragmentation of the precursor ion and a significant reduction in the relative abundance of the peak at *m/z* 619 serves as proof that it is the $[M+H]^+$ ion and also the relative abundance of the sodium adduct peak at *m/z* 641 remains unchanged. The peak at *m/z* 271 represents the most abundant fragment of the $[M+H]^+$ ion at *m/z* 619. Based on the MS/MS spectrum (Figure 4.31B) and the UV spectrum (Figure 4.31A) of compound **6** with the comparison to those of compound **7**, the aglycone of this compound is apigenin. Hence, this compound must also be an apigenin-O-glycoside. Subsequently, the molecular formula of the neutral molecule, $C_{29}H_{30}O_{15}$, was compared to the formulae in the DNP (50) and none of the results were apigenin-O-glycosides.

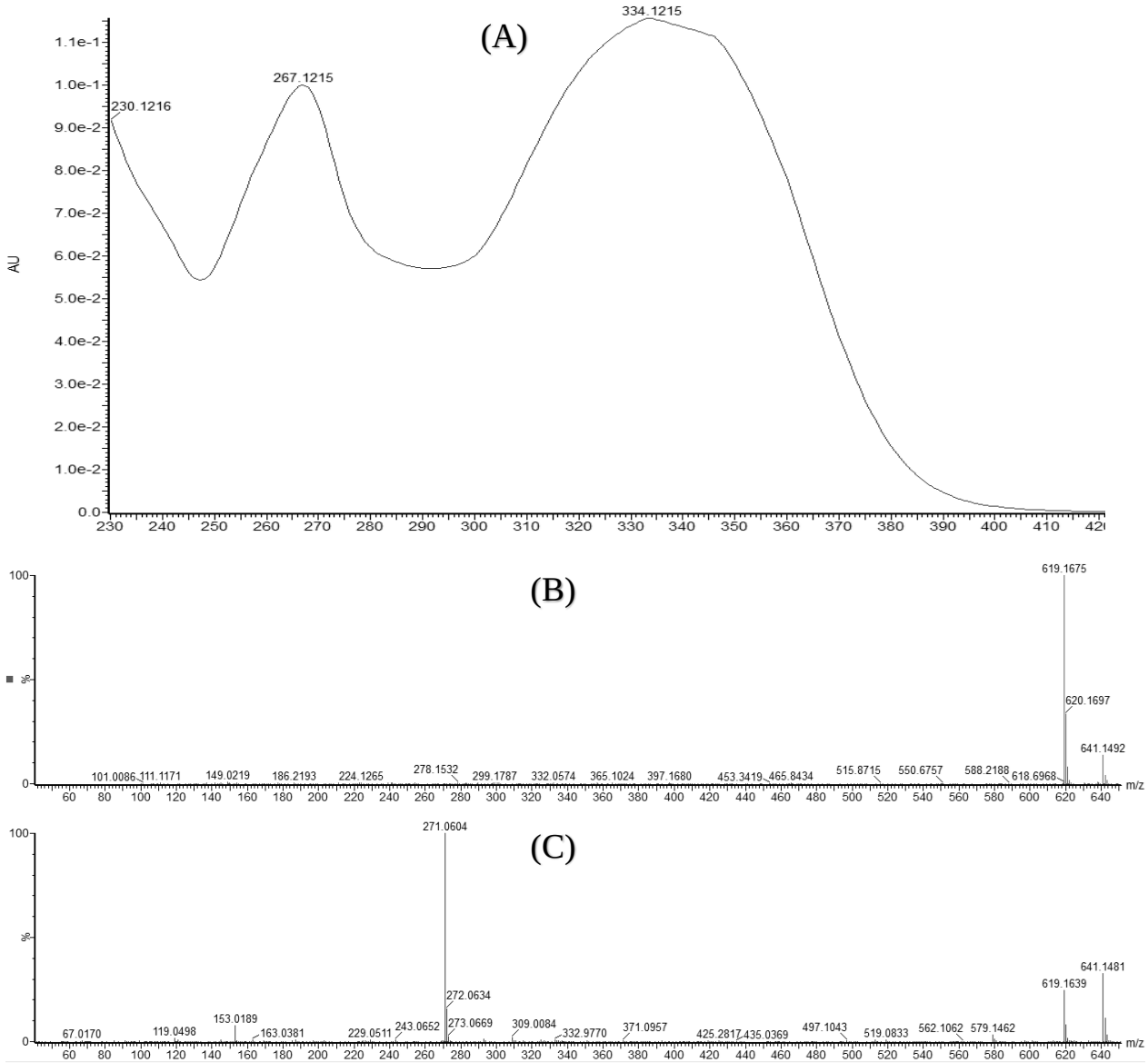

Figure 4.31: UV-vis spectrum (A), MS spectrum (B) and MS/MS spectrum (C) of compound **6**, tentatively identified as an apigenin-7-O-diglycoside in the MeOH extract of the flowers of *H. argyrosphaerum*.

Since the formula of compound **6** was not found in the NIST MS Search 2.0 either, the sugar moiety attached to the apigenin aglycone is still unknown. The difference between the molecular mass of the product ion from that of the precursor ion is the molecular mass of the sugar moiety (348 Da). This suggests that the sugar moiety is

highly substituted or a substituted disaccharide. Possible disaccharide sugar moieties of flavonoids that are commonly found in nature are rutinoside, neohesperidoside, gentiobioside, diglucuronide, apiosyl-glucoside, malonoyl-apiosyl-glucoside and sophoroside (53,54). Rutinoside, neohesperidoside, diglucuronide, apiosyl-glucoside and malonoyl-apiosyl-glucoside were specifically reported for apigenin (54). However, the sugar moiety attached to apigenin remains unknown because none of the sugar moieties mentioned above has a mass that corresponds to 348 Da.

The MS spectrum of compound **3** (Figure 4.32B) displays the $[M+H]^+$ ion at *m/z* 447 with the calculated elemental composition of $C_{21}H_{19}O_{11}$ and the neutral molecule therefore, has the molecular formula of $C_{21}H_{18}O_{11}$. The MS/MS spectrum (Figure 4.32C) of this compound displays a prominent product ion at *m/z* 271 (Y_0) with the calculated formula of $C_{15}H_{11}O_5$ and the neutral molecule having the molecular formula of $C_{15}H_{10}O_5$. As before, it was determined that the aglycone of this compound is also apigenin. The molecular formula of $C_{21}H_{18}O_{11}$ was entered into the DNP and produced two possible matches, apigenin-7-O-β-D-galacturonopyranoside and apigenin-7-O-β-D-glucuronopyranoside, which are flavonoids that consist of the aglycone apigenin and sugar acids (Figure 4.33) of galactose and glucose respectively. Besides the presence of the Y_0 ion in the MS/MS spectrum of compound **3** as proof for the possible structures, the ions $^{0,2}X_0$ and $^{1,3}B_0$ are also observed at *m/z* 315 and 119 respectively. However, it is not possible to distinguish between the two possibilities based on the UV and MS data alone because the sugars do not absorb in the UV range and they are stereoisomers that have identical fragment ions. In addition, without NMR analysis it is also not possible to determine if the molecule is an α or a β anomer or whether it is a D or L enantiomer of either of the two proposed structures. Hence, compound **3** was tentatively identified as apigenin-7-O-galacturonopyranoside or apigenin-7-O-

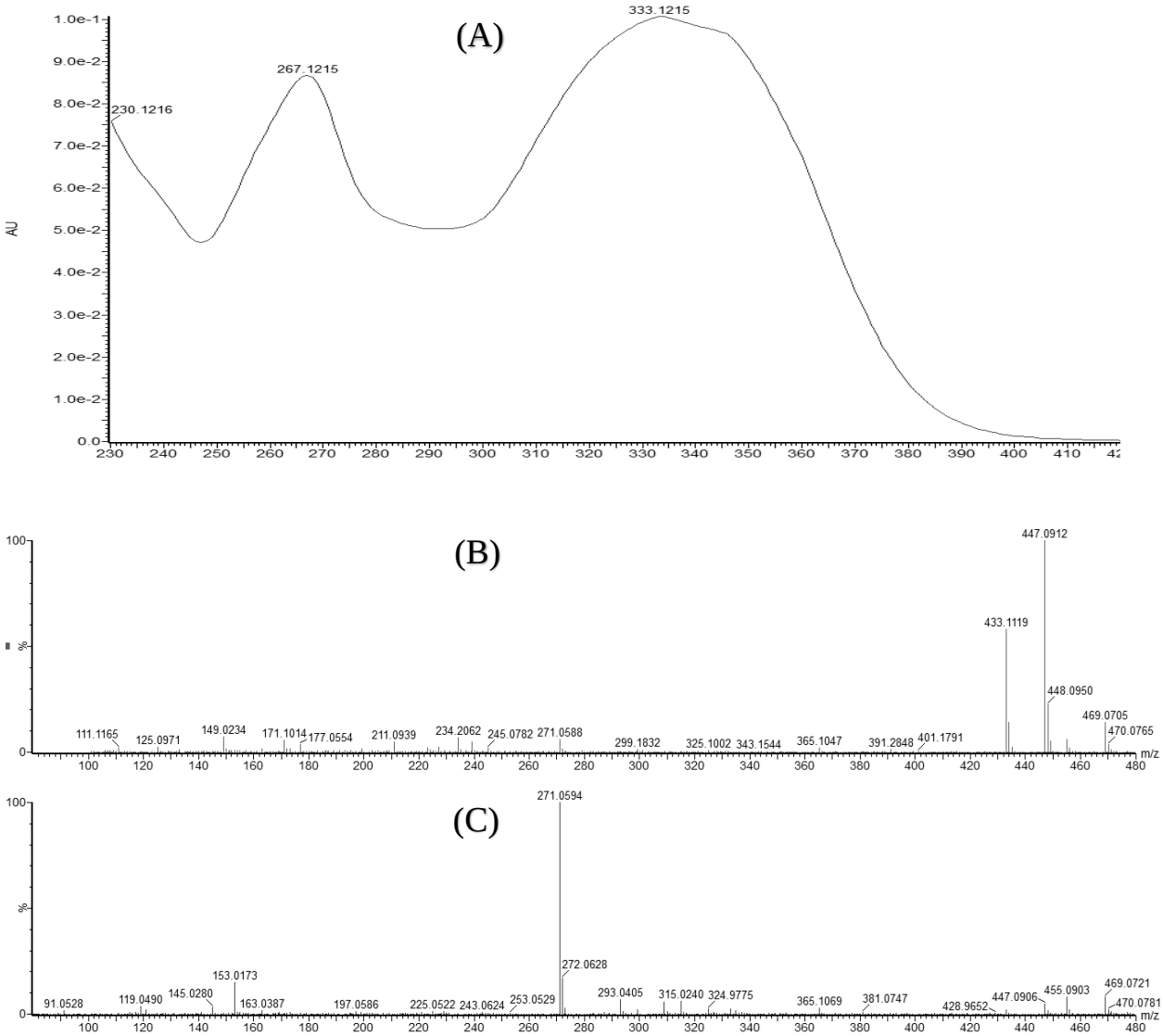

Figure 4.32: UV-vis spectrum (A), MS spectrum (B) and MS/MS spectrum (C) of compound **3**, tentatively identified as apigenin-7-O-galacturonopyranoside or apigenin-7-O-glucuronopyranoside in the MeOH extract of the flowers of *H. argyrosphaerum*.

glucuronopyranoside. These two glycosides are found in *Jacaranda mimosaefolia* and apigenin-7-O-glucuronopyranoside is also found in globe artichoke (54,55).

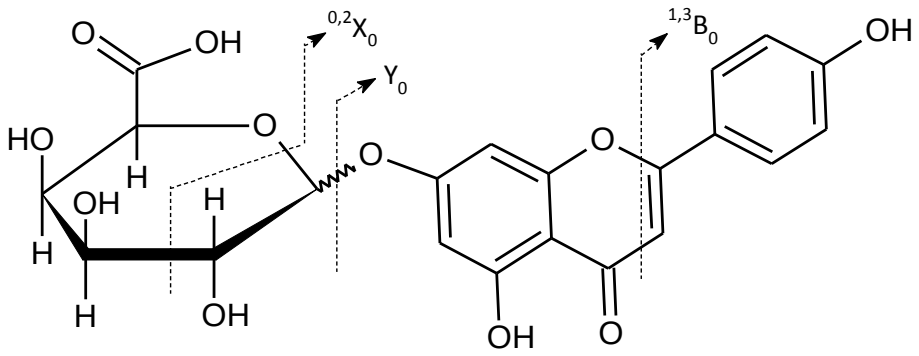

Galacturonopyranoside

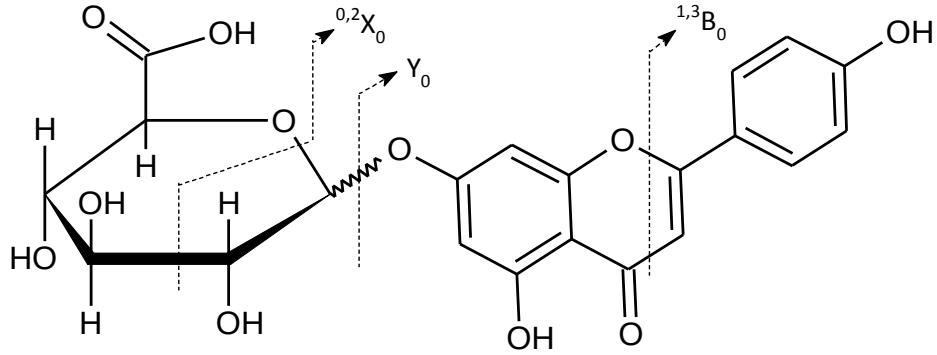

Glucuronopyranoside

Figure 4.33: Apigenin-7-O-glycosides with sugar acids as the sugar moieties that are possible structures of compound **3**.

The MS spectrum of compound **4** (Figure 4.34B) displays the $[M+H]^+$ ion peak at *m/z* 433 with the calculated elemental composition of $C_{21}H_{21}O_{10}$ and the neutral molecule therefore, has the molecular formula of $C_{21}H_{20}O_{10}$. The MS/MS spectrum (Figure 4.34C) displays a product ion (Y_0) at *m/z* 271 and the calculated formula of this ion was $C_{15}H_{11}O_5$ and the neutral molecule has the molecular formula of $C_{15}H_{10}O_5$. Once again, it was found that the aglycone of this molecule is also apigenin. The molecular formula, $C_{21}H_{20}O_{10}$, was entered in the NIST MS Search 2.0 and the DNP (50) to produce a list of possible identities of compound **4**. Since this compound is presumably an apigenin-O-glycoside, the list was reduced to include only the possible compounds that contain apigenin as the aglycone.

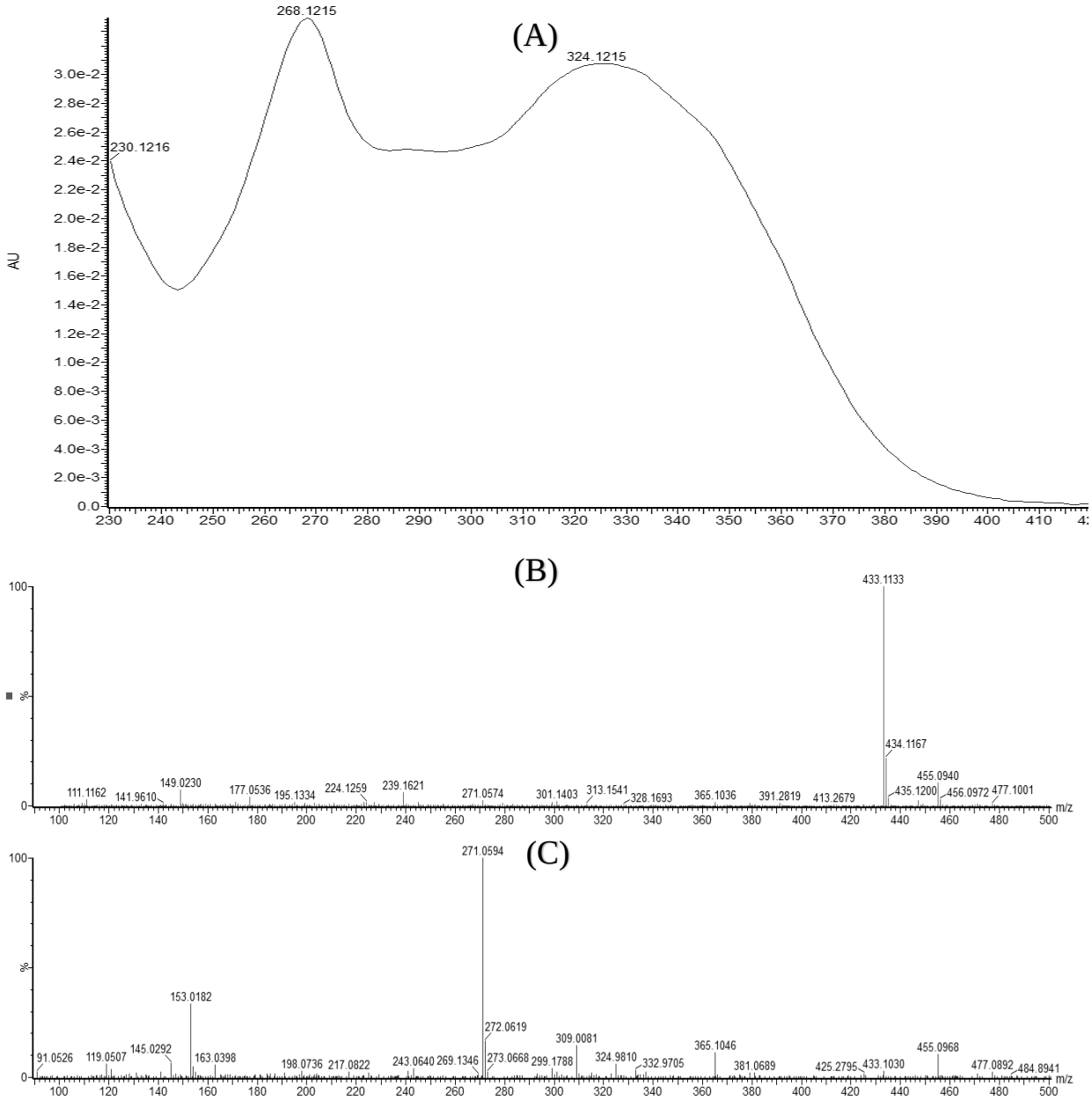

Figure 4.34: UV-vis spectrum (A), MS spectrum (B) and MS/MS spectrum (C) of compound **4**, tentatively identified as apigenin-4'-O-glucopyranoside in the MeOH extract of the flowers of *H. argyrosphaerum*.

The resulting possible structures were apigenin-O-glycosides with different sugar moieties. These sugars include galactose, glucose and allose which cannot be distinguished without the use of NMR. However, glycosylation of the B-ring causes a

shift of band I in the UV spectrum of flavonoids to lower wavelengths. In addition, this effect is more pronounced for a resonant position 4' than for a non resonant position 3' (15). Band I for apigenin appears at 334 nm (Figure 4.27A) and for compound **4** this absorption band has shifted to 324 nm (Figure 4.34A) with a neglegible shift observed for band II. This leads to the conclusion that this apigenin glycoside is glycosylated at resonant position 4'. This additional information reduced the list of possible glycosides to, apigenin-4'-O-α-D-glucopyranoside and apigenin-4'-O-β-D-glucopyranoside, from the DNP (Figure 4.35). The corresponding B_2 and $^{0,2}A_2$ ions appears at *m/z* 163 and 121 respectively, as additional information to support the proposed structures of compound **4**. Apigenin-4'-O-β-D-glucopyranoside is found in *Dracocephalum kotschyi* and as a substituted glycoside in *Gnaphalium affine* (56,57).

There are many apigenin glycosides that are commonly found in literature (Appendix 1) including apigenin-7-O-glucoside, apigenin-6-C-glucoside, apigenin-8-C-glucoside, apigenin-7-O-neohesperidoside, apigenin-7-O-rutinoside, apigenin-8-C-glucoside-4'-O-rhamnoside, apigenin-6-*C*-arabinoside-8-*C*-glucoside, apigenin-6-C-glucoside-8-C-arabinoside and apigenin-6-C-arabinoside-8-C-glucoside (15,17,18,53,56).

4.4.2. Chlorogenic acids

The UV spectrum of compound **1** has absorbance maxima at 326, 295 and 242 nm (Figure 4.37A). This is characteristic of a group of chlorogenic acids, caffeoylquinic acids (CQAs), that have a UV absorbance maxima (λ_{max}) of 325 nm (29). A number of available polyphenol standards were analysed under the same conditions as the MeOH extract of the flowers of *H. argyrosphaerum*. Comparison of the retention times of the standards to those of the sample constituents revealed that compound **1** has the

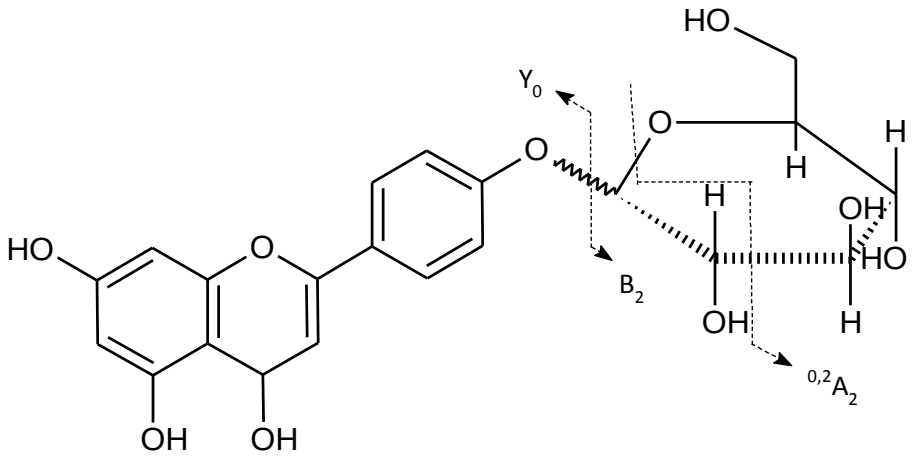

Figure 4.35: The possible chemical structures of compound **4**, apigenin-4'-O-α/β-D-glycoside.

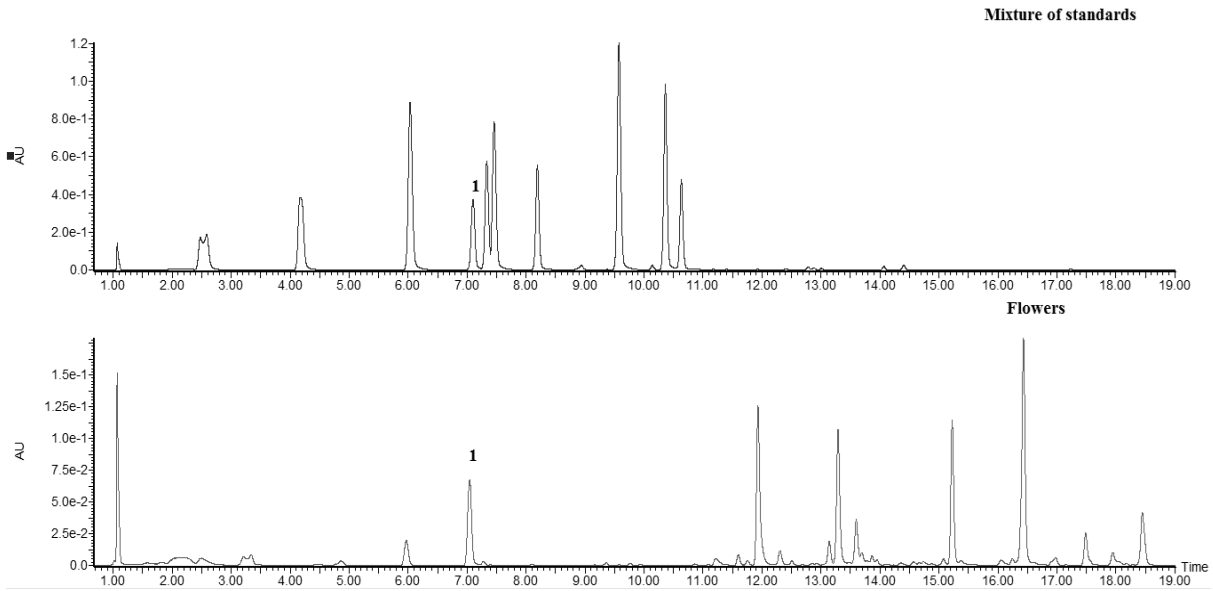

Figure 4.36: TWCs of the RPLC-UV-MS analysis of the polyphenol standards against the MeOH extract of the flowers of *H. argyrosphaerum* reported in positive ionisation mode using a mobile phase containing 0.1 % FA in 5 % MeOH over a gradient of 30 minutes.

same retention time as chlorogenic acid (Figure 4.36). The MS^E and UV spectra of these two compounds were identical (Figure 4.37).

The MS spectrum of compound **1** (Figure 4.38) displays the $[M+H]^+$ ion peak at *m/z* 355 with the calculated molecular formula of $C_{16}H_{19}O_9$ and therefore the neutral molecule has the formula of $C_{16}H_{18}O_9$. The MS^E spectrum (Figure 4.37B) displays the most abundant product ion peak at *m/z* 163, $[M-C_7H_{11}O_6]$, with a calculated molecular formula of $C_9H_7O_3$ and the neutral molecule with the formula of $C_9H_7O_3$. Other prominent peaks that are displayed in the MS^E spectrum of compound **1** as well as chlorogenic acid (Figure 4.37B) are observed at *m/z* 89 ($[M-C_{13}H_{14}O_6]$), *m/z* 107, *m/z* 117, *m/z* 135 ($[M-C_8H_{11}O_7]$) and *m/z* 145. Therefore, based on the retention time comparison to the polyphenol standards, the UV and MS^E spectra data compound **1** was identified as chlorogenic acid (CGA). The $[M-C_7H_{11}O_6]$ ion observed at *m/z* 163 in the MS^E spectrum of chlorogenic acid represents the caffeic acid fragment that results from the loss of the quinic acid unit (Figure 4.39). The UV spectrum of compound **2** (Figure 4.40) is identical to that of CGA suggesting that this compound is clearly a derivative of caffeic acid. This suggests that compound **2** is a derivative of compound **1**.

The MS spectrum (Figure 4.41A) of compound **2** displays the $[M+H]^+$ ion peak at *m/z* 499 and an adduct ion peak, [M+40], at *m/z* 539 which does change in relative abundance in the MS^E spectrum (Figure 4.41). This adduct ion peak could be representing the $[M+H+K]^+$ ion (potassium adduct). The most abundant ion peak at *m/z* 163 is also observed in the MS^E spectrum of compound **2**, therefore, serving as further proof that this molecule is a derivative of CGA. Furthermore, the MS^E spectrum (Figure 4.41B) of compound **2** also displays the same prominent product ions to that of CGA at *m/z* 89, *m/z* 107, *m/z* 117, *m/z* 135 and *m/z* 145. However, additional product

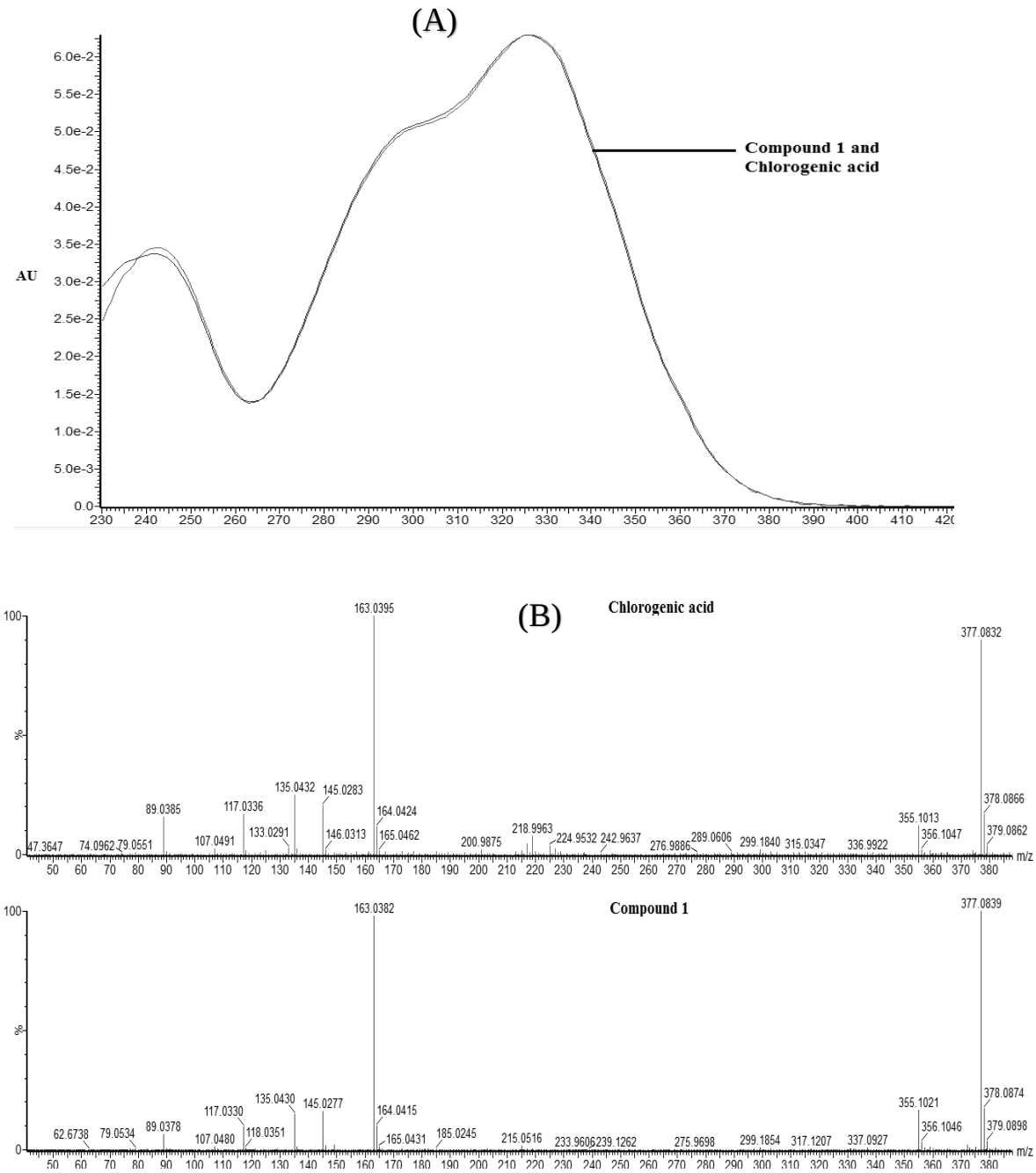

Figure 4.37: UV-vis spectra (A) and the MS^E spectra (B) of the chlorogenic acid standard and compound **1**, identified as chlorogenic acid in the MeOH extract of the flowers of *H. argyrosphaerum*.

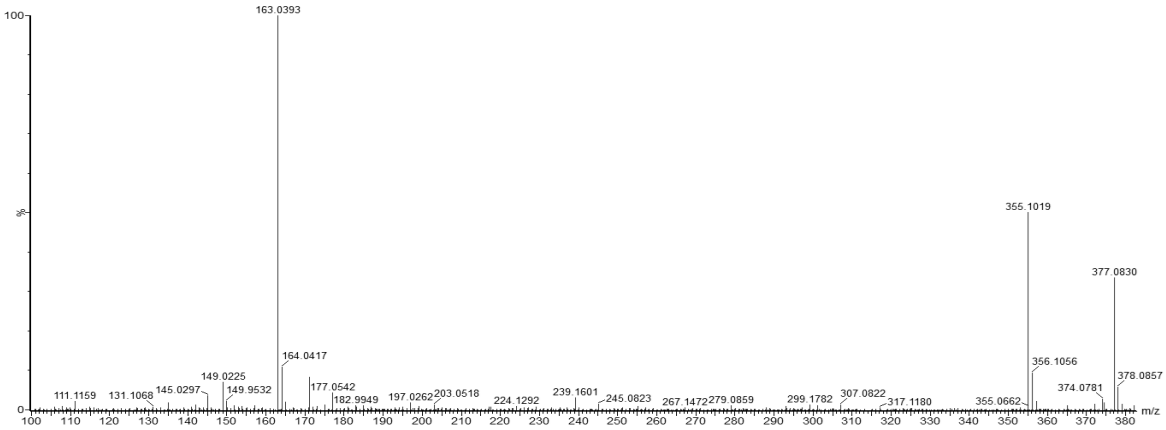

Figure 4.38: The MS spectrum of compound **1**, identified as chlorogenic acid in the MeOH extract of the flowers of *H. argyrosphaerum*.

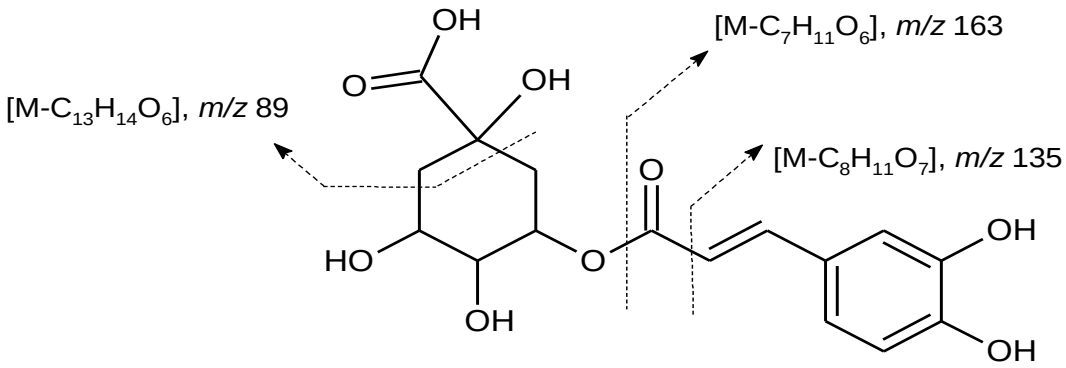

Figure 4.39: The chemical structure of compound **1**, chlorogenic acid.

ions are observed at *m/z* 399, *m/z* 377, *m/z* 317 and *m/z* 287 for compound **2** which are not observed for CGA. Therefore, compound **2** is a CGA derivative with a calculated molecular formula, $C_{25}H_{23}O_{11}$, with the neutral molecular formula of $C_{25}H_{22}O_{11}$. This molecular formula was entered into DNP to produce a match of 1'→3-Lactone-4,5-di-O-caffeoylquinic acid (Figure 4.43). The UV spectrum of compound **8** (Figure 4.40) displays a similar shape to that of CGA, however with a significant shift of λ_{max} to 318 nm suggesting that this might be a *p*-coumaroylquinic acid derivative.

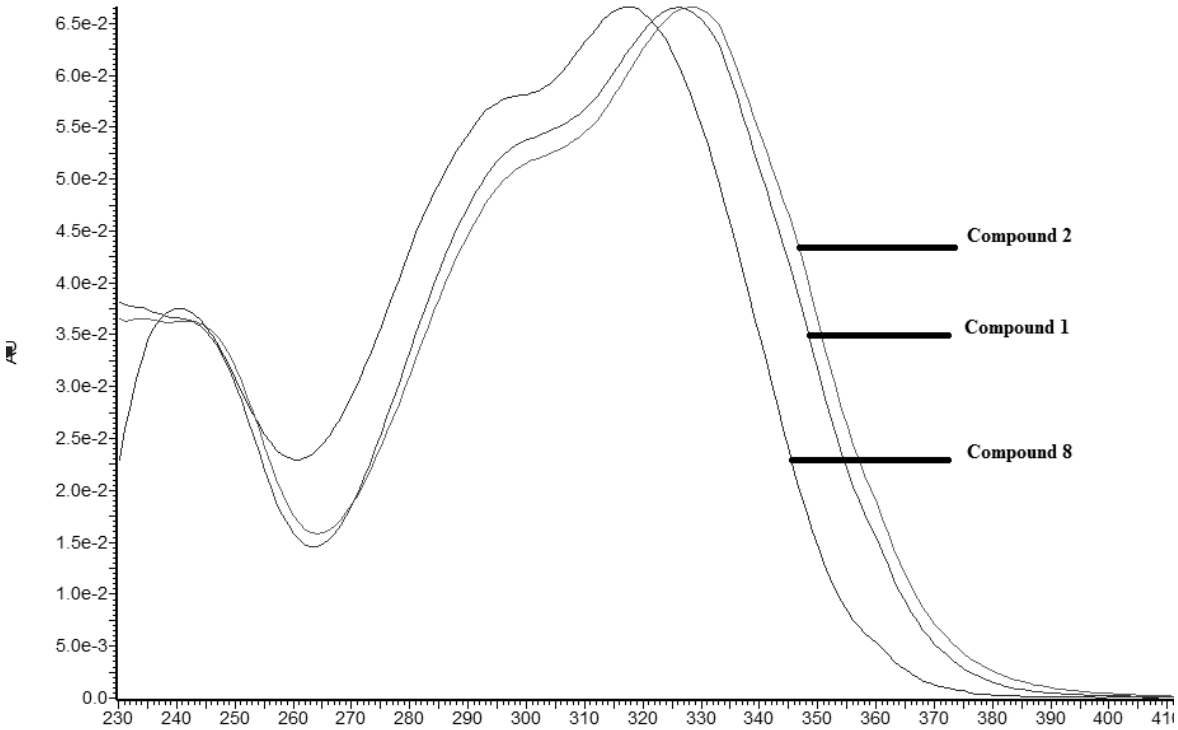

Figure 4.40: UV-vis spectra of compounds **1**, **2** and **8**.

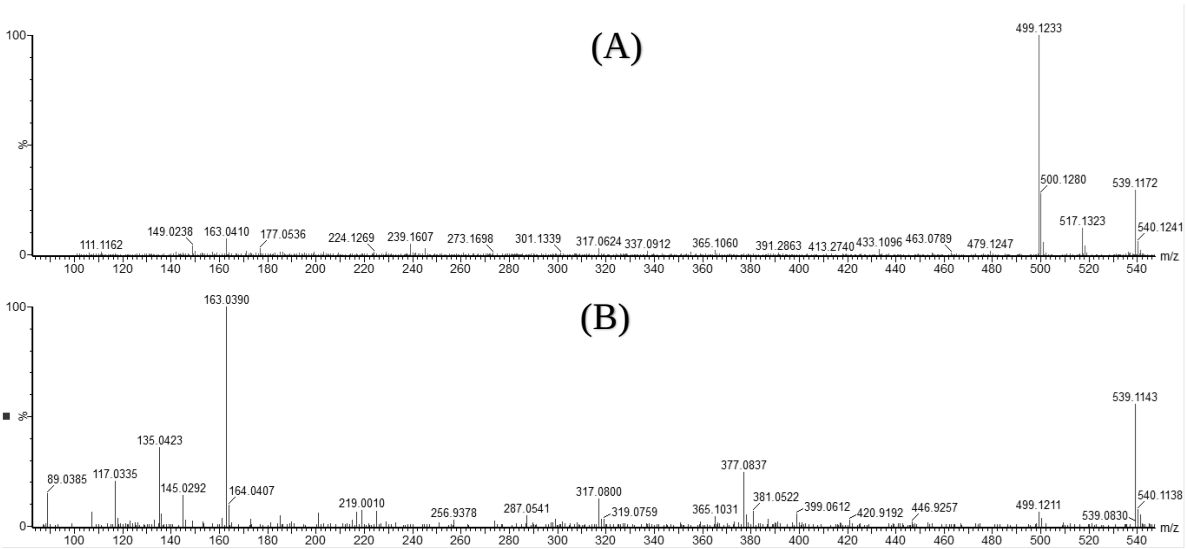

Figure 4.41: The MS spectrum (A) and MS^E spectrum (B) of compound **2**, tentatively identified as 1'→3-Lactone-4,5-di-O-caffeoylquinic acid in the MeOH extract of the flowers of *H. argyrosphaerum*.

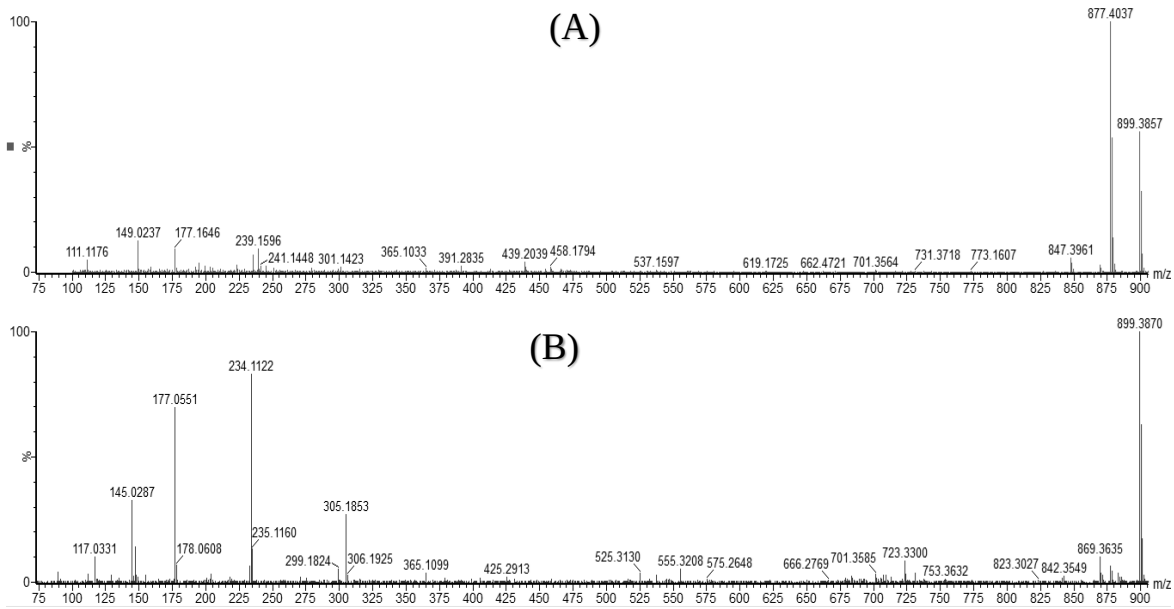

Figure 4.42: The MS spectrum (A) and MS^E spectrum (B) of compound **8**, tentatively identified as a derivative of feruloylquinic acid in the MeOH extract of the flowers of *H. argyrosphaerum*.

The lower λ_{max} compared to that of CGA is characteristic to *p*-coumaroylquinic acid, (λ_{max} 315 nm),but however lacks the typical $[M+H]^+$ ion peak at *m/z* 337 in the MS spectrum (29).

The MS spectrum of compound **8** (Figure 4.42A) displays the $[M+H]^+$ ion peak at *m/z* 877 and the $[M+Na]^+$ ion peak at *m/z* 899. The MS^E spectrum (Figure 4.42B) displays abundant product ions at *m/z* 305, *m/z* 234, *m/z* 177, *m/z* 145 and *m/z* 117. The product ion observed at *m/z* 177, $[M-C_7H_{11}O_6]$, represents the methylated caffeic acid ion 15 amu (methyl-) higher than the typical *m/z* 163. Based on this, compound **8** could be a derivative of feruloylquinic acid (Figure 4.44).

CGAs are one of the most abundant polyphenols in the human diet and they display several important therapeutic properties of many plant extracts, such as antioxidant,

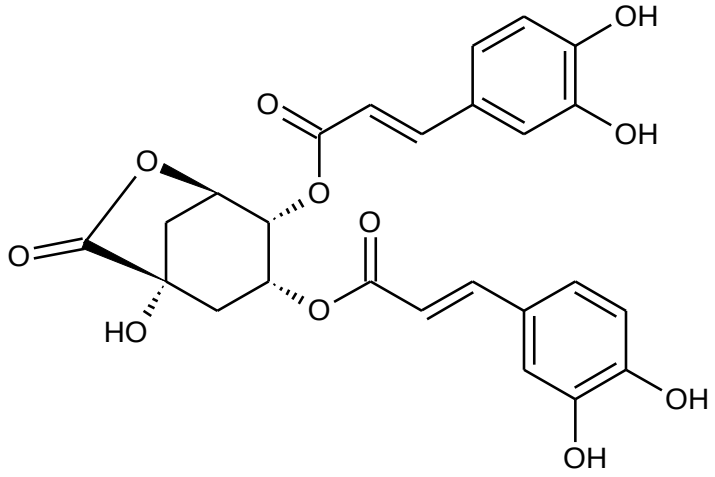

Figure 4.43: 1'→3-Lactone-4,5-di-O-caffeoylquinic acid.

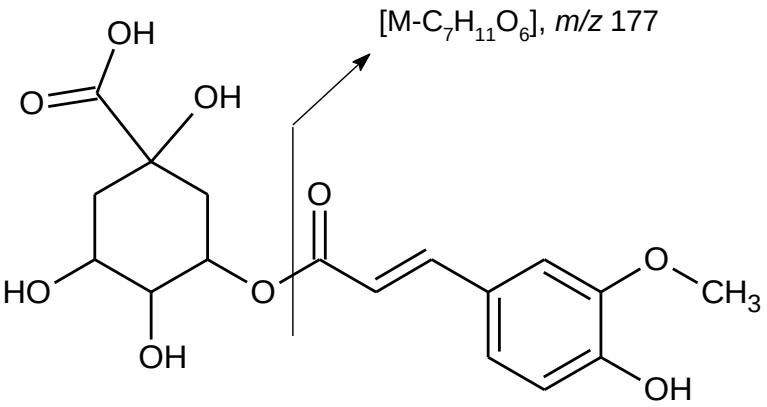

Figure 4.44: Feruloylquinic acid.

antibacterial and anti-inflammatory activity (27,30). CGAs are found in coffee, apples, citrus fruits, grapes, wines, lettuce, artichoke (*Cynara scolymus*), *Artemesia absinthium* and *A. vulgaris* (28). Prevention of hepatocellular carcinoma *in vitro* and *in vivo* was observed on the human hepatocellular carcinoma cell line, HepG2 and HepG2 xenografts in nude mice, by CGA mostly found in coffee (58). Chlorogenic acid caused a significant inhibition of HepG2 cell viability, and *in vivo*, CGA treatment also suppressed the progression of HepG2 xenograft, with 30 and 60 mg/kg of CGA

causing tumour volume decrease by 64.3% and 91.4%, and tumour weight decreased by 26.6% and 77.2% separately. Based on this information CGA appears to be an effective chemo-preventive agent for hepatocellular carcinoma. Chlorogenic acid (5-caffeoylquinic acid), isolated from a plant species, *Baccharis oxyodonta*, was reported to have potential application in snake poisoning treatment and modulation of the pathological effect of inflammation induced by secretory phospholipase A2 (sPLA2) from a rattlesnake, *Crotalus durissus terrificus* (27). CGA significantly decreased the enzymatic activity and the oedema and myonecrosis induced by native sPLA2 and antibacterial activity of CGA was used to confirm the decrease in the enzymatic activity of sPLA2 which induced massive bacterial cell destruction (27). Chlorogenic acid was reported to be a very abundant component of the methanol extracts of various *Helichrysum* species including *H. compactum* that showed strong *in vitro* antioxidant activity in the phosphomolybdenum assay (25).

CHAPTER FIVE

5. CONCLUSIONS

The presence of different classes of plant metabolites in *H. argyrosphaerum* was determined by performing phytochemical screens. HPLC separation methods (RPLC and HILIC) were developed for the analysis of the MeOH extracts of the different plant parts of *H. argyrosphaerum*. Different parameters were optimised to provide good separation between all the compounds that were detected. UPLC separation methods (RPLC and HILIC) were also developed for the LC-MS analysis of the different plant parts of *H. argyrosphaerum*.

Eight major metabolites (5 flavonoids and 3 CGAs) were detected in the MeOH extract of the flowers of *H. argyrosphaerum*. The developed RPLC method was optimised to produce a semi-preparative RPLC method that was used for the isolation of a number of the major compounds from the MeOH extract of the flowers of *H. argyrosphaerum*. Of the eight major metabolites, the identities of compounds **1** (chlorogenic acid) and **7** (apigenin) were confirmed without the use of NMR. Compound **4** was tentatively identified as an apigenin-4'-O-α/β-D-glucopyranoside without confirmation if the molecule is an α or a β anomer. Compound **5** was tentatively identified as apigenin-7-O-glucoside-[6"-O-(4-carboxy-3-methylbutanoyl)]. Compound **6** was tentatively identified as an apigenin-7-O-diglycoside with the identity of the sugar moiety still unknown. Compound **3** was tentatively identified as apigenin-7-O-galacturonopyranoside or apigenin-7-O-glucuronopyranoside were the identity of the sugar moiety could not be confirmed without the use of NMR. Compound **2** and **8** were tentatively identified as 1'→3-lactone-4,5-di-O-caffeoylquinic acid and an unknown derivative of feruloylquinic acid respectively.

Based on this study, *H. argyrosphaerum* contains bioactive compounds, apigenin and chlorogenic acid, that have previously been shown to exhibit antibacterial, antifungal and anti-inflammatory activities and that may be used in the development of chemotherapeutic agents in the future. In addition, *H. argyrosphaerum* has a new-found importance in the drug industry because it possesses bioactive compounds (apigenin and chlorogenic acid) that have been reported to exhibit anticancer properties (47,58).

Since no studies have been found that investigated the chemical composition of *H. argyrosphaerum*, the results presented in this study confirm new insights on the pharmacological potential of the plant. This plant can possibly provide new leads in drug discovery in Namibia, South Africa and all SADC countries where it's distributed (10).

However, only the MeOH extracts were analysed by HPLC and since the identification of the major constituents was limited to the MeOH extract of the flowers only, the study does not serve as a comprehensive chemical characterisation of the plant. In addition, the structure elucidation of the identified compounds in this study was limited to the use of LC-MS data without NMR data because the sample was insufficient for NMR analysis.

RECOMMENDATIONS

Since phytochemical screen procedures sometimes result in false positives, different tests for the same classes of phytochemical compounds should be performed, as well as performing more than one trial for each experiment for confirmation.

Using HPLC-UV-MS/MS, information could be obtained about the aglycone moiety, the types of carbohydrates (mono-, di-, tri- or tetra-saccharides and hexoses, deoxyhexoses or pentoses) or other substituents present, the sequence of the glycan unit, the interglycosidic linkages (O- or C-) and the attachment points (position 7 or 4') of the substituents to the aglycone (15). However NMR analysis must be performed, in order to fully elucidate the structures of the compounds that were tentatively identified in this study. To achieve this, enough material of each of the constituents must be isolated and purified using the semi-preparative method developed in this study.

Investigations on other extracts (e.g. ethanol extracts) of *H. argyrosphaerum* other than MeOH should be carried out including other plant parts (roots, leaves and stems) than flowers only.

Biological assays should also be performed on the extracts and isolated compounds, in order to confirm the biological activities of this plant and its constituents.

REFERENCES

1. Lourens a. CU, Viljoen a. M, van Heerden FR. South African *Helichrysum* species: A review of the traditional uses, biological activity and phytochemistry. J Ethnopharmacol. 2008;119(3):630–52.

2. Botha CJ, Penrith ML. Poisonous plants of veterinary and human importance in southern Africa. J Ethnopharmacol. 2008;119(3):549–58.

3. Lourens a. CU, Van Vuuren SF, Viljoen a. M, Davids H, Van Heerden FR. Antimicrobial activity and in vitro cytotoxicity of selected South African *Helichrysum* species. South African J Bot. 2011 Jan;77(1):229–35.

4. Mathekga ADM. Antimicrobial activity of *Helichrysum* species and the isolation of a new phloroglucinol from *Helichrysum caespititium*. University Of Pretoria; 2001.

5. Mathekga ADM, Meyer JJM, Horn MM, Drewes SE. An acylated phloroglucinol with antimicrobial properties from *Helichrysum caespititium*. Phytochemistry. 2000;53(1):93–6.

6. Rigano D, Formisano C, Pagano E, Senatore F, Piacente S, Masullo M, et al. A new acetophenone derivative from flowers of *Helichrysum italicum* (Roth) Don ssp. *italicum*. Fitoterapia. 2014;99(1):198–203.

7. Jakupovic J, Schuster A, Bohlmann F, Ganzer U, King RM, Robinson H. DITERPENES AND OTHER CONSTITUENTS FROM AUSTRALIAN *HELICHR YSUM* AND RELATED SPECIES. 1989;28(2):543–51.

8. The Plant List. A working list of all plant species. http://www.theplantlist.org/ (accessed 1st January). 2013. p. 1.

9. Austaller Sabine. *Helichrysum argyrosphaerum*, A multipurpose plant of economic importance in Namibia. Spotlight on agriculture. Windhoek: Ministry of Agriculture, Water and Rural Development; 1999. p. No. 19.

10. Hyde M, Wursten B, Ballings P, Coates Palgrave M. Flora of Zimbabwe: Species information: *Helichrysum argyrosphaerum*. 2017 (cited 2017 Apr 3).

11. van der Lugt JJ, Olivier J, Jordaan P. Status spongiosis, optic neuropathy, and retinal degeneration in *Helichrysum argyrosphaerum* poisoning in sheep and a goat. Vet Pathol. 1996;33(5):495–502.

12. Eroğlu HE, Aksoy A, Hamzaoğlu E, Budak Ü, Albayrak S. Cytogenetic effects of nine *Helichrysum* taxa in human lymphocytes culture. Cytotechnology. 2009;59:65–72.

13. Rigano D, Formisano C, Senatore F, Piacente S, Pagano E, Capasso R, et al. Intestinal antispasmodic effects of *Helichrysum italicum* (Roth) Don ssp. italicum and chemical identification of the active ingredients. J Ethnopharmacol. 2013;150(3):901–6.

14. Kellerman TS, Coetzer J a W, Naude TW. Plant Poisonings and Mycotoxicoses of Livestock in Southern Africa. Jl SAfr.vetAss. 2006;77(1):40–1.

15. Abad-García B, Berrueta LA, Garmón-Lobato S, Gallo B, Vicente F. A general analytical strategy for the characterization of phenolic compounds in fruit juices by high-performance liquid chromatography with diode array detection coupled to electrospray ionization and triple quadrupole mass spectrometry. J Chromatogr A. 2009;1216(28):5398–415.

16. Shashank K, Pandey AK. Chemistry and Biological Activities of Flavonoids:

An Overview. Sci World J. 2013;2013:1–16.

17. Abrankó L, Szilvássy B. Mass spectrometric profiling of flavonoid glycoconjugates possessing isomeric aglycones. J Mass Spectrom. 2015;50:71–80.

18. de Villiers A, Venter P, Pasch H. Recent advances and trends in the liquid-chromatography-mass spectrometry analysis of flavonoids. J Chromatogr A. 2015;1430:16–78.

19. Galinski CN, Zwicker JI, Kennedy DR. Revisiting the mechanistic basis of the French Paradox: Red wine inhibits the activity of protein disulfide isomerase *in vitro*. Thromb. 2016;137:169–73.

20. Gibbons S. Anti-staphylococcal plant natural products. Nat Prod Rep. 2004;21(2):263–77.

21. Dehkharghanian M, Adenier H, Vijayalakshmi MA. Study of flavonoids in aqueous spinach extract using positive electrospray ionisation tandem quadrupole mass spectrometry. Food Chem. 2010;121(3):863–70.

22. The Editors of Encyclopædia Britannica. Glycoside. Encyclopædia Britannica. Encyclopædia Britannica, inc.; 2016.

23. Merken HM, Beecher GR. Measurement of Food Flavonoids by High-Performance Liquid Chromatography : A Review. J Agric Food Chem. 2000;48(3):579–99.

24. Antunes Viegas D, Palmeira-De-Oliveira A, Salgueiro L, Martinez-De-Oliveira J, Palmeira-De-Oliveira R. *Helichrysum italicum*: From traditional use to

scientific data. J Ethnopharmacol. 2014;151(1):54–65.

25. Albayrak S, Aksoy A, Sagdic O, Hamzaoglu E. Compositions, antioxidant and antimicrobial activities of *Helichrysum* (Asteraceae) species collected from Turkey. Food Chem 2010;119(1):114–22.

26. Makita C, Chimuka L, Cukrowska E, Steenkamp PA, Kandawa-Schutz M, Ndhlala AR, et al. UPLC-qTOF-MS profiling of pharmacologically important chlorogenic acids and associated glycosides in *Moringa ovalifolia* leaf extracts. South African J Bot. 2017;108:193–9.

27. Toyama DO, Ferreira MJP, Romoff P, Fávero OA, Gaeta HH, Toyama MH. Effect of Chlorogenic Acid (5-Caffeoylquinic Acid) Isolated from *Baccharis oxyodonta* on the Structure and Pharmacological Activities of Secretory Phospholipase A2 from *Crotalus durissus terrificus*. Biomed Res Int. 2014;2014.

28. Clifford MN. Chlorogenic acids and other cinnamates – nature, occurrence dietary burden, absortion and metabolism. J Sci Food Agric. 2000;80(March 1999):1033–43.

29. Clifford MN, Kirkpatrick J, Kuhnert N, Roozendaal H, Salgado PR. LC-MSn analysis of the cis isomers of chlorogenic acids. Food Chem. 2008;106(1):379–85.

30. Liang N, Kitts DD. Role of chlorogenic acids in controlling oxidative and inflammatory stress conditions. Nutrients. 2015;8(1):1–20.

31. Rigano D, Formisano C, Senatore F, Piacente S, Pagano E, Capasso R, et al. Intestinal antispasmodic effects of *Helichrysum italicum* (Roth) Don ssp .

italicum and chemical identi fi cation of the active ingredients. J Ethnopharmacol. 2013;150(3):901–6.

32. Dokli I, Navarini L, Hameršak Z. Syntheses of 3-, 4-, and 5-O-feruloylquinic acids. Tetrahedron Asymmetry. 2013;24(13–14):785–90.

33. Drewes SE, van Vuuren SF. Antimicrobial acylphloroglucinols and dibenzyloxy flavonoids from flowers of *Helichrysum gymnocomum*. Phytochemistry. 2008;69(8):1745–9.

34. van Vuuren SF, Viljoen AM, van Zyl RL, van Heerden FR, Başer KHC. The antimicrobial, antimalarial and toxicity profiles of helihumulone, leaf essential oil and extracts of *Helichrysum cymosum* (L.) D. Don subsp. *cymosum*. South African J Bot. 2006;72(2):287–90.

35. Gouveia S, Castilho PC. Characterisation of phenolic acid derivatives and flavonoids from different morphological parts of *Helichrysum obconicum* by a RP-HPLC-DAD-(-)-ESI-MS n method. Food Chem 2011;129(2):333–44.

36. The Editors of Encyclopaedia Britannica. terpene | chemical compound | Britannica.com. (cited 2017 Sep 8).

37. Harris DC. Quantitative Chemical Analysis. In: Fiorillo J, Anderson V, Thorne A, Varas C, Ranieri D, Byrd ML, editors. Quantitative Chemical Analysis. 7th ed. New York: W. H. Freeman and Company; 2007. p. 508–11.

38. Ouyang X, Leonards P, Legler J, van der Oost R, de Boer J, Lamoree M. Comprehensive two-dimensional liquid chromatography coupled to high resolution time of flight mass spectrometry for chemical characterization of sewage treatment plant effluents. J Chromatogr A. 2015;1380:139–45.

39. Cabooter D, Clicq D, De Boever F, Lestremau F, Szucs R, Desmet G. A variable column length strategy to expedite method development. Anal Chem. 2011;83(3):966–75.

40. Barreca D, Gattuso G, Laganà G, Leuzzi U, Bellocco E. C- and O-glycosyl flavonoids in Sanguinello and Tarocco blood orange (*Citrus sinensis* (L.) Osbeck) juice: Identification and influence on antioxidant properties and acetylcholinesterase activity. Food Chem. 2016;196:619–27.

41. Beelders T, Sigge GO, Joubert E, Beer D De, Villiers A De. Kinetic optimisation of the reversed phase liquid chromatographic separation of rooibos tea (*Aspalathus linearis*) phenolics on conventional high performance liquid chromatographic instrumentation. J Chromatogr A. 2012;1219:128–39.

42. Zhang M, Pace N, Kerns EH, Kleintop T, Kagan N, Sakuma T. Hybrid triple quadrupole-linear ion trap mass spectrometry in fragmentation mechanism studies : application to structure elucidation of buspirone and one of its metabolites. J Mass Spectrom. 2005;40:1017–29.

43. Holčapek M, Jirásko R, Lísa M. Recent developments in liquid chromatography – mass spectrometry and related techniques. J Chromatogr A. 2012;1259:3–15.

44. Camp D, Davis RA, Campitelli M, Ebdon J, Quinn RJ. Drug-like Properties: Guiding Principles for the Design of Natural Product Libraries. J Nat Prod. 2012;75:72–81.

45. Farnsworth NR. Biological and phytochemical screening of plants. J Pharm Sci 1966 Mar (cited 2017 Apr 28);55(3):225–76.

46. Islam MS, Segars JH, Castellucci M, Ciarmela P. Dietary phytochemicals for

possible preventive and therapeutic option of uterine fibroids: Signaling pathways as target. Pharmacol Reports. 2017;69(1):57–70.

47. Erdogan S, Doganlar O, Doganlar ZB, Serttas R, Turkekul K, Dibirdik I, et al. The fl avonoid apigenin reduces prostate cancer CD44 + stem cell survival and migration through PI3K / Akt / NF- κ B signaling. Life Sci. 2016;162:77–86.

48. Shukla S, Gupta S. Apigenin: A Promising Molecule for Cancer Prevention. NIH Public Acces. 2010;27(6):962–78.

49. Sato Y, Suzaki S, Nishikawa T, Kihara M, Shibata H, Higuti T. Phytochemical flavones isolated from *Scutellaria barbata* and antibacterial activity against methicillin-resistant *Staphylococcus aureus*. J Ethnopharmacol. 2000;72(3):483–8.

50. Data P, References B, Unknown. Dictionary of natural products on CD-ROM. (cited 2017 May 10).

51. Tang R, Chen K, Cosentino M, Lee K-H. Apigenin-7-O-β-D-glucopyranoside, an anti-HIV principle from *Kummerowia striata*. Bioorg Med Chem Lett. 1994 Feb;4(3):455–8.

52. Gülcemal D, Alanku-Çalişkan Ö, Karaalp C, Örs AU, Ballar P, Bedir E. Phenolic Glycosides with antiproteasomal activity from *Centaurea urvillei* DC. subsp. urvillei. Carbohydr Res. 2010;345(17):2529–33.

53. Ferreres F, Andrade PB, Valentão P, Gil-Izquierdo A. Further knowledge on barley (Hordeum vulgare L.) leaves O-glycosyl-C-glycosyl flavones by liquid chromatography-UV diode-array detection-electrospray ionisation mass spectrometry. J Chromatogr A. 2008;1182(1):56–64.

54. Rothwell JAJ, Pérez-Jiménez J, Neveu V, Medina-Ramon A, M'Hiri N, Garcia LP, et al. Phenol-Explorer 3.0: a major update of the Phenol-Explorer database to incorporate data on the effects of food processing on polyphenol content. 2013. p. 1–8.

55. Moharram FA, Marzouk MSA. A novel phenylethanoid dimer and flavonoids from *Jacaranda mimosaefolia*. Zeitschrift fur Naturforsch - Sect B J Chem Sci. 2007;62(9):1213–20.

56. Fattahi M, Nazeri V, Torras-Claveria L, Sefidkon F, Cusido RM, Zamani Z, et al. Identification and quantification of leaf surface flavonoids in wild-growing populations of *Dracocephalum kotschyi* by LC-DAD-ESI-MS. Food Chem. 2013;141(1):139–46.

57. Xi Z, Chen W, Wu Z, Wang Y, Zeng P, Zhao G, et al. Anti-complementary activity of flavonoids from *Gnaphalium affine* D. Don. Food Chem. 2012;130(1):165–70.

58. Yan Y, Liu N, Hou N, Dong L, Li J. Chlorogenic acid inhibits hepatocellular carcinoma *in vitro* and *in vivo*. J Nutr Biochem. 2017;46:68–73.

APPENDIX 1: Apigenin glycosides commonly found in nature

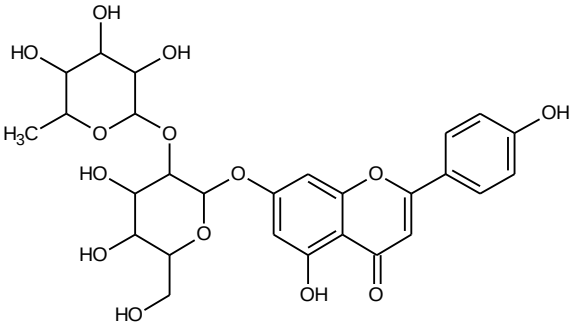

APIGENIN-7-O-NEOHESPERIDOSIDE

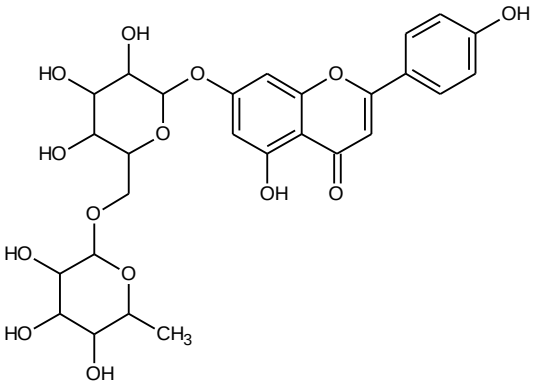

APIGENIN-7-O-RUTINOSIDE

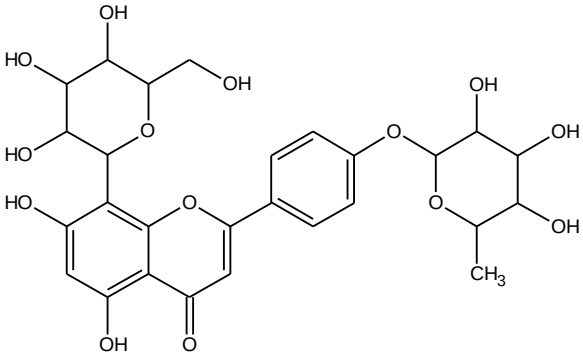

APIGENIN-8-C-GLUCOSIDE-4'-O-RHAMNOSIDE

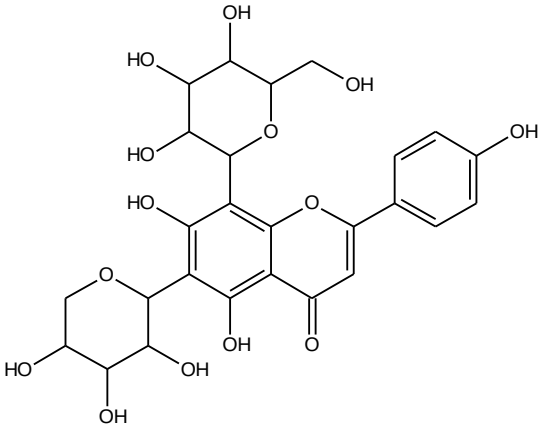

APIGENIN-6-C-ARABINOSIDE-8-C-GLUCOSIDE

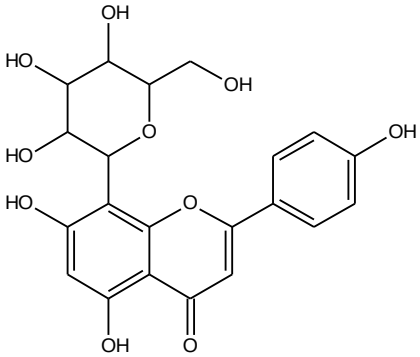

APIGENIN-8-C-GLUCOSIDE

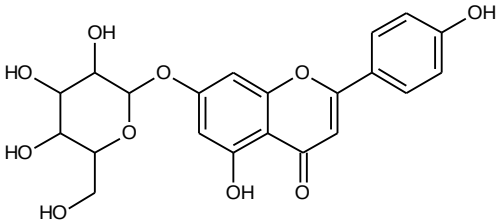

APIGENIN-7-O-GLUCOSIDE

APPENDIX 2: Research permission letter

UNIVERSITY OF NAMIBIA

Private Bag 13301, 340 Mandume Ndemufayo Avenue, Pioneerspark, Windhoek, Namibia.

Date: **21 October 2014**

TO WHOM IT MAY CONCERN

RE: RESEARCH PERMISSION LETTER

1. This letter serves to inform that student: **T. M. Namate** (Student number: **201047624**) is a registered student in the Department of Chemistry and Biochemistry at the University of Namibia. His/her research proposal was reviewed and successfully met the University of Namibia requirements.
2. The purpose of this letter is to kindly notify you that the student has been granted permission to carry out postgraduate studies research. The School of Post- graduate Studies has approved the research to be carried out by the student for purposes of fulfilling the requirements of the degree being pursued.
3. The proposal adheres to ethical principles.

Thank you so much in advance and many regards.

Yours truly,

Name of Main Supervisor: **Dr. Stefan Louw**

Signed: _____

Dr. C. N.S. Shaimemanya

PP

Signed: _____

Director: School of Postgraduate Studies

Tel: 2063523

E-mail: cshaimemanya@unam.na

APPENDIX 3: Ethical clearance certificate

UNIVERSITY OF NAMIBIA

Inspiring minds & shaping the future

ETHICAL CLEARANCE CERTIFICATE

Ethical Clearance Reference Number: SEC/FOS/59/2014 **Date: 29 September, 2014**

This Ethical Clearance Certificate is issued by the University of Namibia Research Ethics Committee (UREC) in accordance with the University of Namibia's **Research Ethics Policy and Guidelines. Ethical approval is given in** respect of undertakings contained in the Research Project outlined below. This Certificate is issued on the recommendations of the ethical evaluation done by the Faculty/Centre/Campus Research & Publications Committee sitting with the Postgraduate Studies Committee.

Title of Project: **ISOLATION AND CHARACTERISATION OF TOXIC COMPOUNDS IN THE WILD EVERLASTING, *HELICHRYSUM ARGYROSPHAERUM*, RESPONSIBLE FOR LIVESTOCK POISONING IN SOUTHERN AFRICA**

Nature/Level of Project: MASTERS

Principal Researcher: T. M. NAMATE (Student No: 201047624)

Host Department & Faculty: Chemistry& Biochemistry, Faculty of Science.

Main Supervisor (s): Dr Stefan Louw (Main), (Co) Dr Renate Hans

Take note of the following:

(a) Any significant changes in the conditions or undertakings outlined in the approved Proposal must be communicated to the UREC. An application to make amendments may be necessary.

(b) Any breaches of ethical undertakings or practices that have an impact on ethical conduct of the research must be reported to the UREC.

(c) The Principal Researcher must report issues of ethical compliance to the UREC (through the Chairperson of the Faculty/Centre/Campus Research & Publications Committee) at the end of the Project or as may be requested by UREC.

(d) The UREC retains the right to:

(i). withdraw or amend this Ethical Clearance if any unethical practices (as outlined in the Research Ethics Policy) have been detected or suspected,

(ii). request for an ethical compliance report at any point during the course of the research.

UREC wishes you the best in your research.

Prof. I. Mapaure
UNAM Research Coordinator
ON BEHALF OF UREC